RESPONSE TIME QUALIFICATION OF RESISTANCE THERMOMETERS IN NUCLEAR POWER PLANT SAFETY SYSTEMS

MILLSTONE NUCLEAR POWER STATION, UNIT NO. 2

NORTHEAST UTILITIES TOPICAL REPORT

DOCKET NO. 50-336

RESPONSE TIME QUALIFICATION OF RESISTANCE THERMOMETERS IN NUCLEAR POWER PLANT SAFETY SYSTEMS

MILLSTONE NUCLEAR POWER STATION, UNIT NO. 2

NORTHEAST UTILITIES TOPICAL REPORT

PREPARED BY

DR. T. W. KERLIN
Analysis and Measurement Services Corp.
1617 Euclid Ave.
Knoxville, Tennessee 37921

TABLE OF CONTENTS

PAGE

Summary

Methods for measuring the response characteristics of resistance thermometers are presented and verified. The methods include loop current step response testing for quantitative response characterization and self heating for monitoring for changes in response time. The loop current step response test provides the transfer function of the sensor (output signal/fluid temperature change). The measured transfer function may be used to give any index of response desired (i.e. response vs. time for a step input, response vs time for a ramp input, time constant, ramp delay time, etc.).

The loop current step response test or the self heating test may be performed at the end of the sensor leads where they are normally connected to their transmitter. The sensor must be disconnected during testing; but, otherwise, normal plant operation is not affected.

The testing procedures have been verified by extensive laboratory testing. Laboratory conditions varied from room temperature and pressure and low flow to full PWR operating conditions. Laboratory tests permitted direct response measurements and loop current step response tests with the sensor in the same condition. Loop current step response results and direct time constant measurements were found to agree very well (within ten percent).

The procedures also have been applied in operating plants. Experiences at six plants are reported herein which show the practicality of the procedures for in-plant testing.

The methods have been found to be reliable, accurate, and practical.

1. Introduction

New techniques for response time testing of resistance thermometers installed in nuclear power reactors have been developed, validated and applied. The techniques are described and their validity is established in this report.

1.1 Regulations and Standards

U.S. Nuclear Regulatory Guide 1.118[1] provides criteria, requirements and recommendations on periodic testing of electric power and protection systems. This guide refers heavily to two Institute of Electrical Engineers Standards (IEEE Std 279-1971[2] and IEEE Std 338-1975[3]). The Regulatory Guide states that the criteria, requirements and recommendations in IEEE Std 338-1975 are considered to be generally acceptable subject to sixteen stated exceptions and/or clarifications. The key points relative to sensor testing in the Regulatory Guide are:

- (Section C - Item 1). "Means shall be included in the design to facilitate response time testing from sensor input to and including the actuated equipment."
- (Section C - Item 5). "Designs that do not require the use of bypasses in order to test all or part of a safety system, are preferred over those that require bypasses."
- (Section C - Item 6). "Instrumentation channel tests should include perturbing the monitored variable wherever practical. Wherever this is not practical, it should be shown that the substitute tests are adequate."
- (Section C - Item 12). "6.3.4 Response Time -ification Tests. Safety system response time measurements shall be made periodically to verify the overall response time (assumed in the safety analysis of the plant) of all portions of the system from and including the sensor to operation of the actuator.

"Where it is not possible to include sensors in in-plant individual or system response time tests, the sensors shall be periodically removed from their normal installations and tested. When this is necessary, the test installation shall duplicate as nearly as possible the expected environment and mechanical configuration of the actual installation.

"For channel testing, not including sensors, test equipment shall include that necessary to simulate sensor output over its full range and simultaneously record input and output conditions for determining the overall response time. The test input should span the normal trip setpoint sufficiently to reset the channel for the untripped condition and ensure complete tripping for the tripped condition.

"For protection tripping functions where two or more variables enter into the tripping action (for example, the trip point is computed from temperature, differential pressure, and nuclear flux signals), the channel response time shall be verified using each of the variables to produce the tripping action. During this tripping action, the test signals for the remaining variables shall be adjusted to within their expected operating range, but to a value that will produce conservative test results.

"The response time test shall include as much of each safety system, from sensor input to actuated equipment, as possible in a single test. Where the entire set of equipment from sensor to actuated equipment cannot be tested at once, verification of system response time may be accomplished by measuring the response times of discrete portions of the system and showing that the sum of the response times of all portions is equal to or less than the overall system requirement.

"Response time testing of all safety system equipment per se is not required if, in lieu of response time testing, the response time of safety

system equipment is verified by functional testing and/or calibration checks where it can be demonstrated that changes in response time beyond acceptable limits are always accompanied by changes in performance characteristics that are detectable during these routine periodic functional tests and/or calibration checks."

These criteria, requirements and recommendations, along with those in IEEE Std 279-71 and IEEE Std 338-75, were taken into account when developing and evaluating a testing procedure for resistance thermometers. Full compliance with these criteria, requirements and recommendations is demonstrated in subsequent sections of this report.

1.2 Candidate Test Procedures

The response of a resistance thermometer is controlled by the rate at which heat diffuses from the fluid to the sensing element. Therefore, a suitable test procedure will involve a variation in the heat diffusion rate.

Several candidate test procedures have been identified and evaluated. These are:

A. Remove and Plunge. The plunge test is the classical response time qualification test for temperature sensors. Most tests involve rapid insertion of the sensor from room temperature air or an ice bath into flowing water. The most common water flow rate is three feet per second. These tests are of questionable value for proper evaluation of the response time of reactor sensors because the conditions in the reactor (flow, pressure, temperature and possibly conditions inside and outside of a thermowell) are different than in the laboratory. Partial resolution of this problem is possible by simulating flow, pressure, and/or temperature conditions, but other environmental conditions (such as the thermowell) cannot

be simulated with confidence. Consequently, the removal and plunge test procedure is judged to have limited usefulness for practical response measurements.

B. Plant Maneuver. Fluid temperature changes can be induced by changing reactor power or by changing the steam flow. This will provide a sensor output transient that depends on its response characteristics. However, there is no way to determine the actual fluid temperature so that the sensor dynamics can be identified. Simulation might be used to estimate the fluid temperature, but the uncertainty in this would be significant. Consequently, the plant maneuver approach is considered to be unsatisfactory.

C. Internal Heating. It is possible to induce a heat diffusion transient by passing an electric current through the normal sensor leads. Since a small current must be used in the bridge used for normal temperature measurement, this approach involves an increase in current from its normal level to a level suitable for obtaining adequate test data. The Joule heating causes a temperature transient which is controlled by heat diffusion from the sensing (and heating) element to the fluid. This is exactly the reverse of the normal heat diffusion path, but the same physical properties control the heat diffusion regardless of the path. This intuitive approach led to the development of an internal heating test method called the loop current step response (LCSR) test. The key to this test method is the ability to construct the response of interest (the response to a fluid temperature change) from information that is measureable in a LCSR test (the response to an internal heating change). This transformation has been developed and validated.[4,5,6,7] The method is suitable for complying with the criteria, requirements and recommendations of Regulatory Guide 1.118. It is discussed in subsequent sections of this report.

D. Fluctuation Analysis.[8,9,10] The output of a temperature sensor that experiences random fluctuation in fluid temperature depends on the sensor response characteristics. Methods have been developed for analyzing these fluctuating signals to determine the response time, but quantitative response time determinations depend on satisfaction of an assumption about the statistics of the process temperature fluctuations. Since this assumption cannot be validated, this method is considered unsuitable for quantitative measurements.

The research program for developing response time testing methods involved theoretical analysis, equipment design, laboratory testing and in-plant testing. The laboratory work involved testing at room temperature, low flow conditions, and testing at plant conditions in a special test loop at Electricite de France. In these tests it was possible to compare the loop current step response test results with plunge tests or injection tests and thereby evaluate the validity of the methods.

1.3 Organization of this Report

Subsequent sections of this report give a complete description of the loop current step response test. This includes basic theory, equipment requirements, analysis procedures, accuracy limitations, laboratory validation and field testing experience. Most of the information was extracted from several earlier publications, but some new information is included also.

2. Resistance Thermometer Characteristics

2.1 Construction Features

A typical resistance temperature detector (RTD) consists of a fine platinum wire mounted inside a metal sheath (usually stainless steel). Two construction methods are commonly used: mandrel mounting and wall mounting. In a mandrel-mount sensor, the platinum element is mounted on a support piece, inserted into the sheath, and held in place by a powder or cement filler (See Figure 2.1). In a wall-mount sensor, a platinum wire coil is attached to the inside wall of a hollow sheath by a cement that also serves to insulate the platinum electrically from the sheath (See Figure 2.2).

Each of the construction methods has advantages. If a support structure is used to mount the filament, stress effects on sensor performance can be minimized; however, the back-fill material needed for electrical insulation has significant thermal resistance. If the filament is very close to the inner wall of the sheath, as is the case for the wall-mount sensor, the time response of the sensor is faster than when the filament is mounted on a separate support. The fast time response is desired for some applications.

RTDs may be designed for direct immersion into a fluid stream (wet-type) or for installation into a well in the stream (well-type). To improve the heat transmission in well-type sensors, a thermal bonding material is often used in the gap between the sheath and the well.

The sensors found in pressurized water reactors manufactured by different vendors are quite different. Table 2.1 gives specifications on some of the commonly-used sensors. Figures 2.3 through 2.5 show some of these sensors.

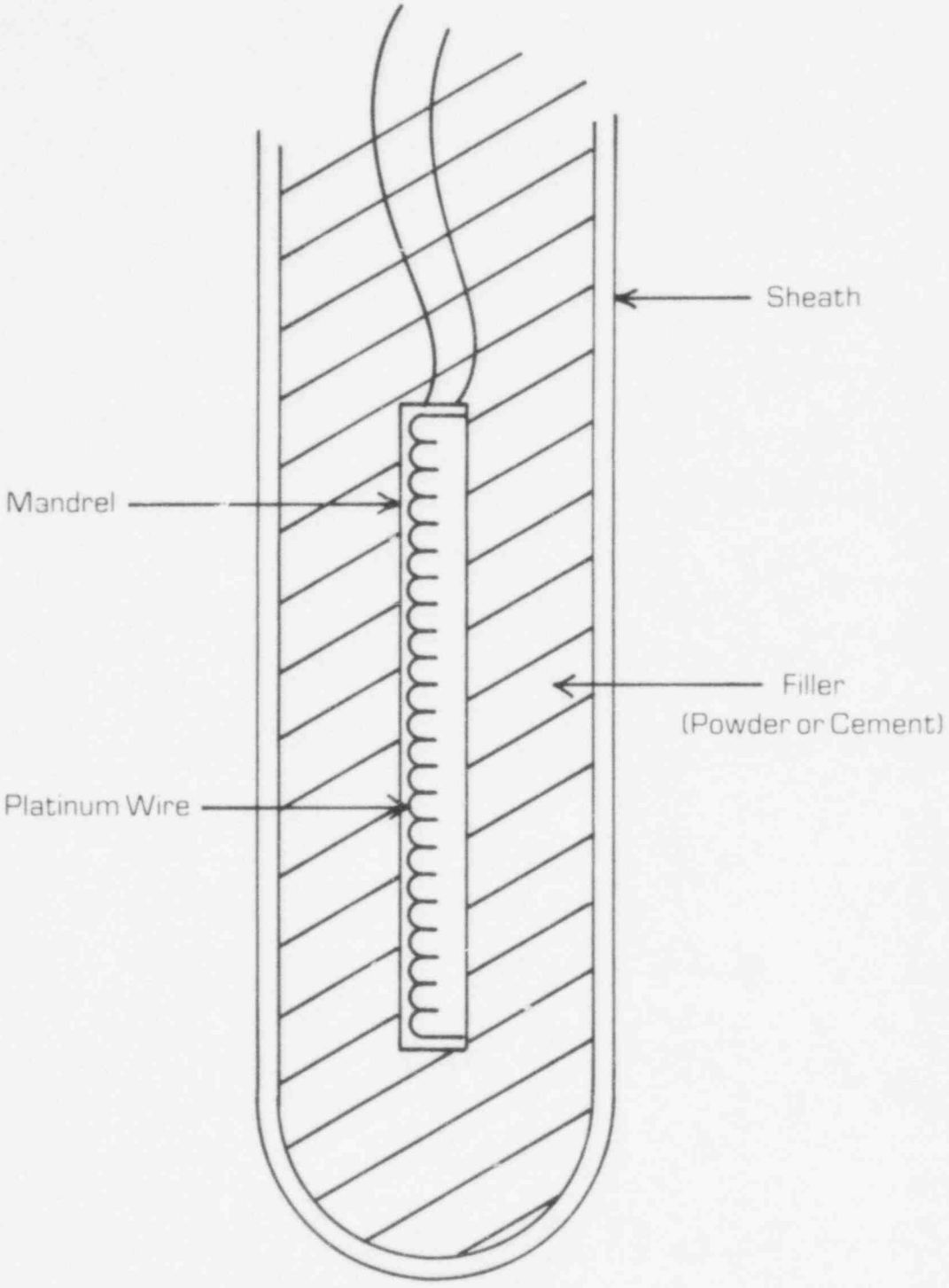

FIGURE 2.1. MANDREL MOUNT RTD

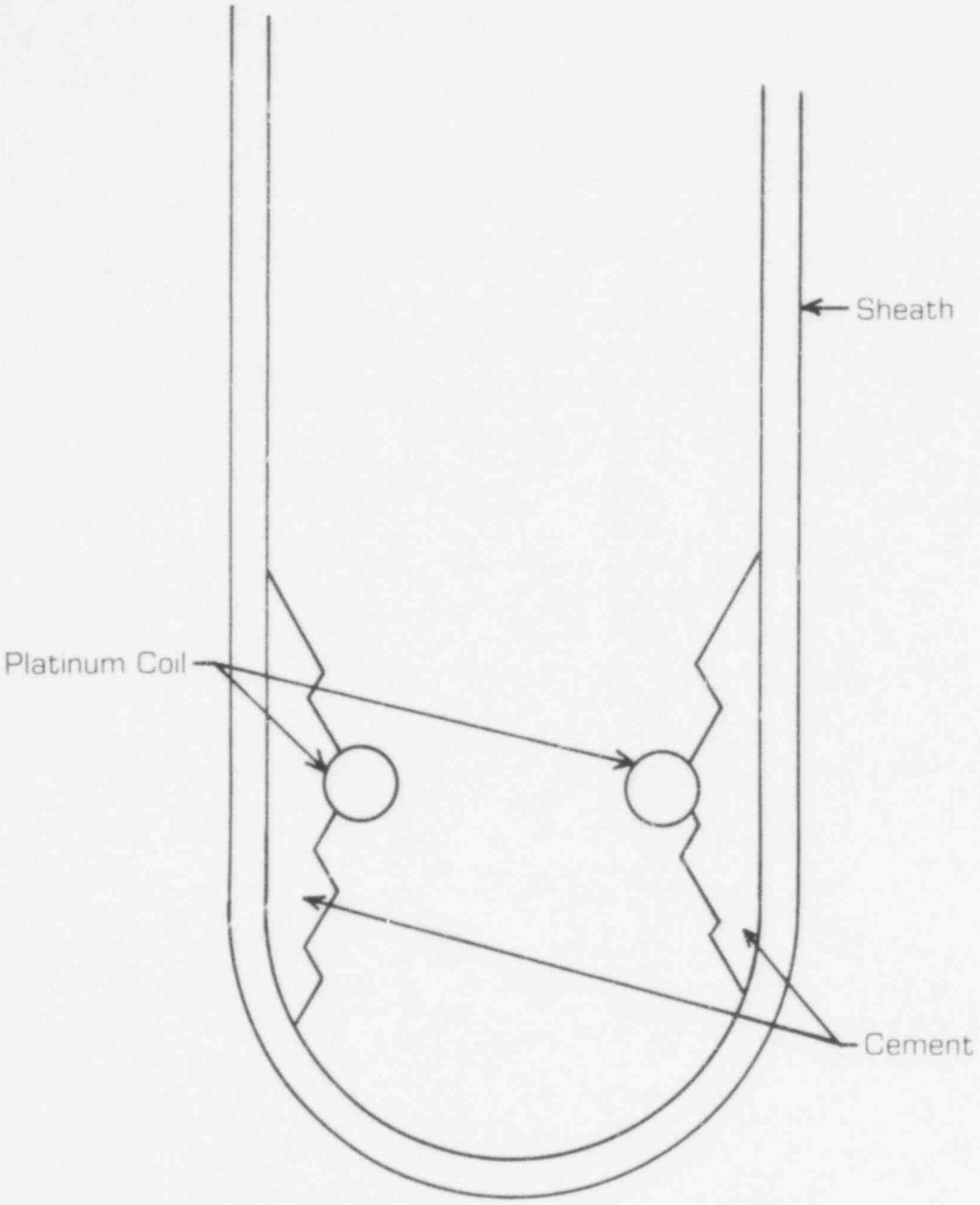

FIGURE 2.2. - WALL MOUNT RTD

TABLE 2.1

SPECIFICATIONS OF THE RTDS USED IN THIS WORK

Sensor Manufacturer	Model Number	Plants Where Used	Wet Type Or Well Type	Sensor Sheath O.D.	Well O.D.	Number of Sensing Elements Per RTD	2 Wire 3 Wire or 4 Wire	Dummy Wire?	Resistance at 0°F R_o (Ω)
REC*	177-GY	B&W**	wet	.335"	NA	2	4	no	100
REC	177HW	B&W**	well	.290"	.410"	2	4	no	100
REC	104-AFC	C.E.	well	.125	.281"	1	2	yes	200
REC	176-KF	Westinghouse	wet	.375"	NA	1	4	no	200
REC	104ADA	C.E.***	well	.125"	.25	1	2	yes	200
REC	104VC	C.E.	well	.125"	.25	1	2	yes	200
Sostman	8606	Westinghouse	wet	.25"	NA	1	4	no	200

*Rosemount Engineering Company.

**Babcock and Wilcox Co.

***Combustion Engineering Inc.

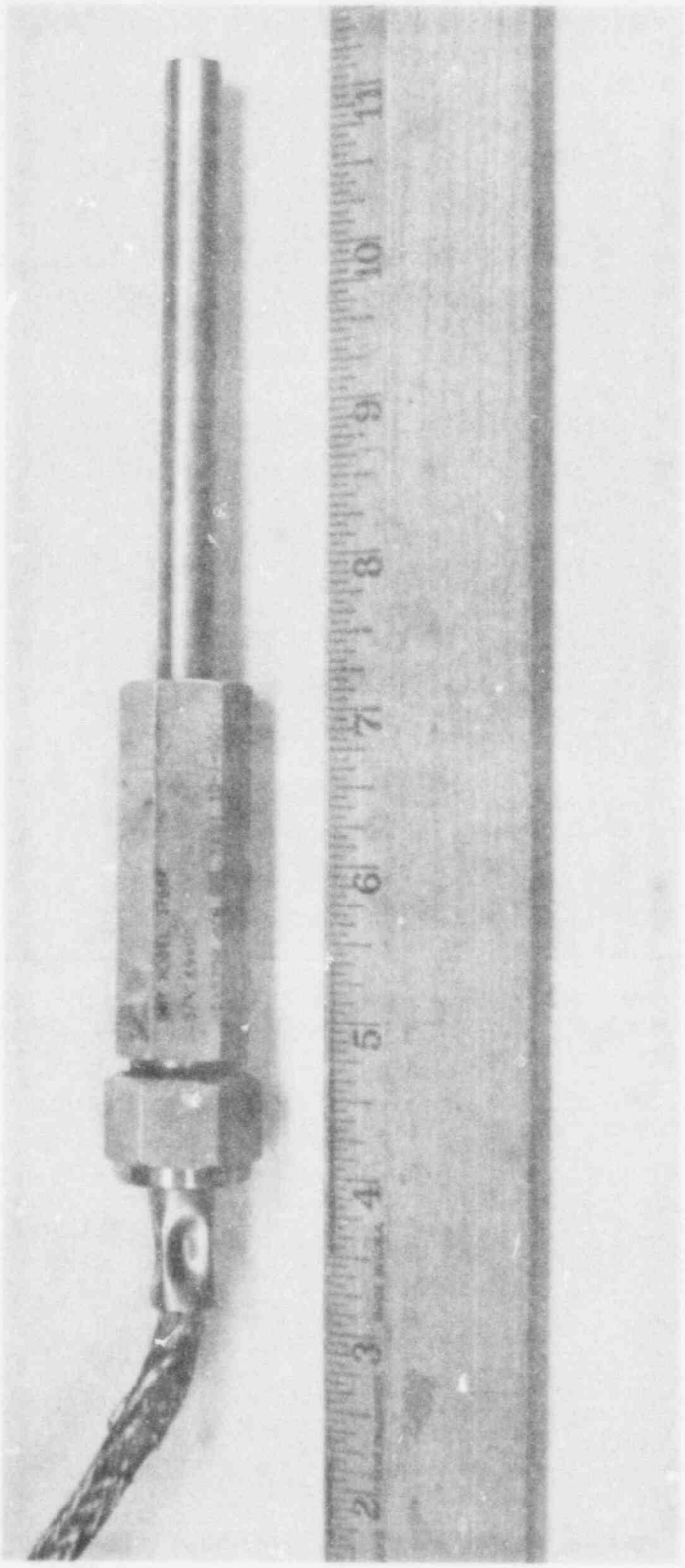

FIGURE 2.3. PICTURE OF THE ROSEMOUNT 176-KF SENSOR

927 066

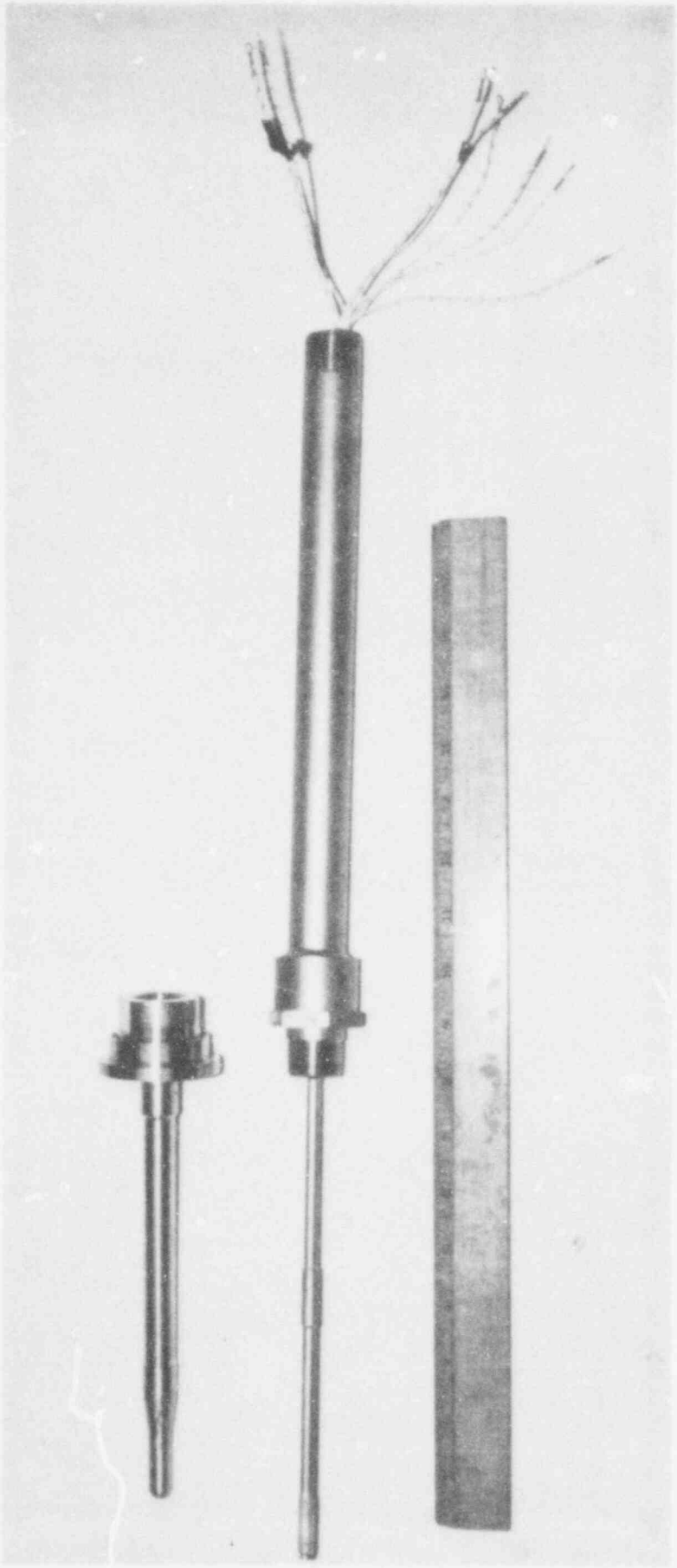

FIGURE 2.4. PICTURE OF THE ROSEMOUNT 177-HW SENSOR

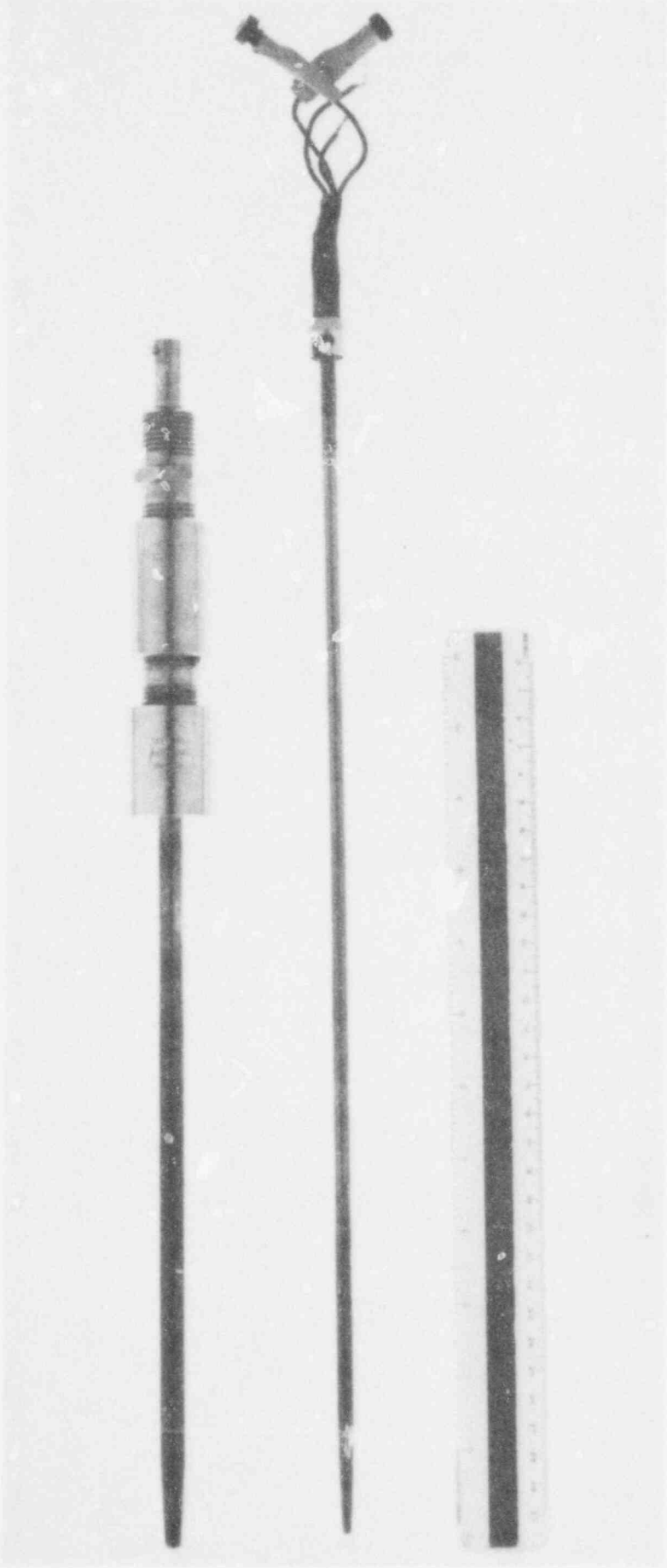

FIGURE 2.5. PICTURE OF ROSEMOUNT 104-ADA SENSOR

The resistance element is connected to lead wires that connect to appropriate instrumentation. Sensors may be constructed with the lead wire configurations shown in Figure 2.6. The multiple lead and dummy wire configurations are used in measurement systems to compensate for lead wire resistance to obtain accurate temperature measurements. RTDs are also made with single sensing elements per sheath and with dual elements that allow two independent measurements with the same sensor.

2.2 Environmental Effects on Response Time

Environmental effects that may influence sensor response time are ambient temperature, fluid flow rate, and ambient pressure. These are discussed below.

2.2.1 Ambient Temperature Influence

Changes in ambient temperature can affect response time by the following mechanisms:

- temperature dependence of heat transfer parameters (thermal conductivities, specific heat capacities and surface film heat transfer coefficients).
- dimensional changes with temperature.

The materials used commonly in RTDs and available information on temperature dependences of thermal conductivities and specific heat capacities are shown in Table 2.2. From Table 2.2, we see that no information is available for several important materials, so a conclusive answer to the temperature dependence of sensor response time cannot be based on the use of physical property data. Experiments on actual sensors must be used to obtain quantitative information.

The heat transfer coefficient at the sensor surface changes with temperature. This occurs because of the temperature dependence of water

a) 2 Wire

b) 3 Wire

c) 4 Wire

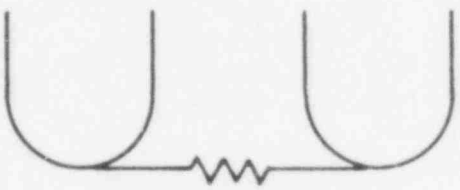

d) 2 Wire with Dummy

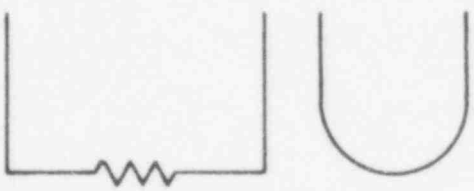

FIGURE 2.6. RTD LEAD WIRE CONFIGURATIONS

927 ~~069~~ 070

Table 2.2

Effect of Temperature on Thermophysical Properties of Resistance Thermometer Materials

Material	Percentage change in Property for a Temperature increase from 70°F to 600°F	
	Specific Heat	Thermal Conductivity
304 SS	+18	+25
316 SS	Negligible	+25
Al_2O_3 (porosity = 0)*	+43	-57
Air	+0.5	+70
Cement Used in RTDs	?	?
Thermal Bonding Compounds (for use as a filler between sensors and their wells)	?	?

*Note - The thermal conductivity of Al_2O_3 depends strongly on porosity. The net effect depends on the combined effect of Al_2O_3 conductivity and the conductivity of the air in the pores. Since the conductivity of Al_2O_3 decreases with temperature and the conductivity of air increases with temperature, these are competing effects. For 53 percent porosity, the temperature dependence is nearly zero.

thermal conductivity, specific heat capacity and viscosity. It has been shown[6] that the film heat transfer coefficient decreases by about a factor of two as water temperature increases from 70°F to 500°F.

An additional (and possibly dominating) factor in establishing the temperature dependence of the response time is the temperature effect on dimensions. The sensor is composed of several layers of materials. Ideally, these materials are homogeneous and in perfect contact with one another. In actuality, it is likely that cracks and gaps exist within regions and at boundaries. As temperature increases, the gaps and cracks may open or close depending on the temperature coefficients of expansion of the sensor materials. Since gas-filled gaps and cracks have a large effect on the heat transfer resistance, this could be a large (but unpredictable) factor with the net effect being an increase or decrease in time constant with temperature.

2.2.2 Fluid Flow Rate Influence

The film heat transfer coefficient for the sensor depends on the fluid flow rate. Correlations show that the film coefficient varies as the flow to the 0.8 power. The importance of the film coefficient in determining the time constant depends on the relative importance of internal heat transfer resistance vs. surface heat transfer resistance. For example, a sensor whose internal heat transfer resistance is ninety percent of the total at low flow can experience only a maximum of ten percent improvement even at very high flow.

2.2.3 Ambient Pressure Influence

If the sensor sheath were compressible, then increased pressure would compact the materials, improve the heat transfer, and reduce the time constant. The effect is insignificant for practical sensor designs.

Ambient pressure also affects the thermophysical properties of water (density, specific heat capacity, thermal conductivity and viscosity), but the effect is small. The total effect of ambient pressure is small.

2.3 Modes of Response Time Degradation

Since the response time is controlled by heat diffusion, response time degradation could occur either by an increase in the overall heat transfer resistance or by an increase in the effective heat capacity of the sensor materials. Response time degradation has occurred, so it is useful to postulate causes. Possible causes are:

- Changes in properties of thermal bonding material. The NEVER-SEEZ compound used for thermal bonding in some well-type sensors undergoes changes with temperature. Experiments[11] showed a tendency for NEVER-SEEZ to change from a pasty material at room temperature to a powder at elevated temperature (500°F). Consequently, tests were performed to determine the influence of temperature on the time constant because of NEVER-SEEZ property changes. Results are shown in Table 2.3. These show that NEVER-SEEZ properties change in a way that increase the time constant of the sensor-well assembly.

- Changes in properties of filler or bonding material. A special cement called PBX (manufactured by the Robert G. Allen Co. of Mechanicsville, N.Y.) is used in most currently used PWR sensors. It is the filler material in mandrel-mounted sensors and the cement used to hold the platinum in place in wall-mounted sensors. Tests in air show that the cement changes from a homogeneous, plastic-like material to a flaky, hard material when heated in air to 500°F. Additional tests[12] with PBX were performed in which special sensors were constructed for material evaluations. Small, iron-constantan thermocouples were placed in the center of 1/2 in. tubes

TABLE 2.3

EFFECT OF NEVER-SEEZ PROPERTY CHANGES WITH TEMPERATURE ON THE TIME CONSTANT

Test Number	Condition	Time Constant (Plunge Test)
1	Fresh NEVER-SEEZ in Well	3.70 sec.
2	After heating sensor and thermowell with NEVER-SEEZ at 500°F for 12 hours	4.55
3	Sensor and Well with NEVER-SEEZ Removed-Sensor and Well cleaned with alcohol (air now in Well)	4.12
4	Repeat of Test Number 1 (fresh NEVER-SEEZ)	3.72
5	After heating sensor and thermo-well with NEVER-SEEZ at 550°F for 16 hours	5.08
6	Repeat Test Number 3	4.13

(Note: The sensor was a Rosemount 104 and matching thermowell)

(13/16 inch long) and then the tubes were packed with PBX. The assemblies were then cured according to the manufacturer's instructions. These sensors were subjected to thermal shock tests, extended exposure at high temperature, and mechanical shock tests. The time constant was measured before and after these tests. The results appear in Table 2.4. These tests show changes (increases and decreases) in time constant, indicating a change in PBX properties or a change in its bonding to the thermocouple or the tube. If similar effects occur in a reactor sensor, then a change in time constant would occur. Furthermore, if the main effect is PBX embrittlement, then mechanical vibrations in a power plant would likely affect the PBX and its heat transfer properties.

- Changes in conditions at the sensor-fluid interface. If any material (such as corrosion products or crud) adheres to the surface, then this would increase the heat transfer resistance and increase the time constant.
- Changes in contact pressure or contact area. In a well-type sensor with no thermal bonding material, the contact pressure between the sensor sheath surface and the inside wall of the well can affect the response time. Higher contact pressure will give a faster response. If a gradual relaxation of a spring caused a gradual decrease in contact pressure, then an increase in time constant would occur. Also, some sensors use bushings with points or groves to establish contact between the sensor and the inside wall of the well. If vibration caused relative motion between the sensor and the well, then wear would cause decreased contact and a slower response time.

This short list of possibilities does not prove that these changes will occur, but sensor response time changes do occur and the postulated mechanisms are plausible. Consequently, they must be taken seriously.

927 075

TABLE 2.4

ENVIRONMENTAL EFFECTS ON PBX CEMENT

Test	Number of Samples	Effect
Thermal shock (450°-550°F then quench in room temperature water)	4	small (<5%) increase in time constant
Exposure to high temperature (450°F-550°F) for at least 4 hours	4	decrease (up to 35%) in time constant
Mechanical shock (36 in. drop onto a hard surface)	4	increase (up to 21%) in time constant

2.4 Effect of Heating Current on RTDs

The response time testing procedures presented in subsequent sections involve heating the sensor filament by Joule heating. Consequently, it is pertinent to consider the possibility of sensor degradation as a result of passing a heating current through the filament.

The sensors used in power plants routinely experience a current of a few milliamperes as a result of the requirements for resistance measurement with a Wheatstone bridge. RTD manufacturers normally specify maximum currents to be used so as to avoid temperature measurement errors due to self heating. A typical maximum recommended value is ten milliamperes. This would give a measurement error of about 0.1°C for a typical PWR sensor.

Some manufacturers also specify maximum safe heating currents to avoid sensor damage. These include large safety factors because there is no need for high currents in the normal temperature measurement applications.

Now that sensor testing by internal heating is an important consideration, several sensor manufacturers have re-examined the question of maximum allowable currents. They agreed to provide their conclusions for use in this report (See Appendix A). The consensus is that currents needed for sensor testing (up to 80 milliamperes) are acceptable.

Additional evidence that Joule heating needed for sensor testing does not harm the sensor has been obtained at Oak Ridge National Laboratory. These results are also documented in Appendix A.

Further experience has been obtained in the EPRI-funded research program at the University of Tennessee. Sensors have been subjected to thousands of Joule heating tests with currents of up to 100 milliamperes with no resultant observable change in sensor characteristics.

It is concluded that heating currents of up to 80 ma range needed for effective testing will cause no deleterious effects on the sensors.

3. Time Response Characterization of Sensors (See Appendix B for details.)

3.1 General

There is considerable confusion about the terms used to characterize the response time of sensors. An attempt will be made here to clarify the situation. There are three basic ways to specify sensor dynamics:

A. Response to a Reference Input. In this case, a reference input (such as a step or a ramp) is imposed and the resulting output curve is recorded. This is unambiguous, but the whole response curves must be specified rather than a single concise numerical index.

B. Mathematical Relation. In this case, a mathematical relation such as a transfer function, a differential equation or a response equation may be used. These may be obtained experimentally. As such, they may be viewed as condensed representations of the same information contained in the response curves. Furthermore, once the mathematical relation is known, it can be used to determine the response to any input.

It is well known[6] that the following mathematical relations are valid for giving the response of temperature sensors to temperature changes:

- Transfer function

$$\frac{O(s)}{T(s)} = \frac{1}{(\tau_1 s+1)(\tau_2 s+1)\ldots} \qquad (3.1)$$

where

O(s) = output

T(s) = temperature

This transfer function has an infinite number of poles (denominator terms), but the higher ones have decreasing importance. The transfer function shown has no numerator terms (zeroes) because experience has shown that they do not occur in typical RTDs used in current PWRs.[6]

It is important to note that a measurement of the transfer function is the preferred way to identify sensor dynamics. Once the transfer function is identified experimentally, all essential information is available. The response to any input (such as a temperature transient expected in a postulated accident) can be determined easily and reliably.

- Response to a step change in fluid temperature.

$$O(t) = a_o + a_1 e^{-t/\tau_1} + a_2 e^{-t/\tau_2} + \ldots \qquad (3.2)$$

Again, an infinite number of terms is required in theory, but the higher terms have a small influence.

- Response to a ramp change in fluid temperature.

$$O(t) = K\,[t - (\tau_1 + \tau_2 + \ldots)] + b_1 e^{-t/\tau_1} + b_2 e^{-t/\tau_2} + \ldots \qquad (3.3)$$

where

K = ramp rate

C. Time Constant and Ramp Delay Time. The concept of a time constant (also sometimes called a response time) was introduced to permit characterization of system dynamics with a single numerical index. The standard definition of the time constant is the time required for the response to cover 63.2 percent of its span following a step input (other definitions based on other percentages are also used sometimes). Figure 3.1 illustrates the concept of a time constant.

Another index is the ramp delay time. It is the time displacement between input and response after the curves become parallel during a ramp input (See Figure 3.2).

Both the time constant and the ramp delay time are very useful, but they are unambiguous only for certain cases. That is, it is possible

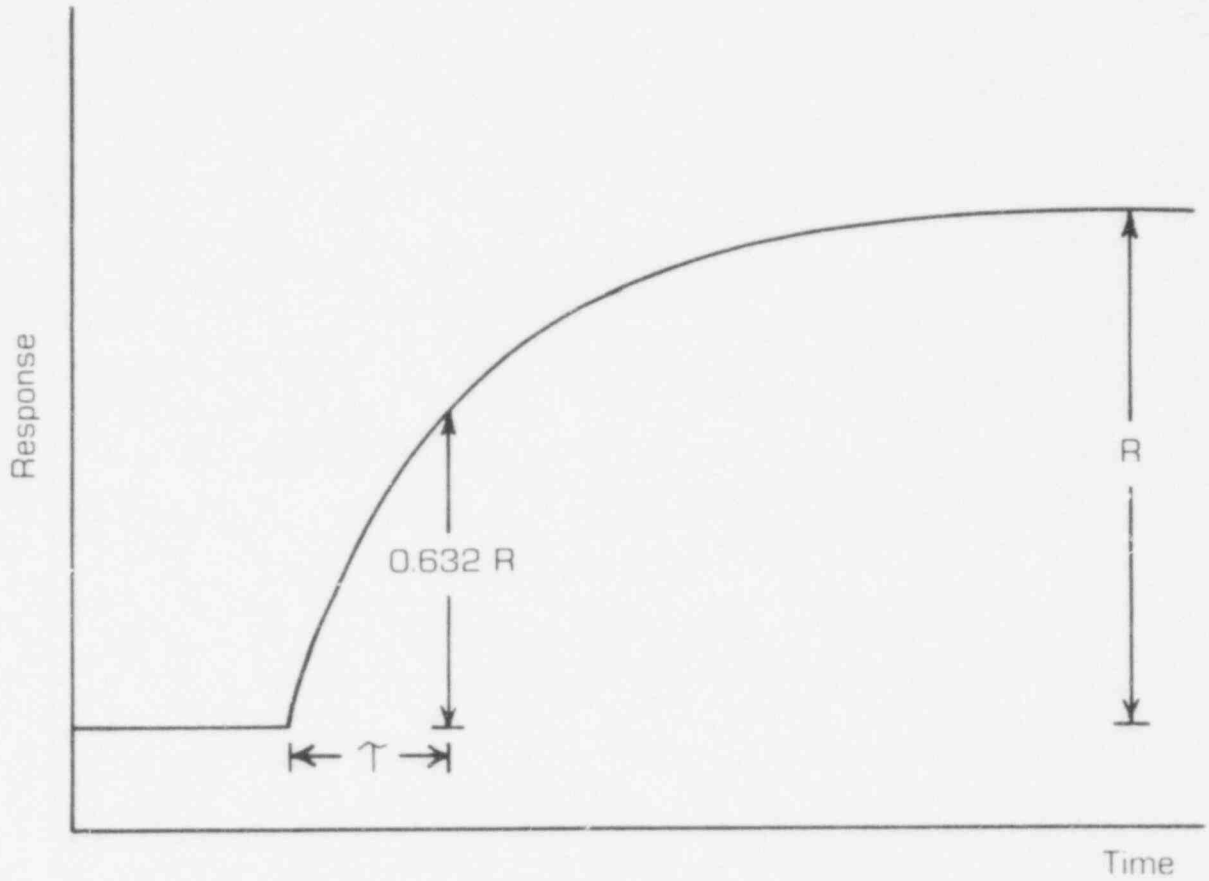

FIGURE 3.1. THE CONCEPT OF A TIME CONSTANT

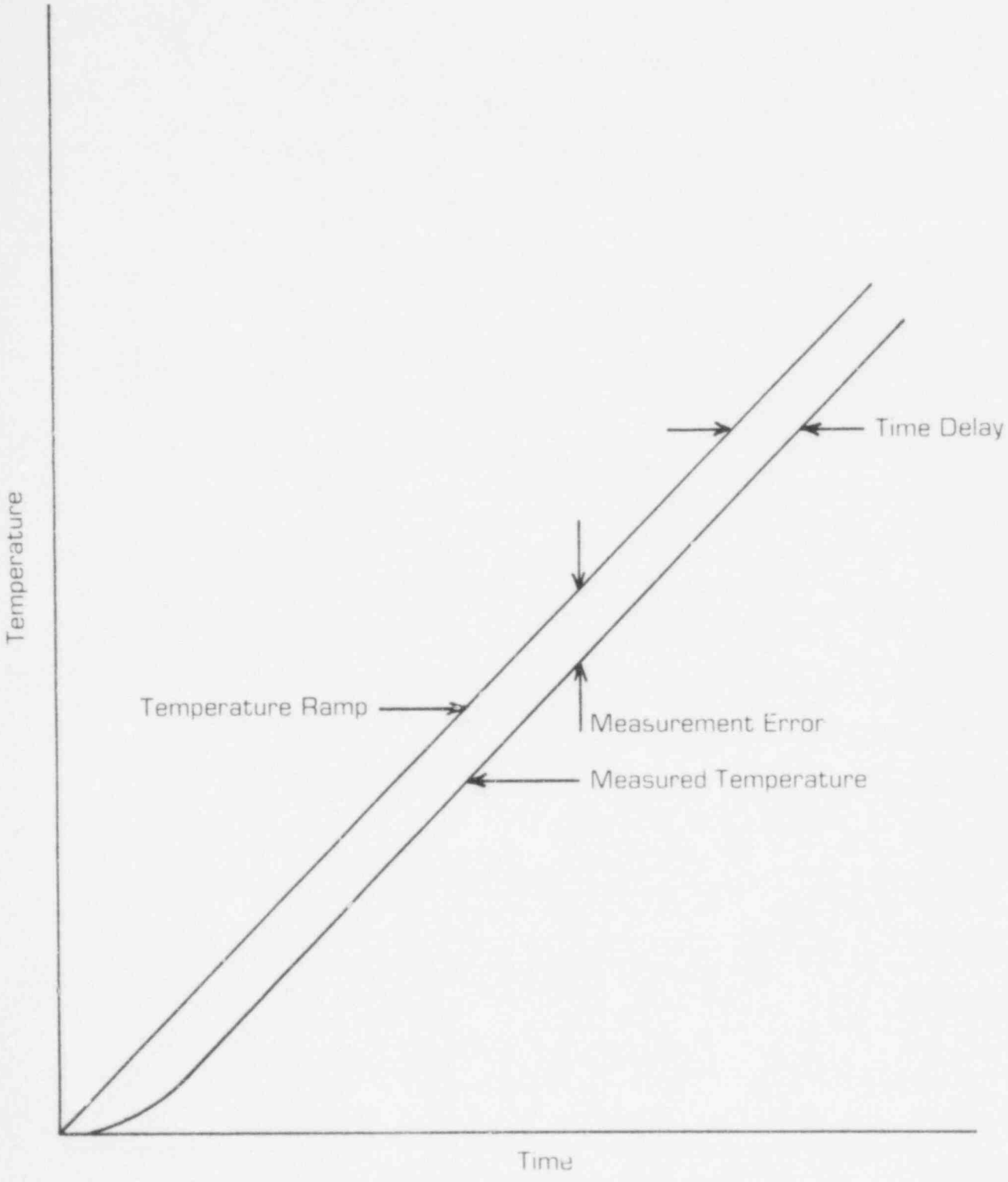

FIGURE 3.2. ILLUSTRATION OF A RAMP RESPONSE AND THE RAMP TIME DELAY.

to have two systems with different dynamic characteristics, but identical time constants (See Figure 3.3).

The time constant is a unique index in the special case of a first order system (only the term involving τ_1 is significant in Equation 3.1, Equation 3.2 or Equation 3.3). In that case, there is only one response for a system characterized by a certain time constant. Furthermore, the time constant and the ramp delay time are numerically identical. (See Appendix B.)

For a higher order system (terms involving τ_2, τ_3, etc. are significant as well as the term involving τ_1 in Equations 3.1, 3.2, and 3.3) it is still possible to use the concept of a time constant or a ramp delay time, but it is not unambiguous as in the case of a first order system. That is, two systems can reach 63.2 percent of their final value at the same time, but have different dynamic characteristics (See Figure 3.3). Figure 3.3 also illustrates a common feature of real sensors that is not observed with a first order system. That is the S shaped curve (derivative equal to zero at the initial time).

The time constant and ramp delay time are useful to characterize even sensors with higher order dynamics in spite of the ambiguity. Formulas have been derived[6] to relate the overall time constant to the τ_i in Equations 3.1, 3.2 and 3.3. These τ_i are usually called modal time constants. The modal time constants are related to the overall time constant, τ, and the ramp delay time, D, as follows:

$$\tau = \tau_1[1 - \ln (1-\tau_2/\tau_1) - \ln (1-\tau_3/\tau_1) - \ldots] \qquad (3.4)$$

$$D = \tau_1 + \tau_2 + \tau_3 + \ldots \qquad (3.5)$$

While τ and D are numerically equal for first order systems, they are

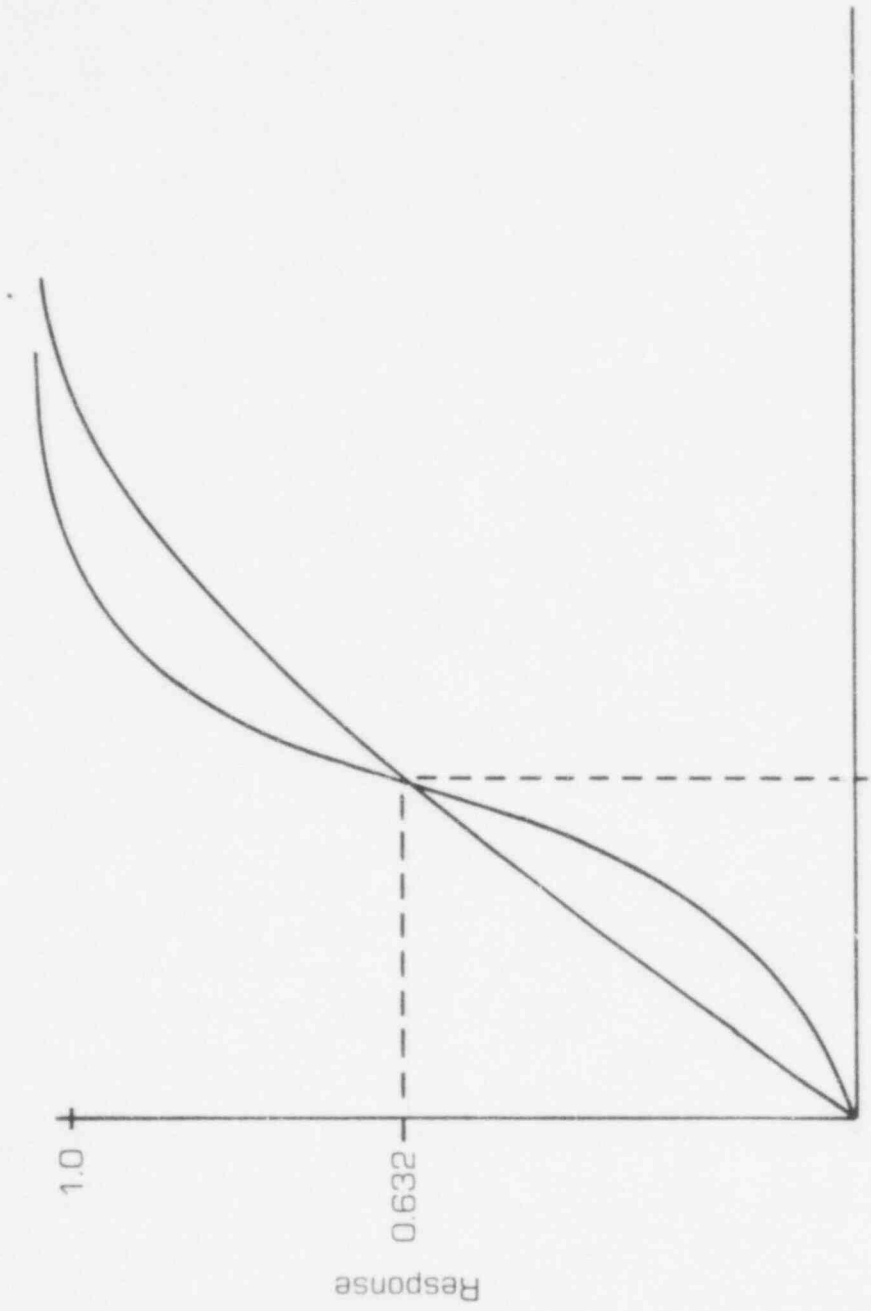

FIGURE 23. TWO RESPONSES WITH IDENTICAL TIME CONSTANTS

slightly different for higher order systems. However, the difference is small. Figure 3.4 shows the percent difference between τ and D for a second order system. For all practical purposes, they may be considered equal.

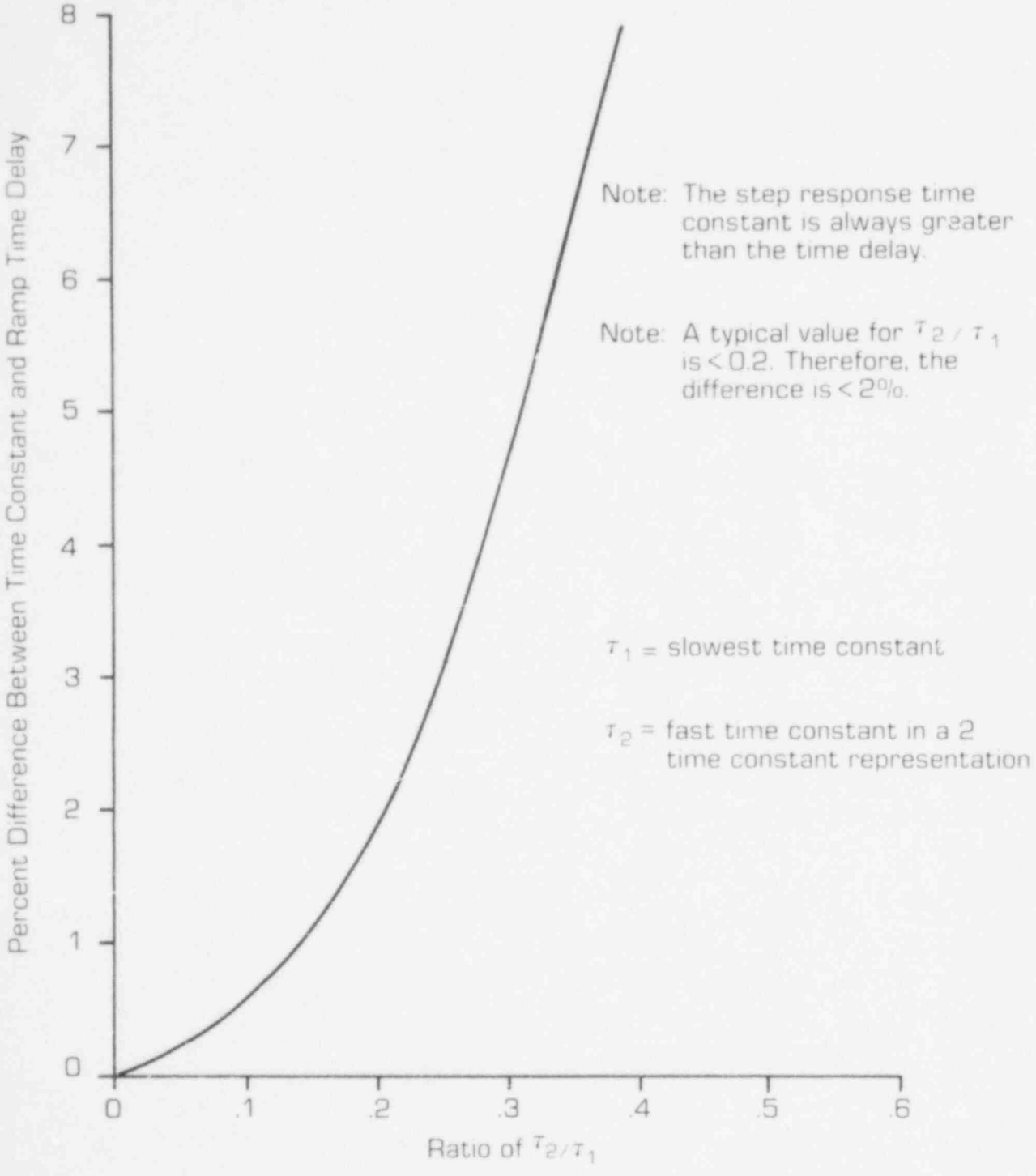

FIGURE 3.4: RELATION BETWEEN PLUNGE TIME CONSTANT AND RAMP TIME DELAY

4. Sensor Heat Transfer

4.1 Introduction

Theoretical heat transfer analysis has a very important role in developing LCSR data analysis procedures and in determining limitations on accuracy. However, the theory is suitable only for determining how to use data from experiments. Any analysis or correction based entirely on theory is unsuitable because of the impossibility of specifying adequately the geometrical, dimensional and physical property information that would be required. Consequently, this section is devoted to heat transfer theory as a tool for using the information in a LCSR transient.

The approach will be to study a range of sensor configurations in search of correlations (which are independent of geometry, dimensions, or physical properties) that are useful in LCSR data analysis. Exact solutions for homogeneous solid cylinders and for homogenous annular cylindrical geometries will be used. Also, finite difference methods will be used for non-homogenous assemblies. The results will reveal the sensor characteristics and environmental conditions that control response time and will provide information needed to improve the accuracy of test results (from approximately twenty-five percent maximum without the improvement to approximately ten percent maximum with the improvement).

4.2 Homogeneous Systems

Sensors are not really homogeneous assemblies. They consist of layers of materials with varying heat transfer properties. Nevertheless, homogeneous models provide a useful starting point in analyzing sensor heat transfer.

Many standard references give the equations, boundary conditions and solutions for unsteady state heat transfer in homogeneous cylinders

(solid or hollow). The heat conduction equation is:

$$\frac{\partial T(r,t)}{\partial t} = \alpha \left[\frac{\partial^2 T(r,t)}{\partial r^2} + \frac{1}{r}\frac{\partial T(r,t)}{\partial r}\right] + \frac{\dot{Q}(r,t)}{\rho c} \qquad (4.1)$$

where

T = temperature

r = radius

t = time

α = thermal diffusivity = $k/\rho c$

k = thermal conductivity

ρ = density

c = specific heat capacity

$\dot{Q}$ = heat generation rate.

The solution is specialized to selected geometries and surface conditions by selection of suitable boundary conditions.

4.2.1 Solid Cylinders

The proper boundary conditions for a solid cylinder are:

$$T(0,t) \neq \infty \qquad (4.2)$$

$$k\frac{\partial T}{\partial r}(R,t) = h\,(T(R,t) - \theta(t)) \qquad (4.3)$$

where

R = outer radius

h = film heat transfer coefficient

A = heat transfer area

θ = bulk fluid temperature

The second boundary condition is called Newton's law of cooling. The solution of Equation 4.1 for a step change in θ with these boundary conditions is:

$$\frac{T(r,t) - T(r,\infty)}{T(r,0) - T(r,\infty)} = \sum_{n=1}^{\infty} K_n e^{-(\lambda_n^2 \alpha)t} \qquad (4.4)$$

where

$$K_n = \frac{2}{M_n} \frac{J_1(M_n)J_o(M_n r/R)}{[J_o^2(M_n) + J_1^2(M_n)]} \tag{4.5}$$

$$M_n = \lambda_n R$$

$$\frac{\lambda_n R}{\frac{hR}{k}} = \frac{J_o(\lambda_n R)}{J_1(\lambda_n R)} \tag{4.6}$$

J_o, J_1 = Bessel functions

There are several key points to note:

a. The response is an infinite sum of exponentials

b. The exponential coefficients depend on the solution of a transcendental equation (Equation (4.6)). The λ_n that cause validity of Equation (4.6) are called eigenvalues. The model time constants, τ_i, are inversely proportional to λ_i^2.

c. The quantity, $\frac{hR}{k}$, appears in Equation 4.6. This very important parameter is called the Biot Modulus, N_{Bi}. It represents the ratio of internal heat transfer resistance to surface heat transfer resistance. It will prove to be a very important item in developing LCSR theory and in understanding sensor behavior.

The eigenvalues (values of λ_n that cause the equality in Equation (4.6) to be valid) may be found by a graphical procedure. The procedure requires specification of the following information about the sensor:

- outer radius
- Biot modulus

A plot with separate curves for the left hand side ($\frac{R}{N_{Bi}} \lambda$ vs. λ) and for the right hand side ($\frac{J_o(\lambda R)}{J_1(\lambda R)}$ vs. τ) will have intersections at values of λ that satisfy Equation 4.6. A plot of this type is shown in Figure 4.1. From

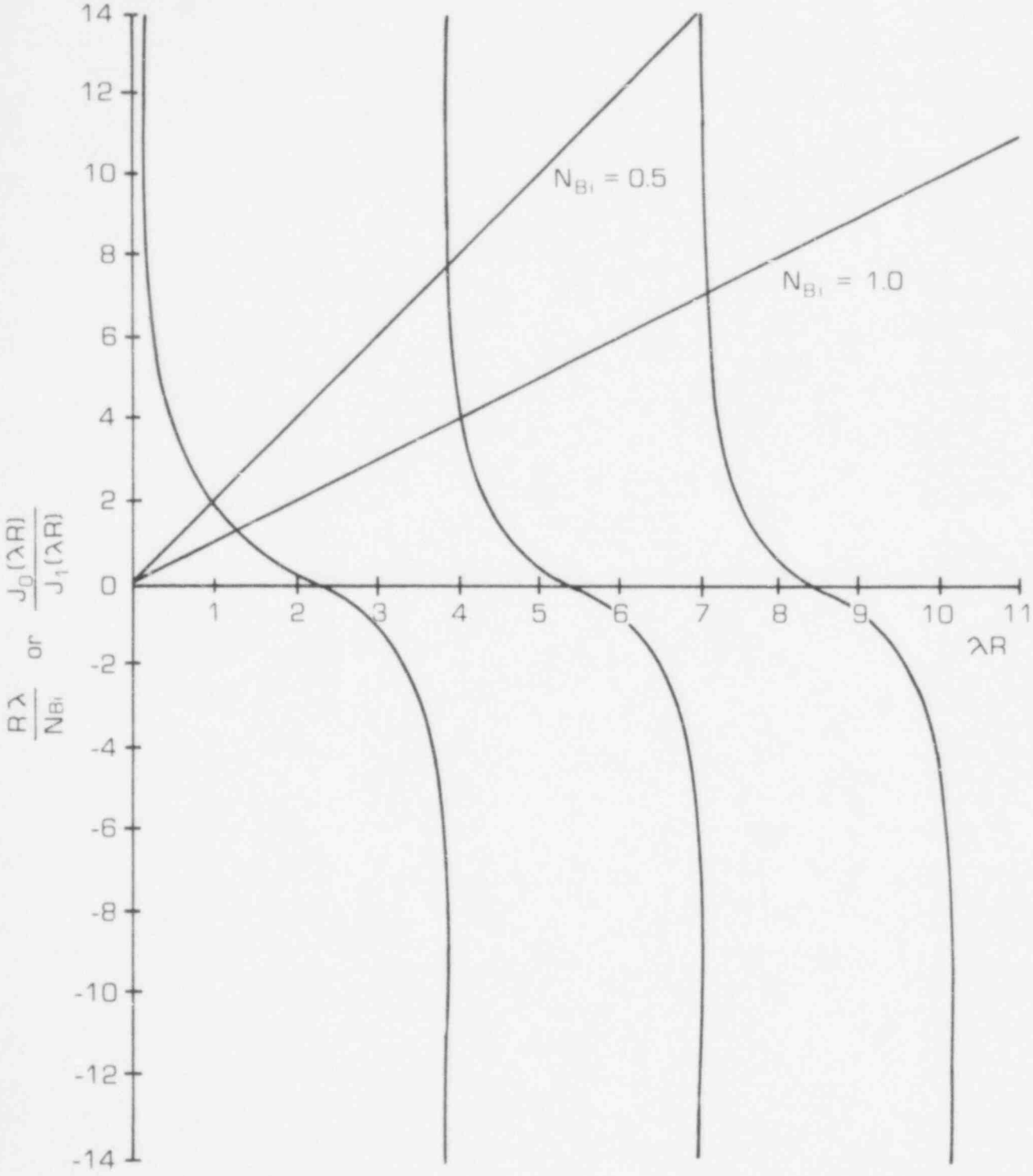

FIGURE 4.1. GRAPHICAL SOLUTION OF EQUATION 4.6

this curve, several properties relative to the eignvalue spacing (which will be useful in subsequent development of LCSR transformation theory) can be determined:

- The smallest λ_i (largest τ_i) is much more sensitive to the Biot modulus than the other λ_i.
- The value of $J_o(\lambda R)/J_1(\lambda R)$ goes to infinity at values of λR equal to $(n + 1/4)\pi$ for large, integer values of n. The intersections occur near these values for large n. Since the exponential terms in the response equation involve λ_i^2, we observe that the modal time constants, τ_i, are inversely related to λ_i^2. Therefore

$$\tau_i = \frac{R_2}{\alpha\pi^2(i + 1/4)^2}$$

- The value of $J_o(\lambda R)/J_1(\lambda R)$ goes to zero at values of $(n - 1/4)\pi$ for large integer values of n.
- Since the straight line (with slope $1/N_{Bi}$) intersects the $J_o(\lambda R)/J_1(\lambda R)$ curve at progressively larger values of the abscissa, the intersections occur nearer the vertical asymptotes at the larger values of λR. This means that the larger values of λ_i are given by

$$\lambda_i = \frac{(i + 1/4)\pi}{R}$$

The ratio of the higher eigenvalues is given by:

$$\frac{\tau_i}{\tau_{i+1}} = \frac{(i + 1.25)^2}{(i + 0.25)^2}$$

This is independent of the Biot modulus.

The response to a step change in heat generation rate is also possible. The results are:

$$T(r,t) - T(r,0) = \sum_{n=1}^{\infty} L_n e^{-\lambda_n^2 \alpha t/R^2} \qquad (4.7)$$

where

$$L_n = \frac{\dot{Q}_o - \dot{Q}_\infty}{\pi k} \frac{J_o(\lambda_n r) J_o(\lambda_n R)}{(\lambda_n R^2)[J_1^2(\lambda_n R) + J_o^2(\lambda_n R)]}$$

$\dot{Q}_o$ = initial heat generation rate

$\dot{Q}_\infty$ = final heat generation rate

The eignvalues (λ_n) are the same as for the previous case. Consequently, the exponential terms are the same for both cases, but the factors that multiply the exponentials are different.

The modal time constant ratios for different values of Biot Modulus are shown in Table 4.1. It is clear that for a solid cylinder, the eigenvalue ratios increase when the Biot modulus decreases (internal heat transfer resistance decreases relative to surface heat transfer resistance). This shows that higher modes are more important when the Biot modulus is large (internal heat transfer resistance dominates over surface heat transfer resistance).

4.2.2 Hollow Cylinders

The heat conduction equation (Equation 4.1) applies for hollow cylinders as well as solid cylinders. Also, the Newton's law of cooling boundary condition at the surface (Equation 4.3) is still applicable. The other boundary condition must be changed. A suitable choice is to assume that there is no heat transfer at the inner radius. This means that the surface is insulated or that the material across the inner boundary has no heat capacity. In this case, the boundary condition becomes:

$$\frac{\partial T(R_1, t)}{\partial t} = 0. \qquad (4.9)$$

As for the solid cylinders, the response to a fluid temperature step or an internal heat generation step is a sum of exponentials. As

TABLE 4.1

EFFECT OF THE BIOT MODULUS ON THE MODAL TIME CONSTANTS

Biot Modulus	τ_2/τ_1
.4	21.69
1	10.49
2	7.18
5	5.64
10	5.34
20	5.28

before, the exponentials are the same for both types of coefficients, but the factors that multiply the exponentials differ. The solutions are given in reference (12).

4.3 Multi-Layer Modal Models

Transient heat transfer models may also be constructed using a finite difference approach. Dynamic energy balances may be written over each section. This method gives results that approach the exact solution as the number of sections increases. For a one-dimensional case, the equation for the temperature of the $i^{\underline{th}}$ node is:

$$(MC)_i \frac{dT_i}{dt} = \frac{1}{R_{i,i-1}} (T_{i-i} - T_i) - \frac{1}{R_{i,i+1}} (T_i - T_{i+1}) + \dot{Q}_i$$

where

T_i = average temperature in the $i^{\underline{th}}$ section

$R_{i,i-1}$ = heat transfer resistance between section i and section 1-1

M_i = mass in section i

C_i = specific heat capacity of material in section i

$\dot{Q}_i$ = heat generation rate in section i

The advantage of a model of this type is that it is easy to simulate non-homogeneous systems. The variations in heat transfer characteristics in different regions shows up in the model in values for the resistances which differ in different equations in the set.

The overall model for the sensor consists of a set of coupled, linear differential equations. The solution for the temperature response in the $i^{\underline{th}}$ section is:

$$T_i(t) = a_{0i} + a_{1i} e^{\lambda_1 t} + a_{2i} e^{\lambda_2 t} + \ldots$$

If the model involves n equations, there will be n exponential terms in

the response equation. Note that the response equation for each section contains the same exponentials, but the coefficients that apply for different sections are different. Also, note that the solution is a sum of exponentials, just like for the analytical approach in the previous section.

The equations may be solved to give the time responses of interest or they may be solved to give the λ_i. The approach used[12] was to solve the finite difference equations for homogeneous systems as a first step. Comparisons with analytical results confirmed that the coefficients were being calculated correctly and that a sufficient number of sections was being used. Subsequently, the coefficients were re-formulated to approximate the multi-layer structure of typical commercial sensors and simulations were performed.

4.4 Results of Simulation Studies

A large number of simulations was performed to find general correlations of potential use in interpreting sensor response tests. One question that was considered is, "Is it possible to find a correlation that permits estimation of higher mode effects when only the first few dominant modal time constants are known?" Particularly, can one use a knowledge of τ_1 and τ_2 to estimate the influence of τ_3, τ_4, etc. on the sensor response?

The approach is to define an approximate time constant $\tau(N)$ based on N modes. For example:

$$\tau(1) = \tau_1$$

$$\tau(2) = \tau_1(1 - \ln(1 - \tau_2/\tau_1))$$

$$\tau(3) = \tau_1(1 - \ln(1 - \tau_2/\tau_1) - \ln(1 - \tau_3/\tau_1))$$

Note the $\tau(\infty)$ is the true time constant (infinite number of modes).

It was found that $\tau(\infty)/\tau(2)$ correlates uniquely with τ_2/τ_1 regardless of sensor geometry, size or materials. The basis for this may be

reasoned as follows:

- The ratio of τ_2/τ_1 correlates uniquely with the Biot modulus
- The Biot modulus completely defines the required sensor heat transfer information
- The availability of the required sensor heat transfer information allows assessment of higher mode contributions.

The correlation appears in Figure 4.2. It shows results for homogeneous solid cylinders, homogeneous annular cylinders, and inhomogeneous (multi-layer) assemblies. Clearly, they all follow the same correlation.

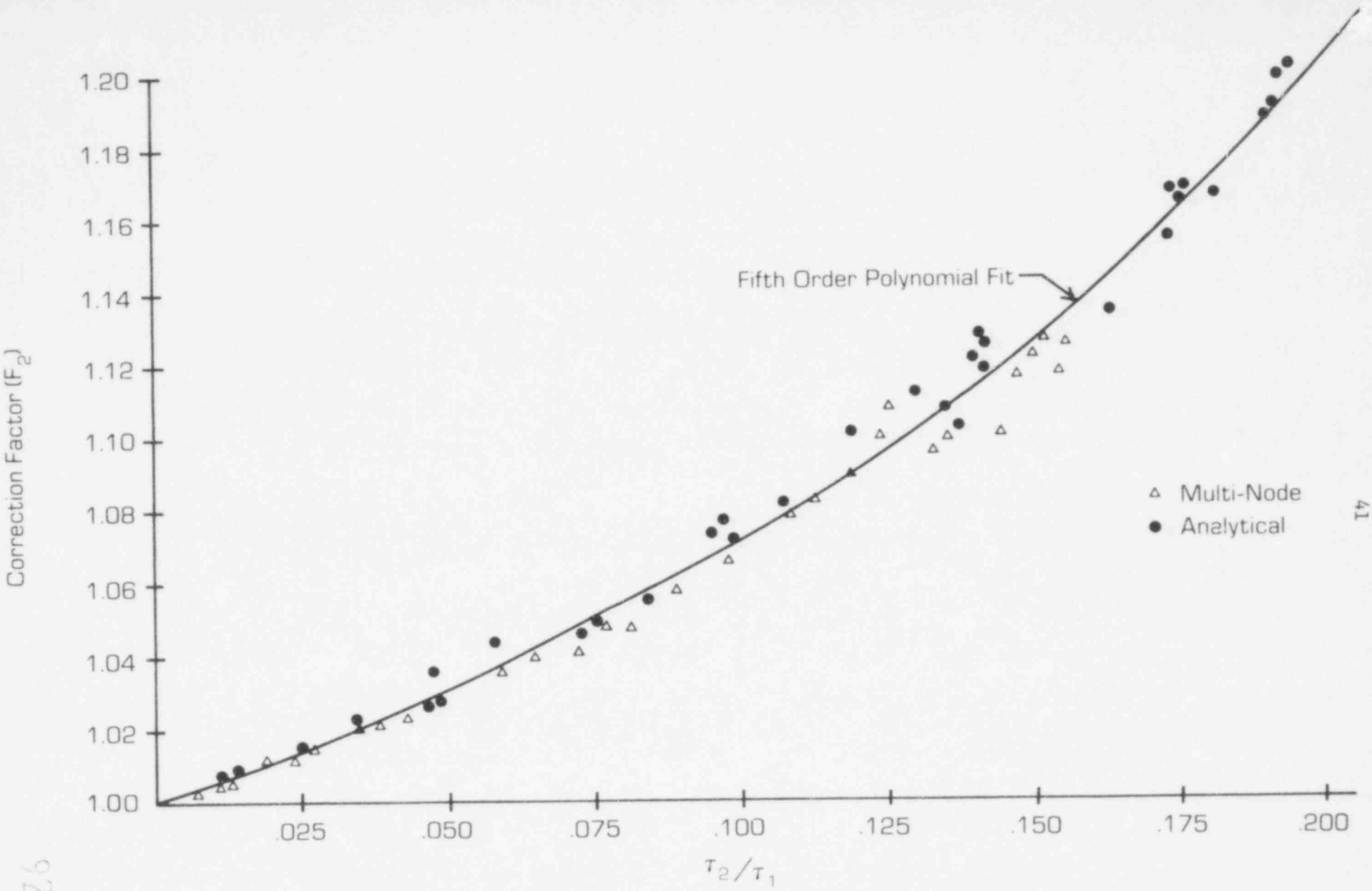

FIGURE 4.2. CORRECTION FACTOR FOR CYLINDRICAL SENSOR ASSEMBLIES.

5. Loop Current Step Response Theory

5.1 Derivation of the Loop Current Step Response Transformation

The loop current step response transformation provides a means to determine the response to a fluid temperature change from information extracted from a loop current step response transient. The transformation provides the sensor transfer function. Consequently, it enables one to determine the response of the sensor output to any fluid temperature disturbance. In addition the time constant or the ramp delay time may be determined.

The mathematical details of the development of the transformation are given in Appendix C. The key points to understand about the basis for the transformation are:

- No physical property information or dimensions are required to implement the transformation. All information needed in the transformation is contained in the loop current step response transient data.
- The validity of the mathematical model used in the analysis is assured. The deriviation depends only on the form of the model. The form assumed is based on a model developed by performing dynamic energy balances on a series of adjacent slices to represent the sensor. The LCSR transformation theory does not require a specification of the number of sections or the coefficients. The model used in the theory can then be said to be free of any restrictions that limit the validity of the transformation.

Two assumptions are made about sensor geometry.

A. The heat transfer is one dimensional

B. There is insignificant heat capacity between the sensing element and the center line of the sensor.

The implications of these assumptions are important in assessing

the validity of sensor response time evaluation by loop current step response testing. The effects of imperfectly satisfying the assumptions have been evaluated theoretically and experimentally. These topics are discussed in Chapters 9 and 10 of this report.

Analysis based on the model and the two required assumptions gives the following results (See Appendix C for details):

- LCSR transient

$$x(t) = a_o + a_1 e^{-t/\tau_1} + a_2 e^{-t/\tau_2} + \ldots \tag{5.1}$$

- Sensor transfer function

$$\frac{\delta O(s)}{\delta \theta(s)} = \frac{1}{(\tau_1 s + 1)(\tau_2 s + 1)\ldots} \tag{5.2}$$

where

δO = sensor output variation

$\delta \theta$ = fluid temperature variation

- Sensor response to a step change in fluid temperature

$$\delta O(t) = b_o + b_1 e^{-t/\tau_1} + b_2 e^{-t/\tau_2} + 1 \ldots \tag{5.3}$$

where $b_i = f(\tau_i)$

The noteworthy aspect of these results is that the τ_i are necessary and sufficient to specify the sensor transfer function. Furthermore, the same τ_i determine the LCSR transient and the response to a fluid temperature perturbation. Consequently, identification of the τ_i from the LCSR transient provides all of the information needed to determine the sensor's response to fluid temperature changes. The result for a step change in fluid temperature given above is one example.

The steps in a LCSR test and analysis program are:

A. Measure the time varying resistance following a step change in Joule heating of the sensor.

B. Identify the τ_i by analyzing the LCSR transient.

C. Use the τ_i to identify the sensor's response to fluid temperature changes. Identification may provide any of the following:

- transfer function (sensor output/fluid temperature changes)
- response vs. time for a fluid temperature step change
- response vs. time for a fluid temperature ramp change
- time constant (time required to reach 63.2 percent of the final output following a fluid temperature step)
- ramp time delay.

This list illustrates the completeness of the information from a LCSR test and analysis. The usual desired quantity is the time constant, but much more information is available if desired.

5.2 Correction Factors

It has been shown that the sensor response can be specified if all of the τ_i are identified. For example, the time constant can be evaluated from the τ_i using

$$\tau = \tau_1 [1 - \ln(1 - \tau_2/\tau_1) - \ln (1 - \tau_3/\tau_1) - \ldots] \qquad (5.4)$$

The contribution of the term involving τ_i gets smaller as i gets larger. Nevertheless, a good determination of τ may require a number of τ_i. In analysis of practical data sets, it is possible to identify only two, or possibly three, τ_i from a LCSR transient. If the additional, unmeasureable τ_i contribute a significant fraction to the total response, then the time constant based on two or three terms will be too small.

The results of the theoretical studies may be used to develop correction factors that account for the important modes (terms containing

the exponential factors) that cannot be identified from practical LCSR data. The relation between the modal time constants, τ_i, and the overall time constant, τ, was given in Equation 5.4.

This is rewritten as follows:

$$\tau = \tau_1 [1 + C_1 + C_2 + \ldots] \tag{5.5}$$

where

$$C_i = - \ln(1 - \tau_i/\tau_1) \tag{5.6}$$

The true time constant (based on an infinite number of terms) is

$$\tau = \tau_1 [1 + \sum_{i=2}^{\infty} C_i] \tag{5.7}$$

The approximate time constant (based on a finite number of terms, N) is

$$\tau(N) = \tau_1 [1 + \sum_{i=2}^{N} C_i] \tag{5.8}$$

A correction factor is defined as:

$$\text{Correction Factor} = F_N = \frac{\text{True time constant}}{\text{Time constant based on N terms}} = \frac{\tau(\infty)}{\tau(N)}$$

If two modal time constants (τ_1 and τ_2) can be identified experimentally, then the appropriate correction factor is F_2. The theoretical studies show that a measurement of τ_2/τ_1 provides all of the information required to give F_2. This very important correlation appears in Figure 4.2. Note that F_2 varies from 1.0 to 1.2. It should be noted that the correlation is based on simulations that include a wide range of geometries, dimensions and physical properties. The striking feature is that the correlation is independent of these properties. The procedure for determining the time constant is:

- perform a LCSR test
- identify τ_1 and τ_2 from the test data
- evaluate $\tau(2)$ based on τ_1 and τ_2

- determine F_2 from the measured τ_2/τ_1

- evaluate the true time constant $\tau = F_2\ \tau(2)$.

The validity of this approach is confirmed experimentally in Chapter 10.

Other correction factors besides F_2 are sometimes useful. Particularly, F_1 may be required in cases where experimental conditions make it impossible to identify τ_2. In this case, τ_1 is the only available modal time constant and it may be inadequate to evaluate the overall time constant. In this case, it is not possible to evaluate the higher mode contributions without knowing the Biot modulus. Since the Biot modulus is just as poorly known as the time constant that is being measured, it is not possible to specify a proper value to use in order to give F_1. However, we can use F_1 to set an upper limit on τ. The theoretical studies show that the maximum value for F_1 is 1.4. Since $\tau = F_1\tau_1$ the maximum possible τ is $1.4\tau_1$.

6. The Self Heating Test

The heat transfer resistance affects two measurable quantities following a change in internal heating: the rate of temperature change and the magnitude of the resulting steady state temperature change. The heat capacity affects only the rate of change. Consequently, a change in heat transfer resistance (and a concomittant change in time constant) may be detected by measuring the magnitude of the temperature change per unit of power dissipated in the filament. Since the temperature change in an RTD is proportional to its change in resistance, the measurement may also involve determination in the steady state change in resistance per unit of power (typically ohms/watt). This index, which is called the self-heating index, is easily measureable. Its suitability for detecting changes in response characteristics is demonstrated in Chapters 10 and 11.

7. Equipment

Several options are available for the test equipment needed in a loop current step response test. The instrument should permit switching from one constant power condition to another constant power condition while simultaneously providing a measurement of the time-varying resistance. Bridge-type instruments are well suited for this. The bridge may be run using a constant voltage source or a constant current source. Also, a simple voltage measurement on a resistance element being heated by a constant current may be used. These are considered below.

7.1 Constant Current Source With Voltage Measurement Across the Resistance

In this case, the equipment involves the simple circuit shown in Figure 7.1. The resistance changes because of Joule heating and this affects the voltage measurement. The voltage drop increases linearily as the resistance increases and the power also increases linearily as the resistance increases. Therefore, if the resistance changes significantly, the constant power assumption used in the development of LCSR theory is not valid. This can be overcome, but at the expense of a more complicated analysis procedure.

7.2 Bridge, Constant Voltage

The voltage drop, V, across the arms of a Wheatstone bridge with applied voltage E is (See Figure 7.2):

$$V = \frac{(R_{RTD} - R_d)R_1}{(R_1 + R_d)(R_1 + R_{RTD})} E. \qquad (7.1)$$

If the bridge is initially balanced, then

$$R_{RTD} = R_d + \delta R$$

and

$$V = \frac{R_1}{R_1 + R_d} \frac{\delta R}{(R_1 + R_d + \delta R)} E \qquad (7.3)$$

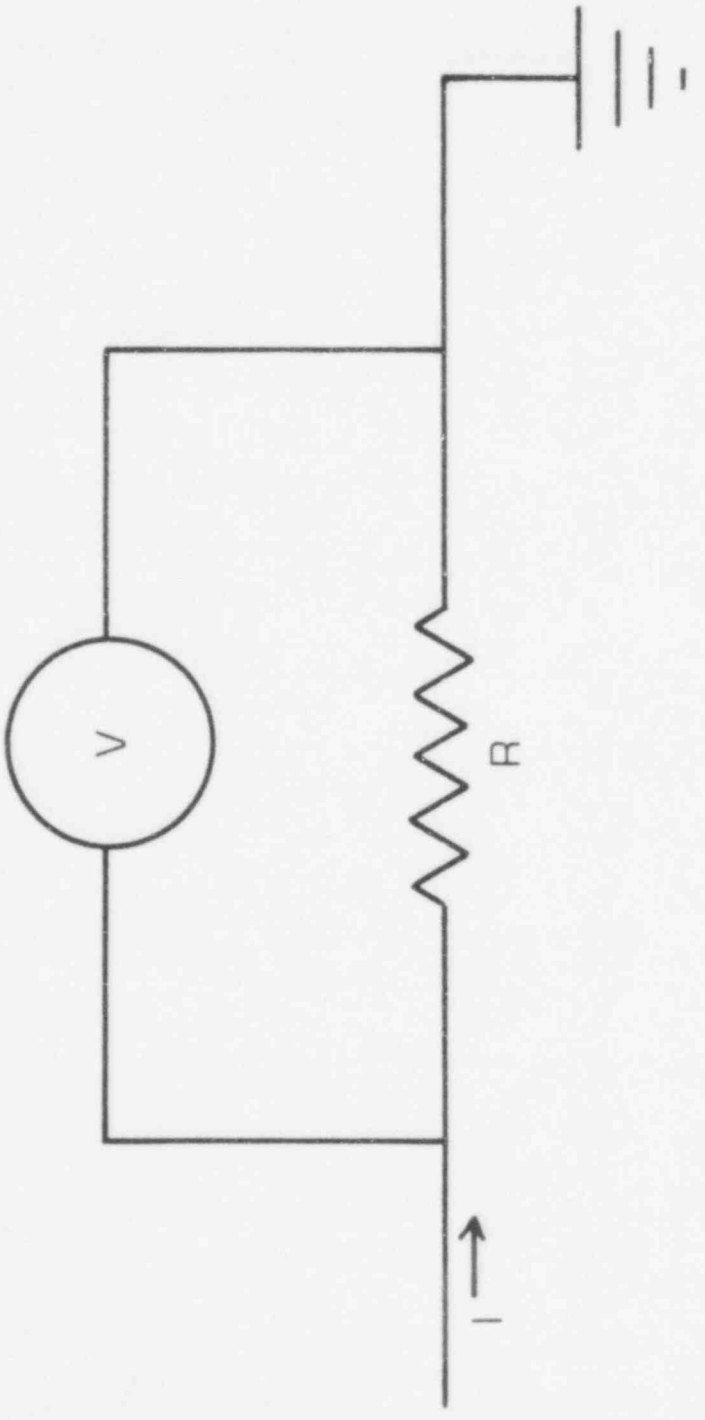

FIGURE 7.1. CIRCUIT FOR LCSR TESTING

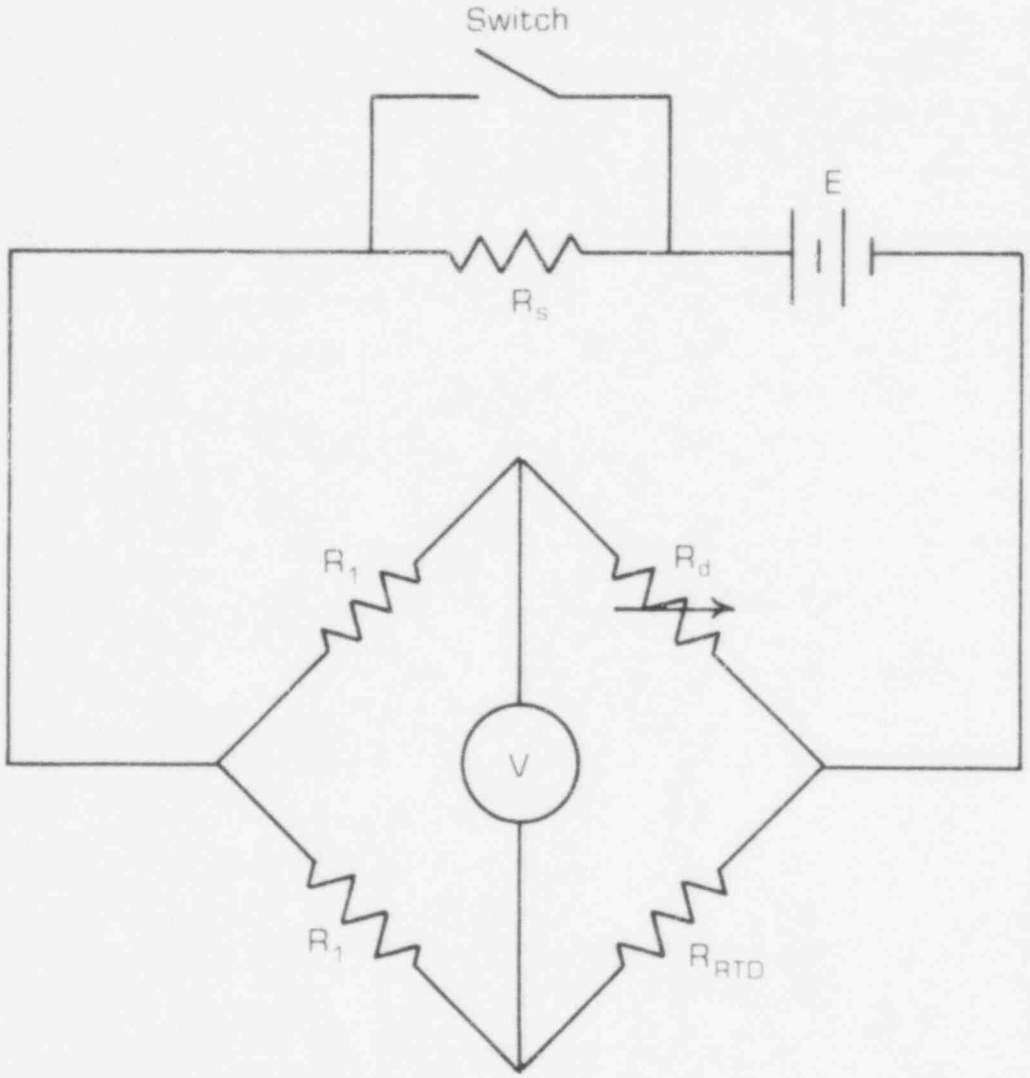

FIGURE 7.2. WHEATSTONE BRIDGE FOR LCSR TESTING

The power dissipated in the RTD is

$$P = \frac{E^2 (R_d + \delta R)}{(R_1 + R_d + \delta R)^2} \tag{7.4}$$

The relation between resistance change and measured voltage is

$$\delta R = \frac{(R_1 + R_d)}{\left(\frac{R_1 E}{R_1 + R_d} - V\right)} V \tag{7.5}$$

The relation between V and δR is nonlinear, but, if δR is small compared to $R_1 + R_d$, then assuming linearity is satisfactory. Typical values for δR are two to ten ohms and R_d is 200 to 500 ohms. R_1 may be chosen large enough to ensure adequate linearity, but 100 to 500 ohms is generally satisfactory.

For a bridge with constant voltage, the power changes when the resistance changes. For typical cases where δR is small compared to R_1 and R_d, the effect is small. If cases are encountered where δR is significant compared to R_1 and R_d, then the analysis procedure may be modified to account for the varying power

7.3 Bridge, Constant Current

In this case, the relation between voltage measured and resistance change is

$$V = \frac{R_1 I}{2R_1 + 2R_d + \delta R} \delta R \quad . \tag{7.6}$$

The power dissipated in the sensor is

$$P = \left[\frac{(R_1 + R_d)}{2(R_1 + R_d) + \delta R}\right]^2 I^2 (R_d + \delta R) \tag{7.7}$$

The linearity of V vs. δR and the effect of resistance change on power are similar to the previous results for a constant voltage bridge.

7.4 Conclusions Concerning Equipment

The equipment is simple and its operation is fully understood. Equipment design or data processing features may be specified so as to ensure adequacy of the data collected by the instrumentation.

8. Typical Test and Analysis Procedures

8.1 Performing a LCSR Test

The loop current step response is performed as follows:

a. connect a lead from each side of the resistance element to the test equipment. The additional leads used in multiple wire sensors are not needed since the absolute temperature is not measured.

b. set the bridge to the low voltage condition. The voltage is selected to give a sensor current of 1 to 4 ma so as to cause negligible Joule heating.

c. balance the bridge by adjusting the variable resistor so as to give a zero voltage drop, V, across the arms of the bridge.

d. Switch to the high voltage condition. The voltage is selected to give 25 to 75 ma through the sensor. For a 400 ohm sensor this gives 0.25 to 2.25 watts. This causes a resistance change of 2 to 20 ohms in typical PWR sensors. The temperature increase is 3 to 30°C. A typical transient is shown in Figure 8.1.

It is also possible to use the data obtained upon switching from high voltage to low voltage. However, the measured signal is smaller and the signal-to-noise ratio is lower. Consequently, the preferred test involves a transition from low voltage to high voltage.

Appendix D gives a detailed test procedure.

8.2 Analyzing LCSR Data

The data analysis procedure discussed in Section 5.1 requires the identification of exponential coefficients from step response data. This may be done graphically using well-known exponential peeling techniques or it may be done using a computer fit. The fit is usually based on a least squares principle that finds the coefficients in a sum of exponentials that give the best fit to the data.

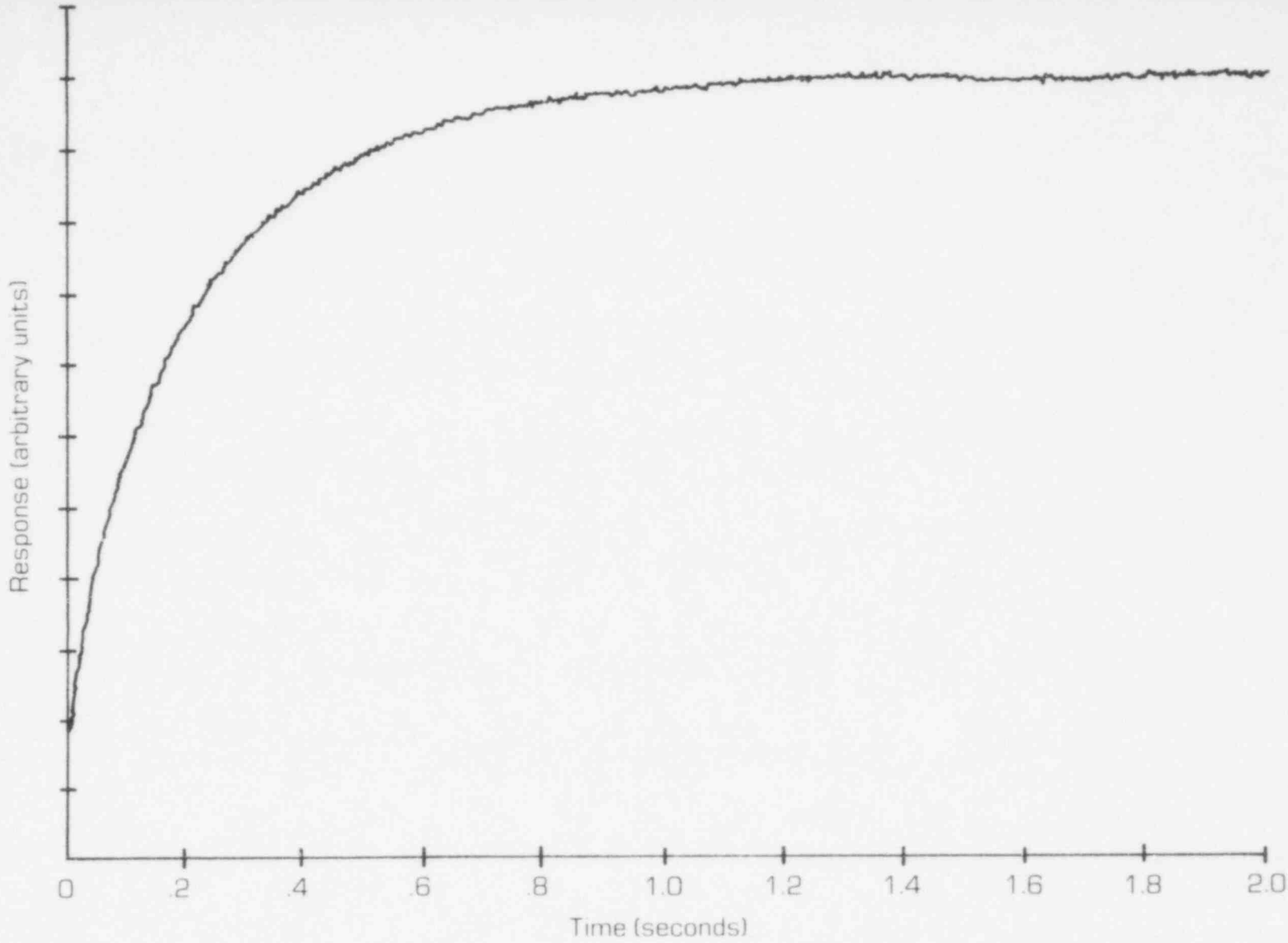

FIGURE 8.1. TYPICAL LABORATORY LOOP CURRENT STEP RESPONSE DATA

8.2.1 Graphical Analysis

The function has the form

$$X(t) = a_o + a_1 e^{-t/\tau_1} + a_2 e^{-t/\tau_2} + \ldots \quad (8.1)$$

Since $a_o = X(\infty)$, we may write

$$X(\infty)-X(t) = - a_1 e^{-t/\tau_1} - a_2 e^{-t/\tau_2} + \ldots \quad (8.2)$$

If $\tau_1 > \tau_2$, then higher terms (τ_i for $i > 1$) have a small influence relative to the τ_1 term as time increases. If one waits until the higher terms are negligible, then

$$X(\infty)-X(t) \cong - a_1 e^{-t/\tau_1} \quad . \quad (8.3)$$

In this portion of the data, a semi-logarithmic plot of $X(\infty)-X(t)$ is a straight line and $-\frac{1}{\tau_1}$ is the slope. The intercept of this line at $t = 0$ gives the value of a_1.

The identification of the second exponential involves using the identified a_1 and τ_1 to construct a modified data set:

$$y(t) = X(t)-X(\infty) - a_1 e^{-t/\tau_1} = a_2 e^{-t/\tau_2} + a_3 e^{-t/\tau_3} + \ldots \quad (8.4)$$

The same procedure may be applied to find τ_2 that was used to find τ_1.

In principle, this could go on until a large number of τ_i were identified. In practice, the small influence of the higher terms and the limited accuracy of actual test data restrict the graphical analysis to identification of one or two τ_i.

An example of a graphical analysis of laboratory data is shown in Figure 8.2

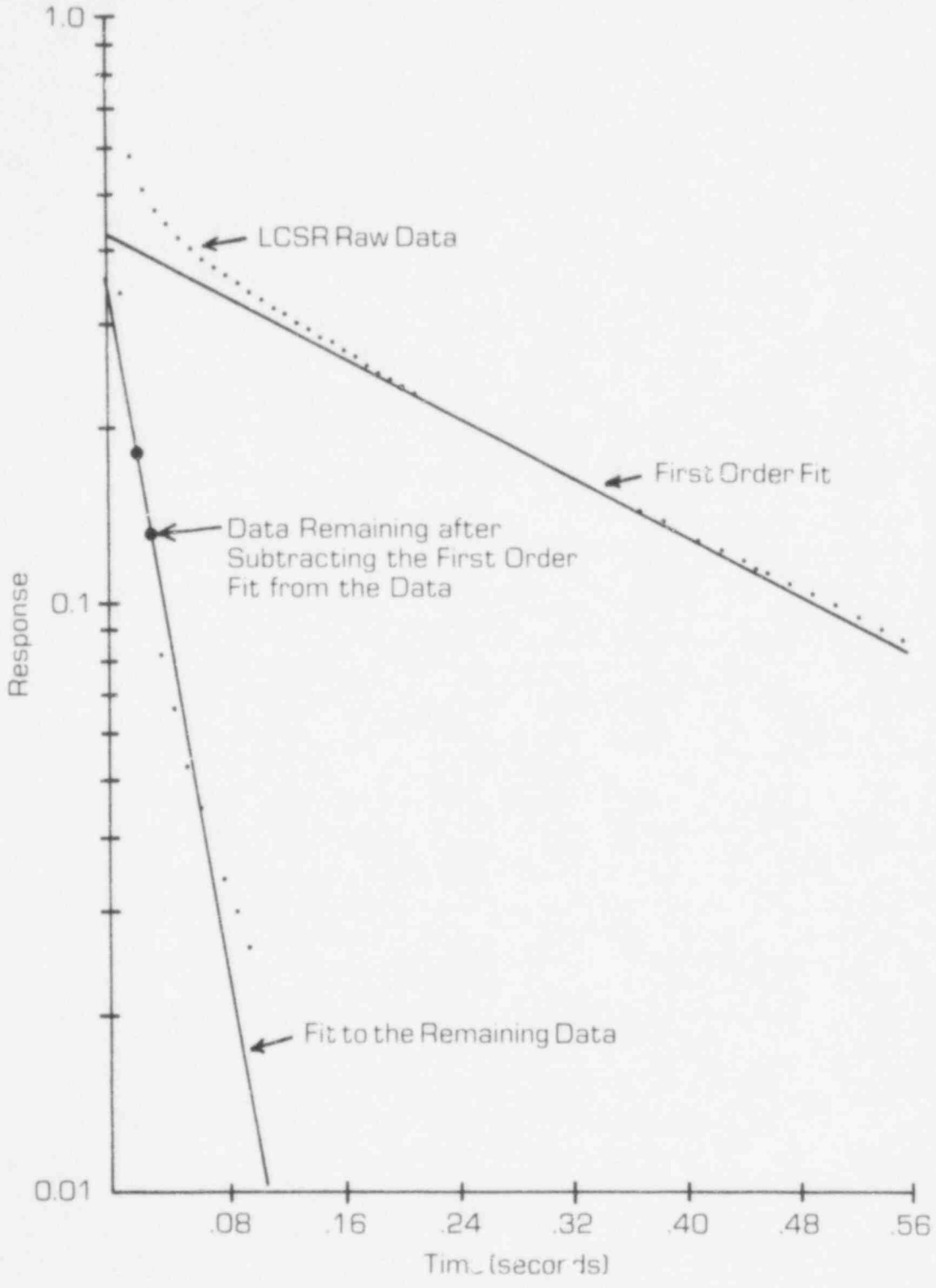

FIGURE 8.2. GRAPHICAL EXPONENTIAL STRIPPING

8.2.2 Computer Analysis

Numerous algorithms are available for identifying exponential coefficients from data records. Most involve minimization of the error between the data and the equation prediction of the response:

$$E = \sum_{i=1}^{N} \varepsilon_i^2 \tag{8.5}$$

$$\varepsilon_i = X(t_i) - a_o - a_1 e^{-t/\tau_1} - a_2 e^{-t_i/\tau_2} - \ldots \tag{8.6}$$

where

E = error

N = number of samples

The identification involves finding the parameters (a_i and τ_i) that minimize E. Experience has shown that two τ_i can usually be identified using computer fitting methods.

Results of a computer fit are shown in Figure 8.3. The figure shows the raw LCSR data, the fitted curve and the predicted response to a step change in fluid temperature as determined from the identified transfer function. It is seen that the fit is indistinguishable from the raw data. This is typical of LCSR analysis results.

8.3 The Self-Heating Test

In a self heating test, the sensor is connected to the test equipment as for the LCSR test. The steps are as follows:

a. Set the applied voltage to obtain a low current (typically 5 to 10 ma) through the sensor.

b. Measure the sensor resistance. In a bridge-type instrument, this means adjusting the variable resistor to achieve a voltage drop of zero across the arms of the bridge.

c. Measure the power (I^2R) dissipated in the sensor.

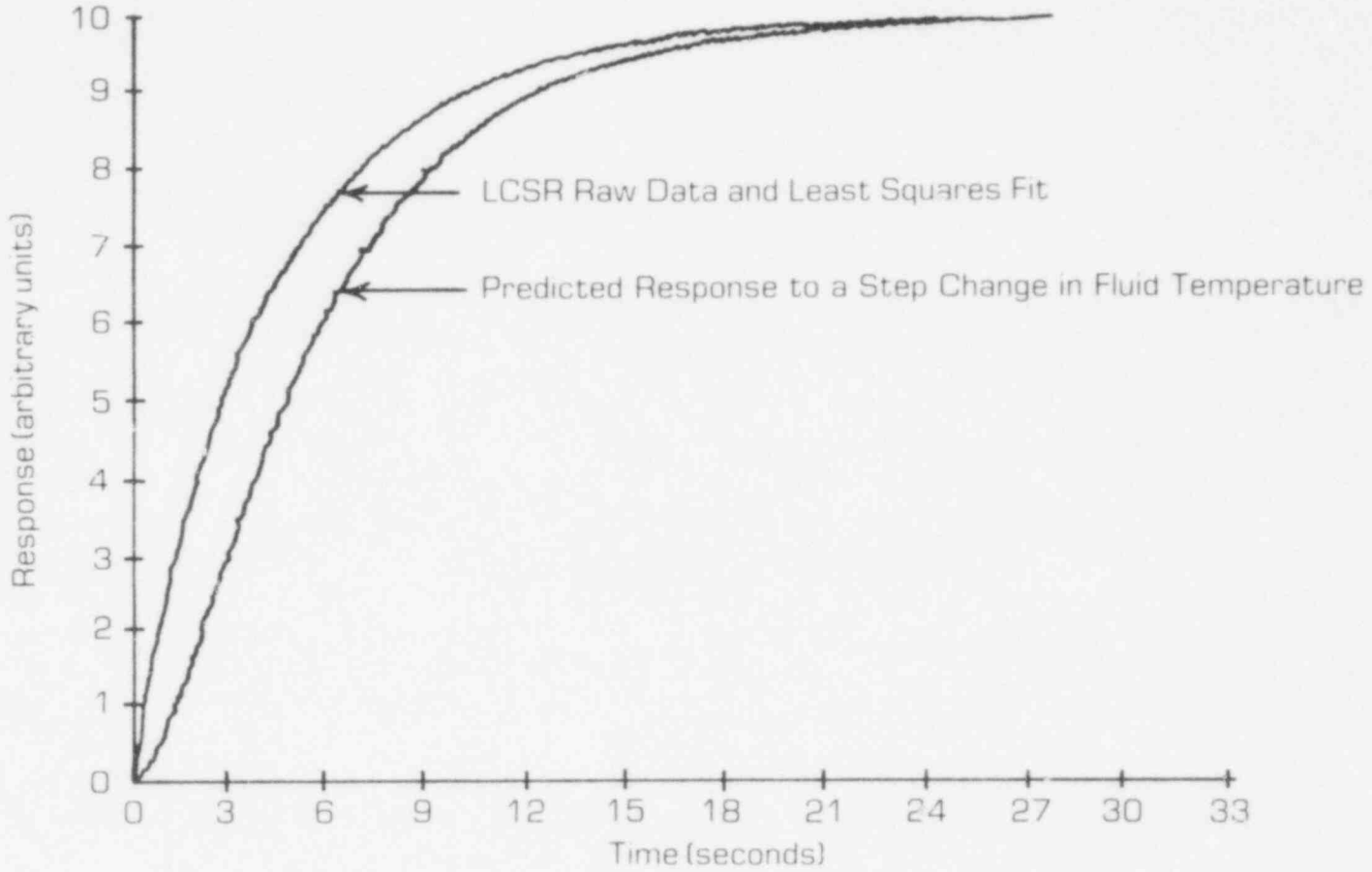

FIGURE 8.3. TYPICAL LABORATORY RESULTS FROM A LOOP CURRENT STEP RESPONSE TEST ON A ROSEMOUNT 104 ADA.

d. Repeat steps a through c for several different applied voltages (usually ten or more values are measured).

A detailed self heating procedure is included in Appendix D.

8.4 Self Heating Test Analysis

The self heating data are plotted (steady state changes in resistance vs. power). The plot is a straight line. The slope (ohms/watt) is called the self heating index. The self heating index is proportional to the overall heat transfer resistance for the sensor. Typical laboratory results appear in Figure 8.4. Self heating index values for typical PWR resistance thermometers are 5 to 10 ohms/watt.

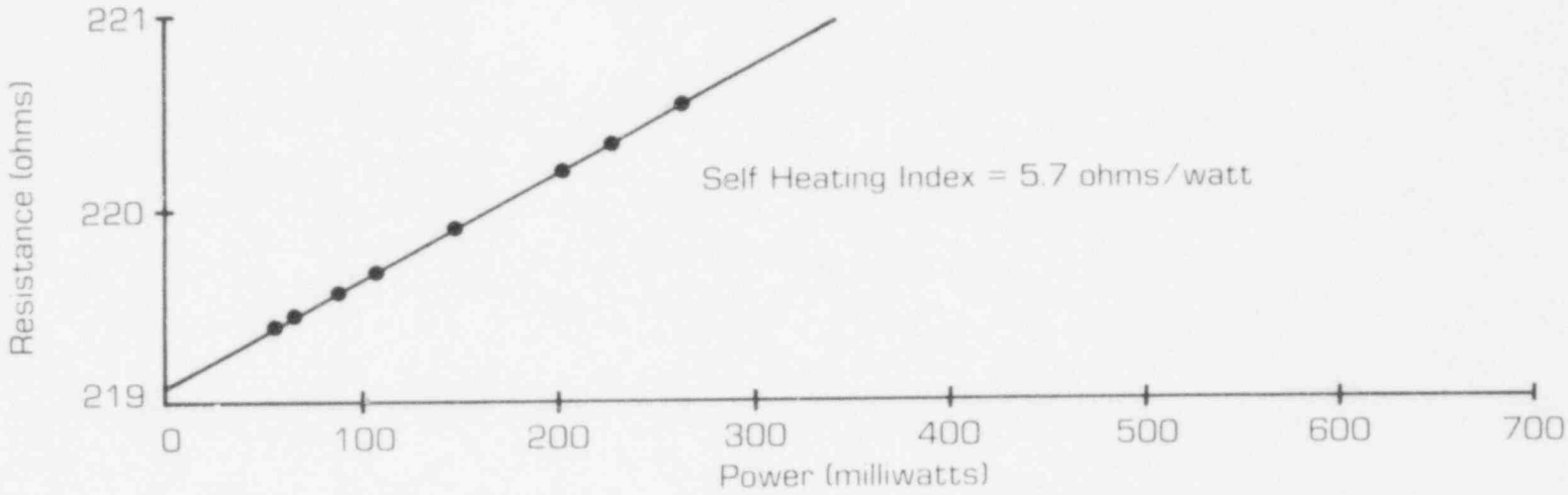

FIGURE 8.4. SELF HEATING CURVE FOR ROSEMOUNT RTD

9. Accuracy Limitations

The accuracy of the results of a loop current step response test depends on the significance of two types of errors:

Mathematical errors - Those errors due to violation of the conditions for validity of LCSR transformation theory.

Measurement errors - Those errors due to measurement conditions that prevent accurate identification of all of the exponential coefficients (τ_i) that are needed to permit accurate specification of sensor dynamics.

These errors are assessed below.

9.1 Mathematical errors

The LCSR transformation depends on the absence of zeroes in the transfer function for the sensor. This is guaranteed (See Appendix C) if the following two essential assumptions of LCSR transformation theory are satisfied:

1. insignificant branching in the heat transfer path between the sensing filament and the fluid.
2. insignificant heat capacity between the sensing filament and the sensor center line.

Analysis shows[13] that the presence of zeroes that would occur if these assumptions were violated causes the response to be slower than the true value. Consequently, if these assumptions are violated, the results are conservative and there is no possibility of failing to detect an unsafe condition because of mathematical errors.

9.2 Measurement errors

Measurement errors have to do with the test conditions that limit the amount of necessary information that can be extracted from the data. In an ideal test, the LCSR transient will obey the following type

of equation:

$$X(t) = a_o + a_1 e^{-t/\tau_1} + a_2 e^{-t/\tau_2} + a_3 e^{-t/\tau_3} + \ldots \qquad (9.1)$$

Experimental and data handling problems that limit the accuracy of the identification of the τ_i are:

- noise (either due to electrical pick-up or process fluctuations)
- drift in the process
- finite resolution in the sampling of the data and in the digital computations.

The noise problem can be overcome by using large heating currents or by averaging multiple data sets. In some power plants, adequate signal-to-noise ratios have been obtained with moderate heating currents (50 ma). In others, the noise was too high to overcome with safe heating currents so averaging was used.

Drift is easily removed by identifying the drift rate and subtracting it from the data before analysis.

The finite resolution in data sampling and computer calculations is unavoidable. This effect usually limits the analysis to identification of two modes (τ_1 and τ_2). These alone are inadequate to specify the complete response for some sensors. However, the identification of τ_1 and τ_2 has been shown to reveal all of the information required about sensor heat transfer and permits evaluation of the contributions of τ_3, τ_4, etc. (See Section 5.2 for details).

Further assessment of the validity of the method must rely on tests performed under conditions when the response can be measured directly and compared with the prediction. This is reported in Chapter 10.

10. Laboratory Testing

Laboratory tests were performed to check the validity of the test procedures. These were performed by University of Tennessee personnel in two different laboratories: the Thermometry Laboratory in the Nuclear Engineering Department at the University of Tennessee and the RTD test facility at the Renardieres facility of Electricite de France in France. In each laboratory, it was possible to perform the tests developed for use in a power reactor and to perform a direct response time measurement for the RTD under the same conditions (ambient temperature, flow, pressure). Comparison then showed the adequacy of LCSR testing and analysis.

10.1 Description of Facilities

10.1.1 University of Tennessee Thermometry Laboratory

The tests at the Thermometry Laboratory at the University of Tennessee were performed in a rotating tank of water. The radial position where a velocity of three feet per second occurs was found and used for the tests. For LCSR or self heating tests, the sensor was mounted vertically with an insertion depth of about six inches. For direct response time measurements, the following procedure was used:

1. Mount the RTD vertically on the shaft of a pneumatic cylinder positioned such that the stroke of the shaft carries the sensor from air down into the flowing water.
2. Place a container of ice water under the RTD. The container had a thin membrane at the bottom.
3. Actuate the solenoid to move the cyli. er down (penetrating the membrane).
4. Record the sensor resistance and a timing signal that marks the entrance of the RTD into the water.

5. Measure the time constant (time to achieve 63.2% of the total response) from the recorded trace.

10.1.2 EDF Facility

The EDF facility is a large loop designed primarily for testing full size PWR pumps and valves at operating conditions. A special RTD test loop was added. It includes a test section for mounting the sensor in water flowing at typical PWR flow, temperature and pressure conditions. A special injection system with a fast valve is used to feed a small stream of colder water into the test section. This approximates a step change (rise time of 20 to 60 ms) for direct measurement of the sensor time constant. The LCSR test is performed with the sensor in the same position.

10.2 LCSR Test Results

10.2.1 University of Tennessee Thermometry Laboratory

Results of loop current step response testing in the thermometry Laboratory at the University of Tennessee[12] appear in Table 10.1. These results show that the correction factor of Section 5.2 is capable of improving LCSR estimates and that the final LCSR estimates agree very well with plunge test results (differences of 0 to 8.7 percent).

10.2.2 EDF Facility

Results of loop current step response testing in the EDF facility appear in Table 10.2. These results also show the validity of the LCSR testing method and of the correction factor of Section 5.2. The maximum discrepancy between direct measurements via fluid injection and by LCSR testing is 9.8 percent. These tests demonstrate clearly that the tests are suitable at PWR operating conditions as well as at laboratory conditions.

10.3 Self-Heating Test Results

Self-heating tests were performed in room temperature water

TABLE 10.1

RESULTS OF LCSR AND PLUNGE TESTING IN THE UNIVERSITY OF TENNESSEE THERMOMETRY LABORATORY

Sensor	Plunge Time Constant (Sec.).	LCSR Estimate of Time Constant		Percent Error
		Without Higher Mode Correction of Section 5.2	With Higher Mode Correction of Section 5.2	
Rosemount 176KF	0.38	0.39	0.41	+ 7.9
Rosemount 104ADA (without thermowell)	3.1	2.9	3.1	0
Rosemount 104ADA (with thermowell)	7.1	5.9	7.2	+ 1.4
Rosemount 104VC (without thermowell)	2.3	1.7	2.1	- 8.7
Rosemount 104VC (with thermowell)	5.3	4.5	5.5	+ 3.8
Rosemount 177GY	5.8	5.1	6.2	+ 6.9
Rosemount 177GY	6.1	5.2	6.3	+ 3.3
Sostman 8606	2.0	1.7	2.1	+ 5.0

TABLE 10.2

RESULTS OF LCSR AND INJECTION TESTING IN THE EDF FACILITY

Sensor	Time Constant from Injection Test (Sec.)	LCSR Estimate of Time Constant		Percent Error
		Without Higher Mode Correction of Section 5.2	With Higher Mode Correction of Section 5.2	
Rosemount 176KF	0.14	0.11	0.13	- 7.1
Rosemount 177HW (with thermowell)	8.8	7.0	8.4	- 4.5
Rosemount 104 (with thermowell with air in gap)	6.2	4.9	5.9	- 4.8
Rosemount 104 (with thermowell with NEVER-SEEZ)	4.1	3.3	3.7	-9.8

flowing at three feet per second. The main purposes of the tests were to develop testing procedures and to determine the sensitivity of the measured self-heating index to changes in the sensor's response characteristics. Typical self-heating test results appear in Figure 8.4.

The sensitivity of the self-heating index to changes in response characteristics was evaluated using sensors with artifically degraded heat transfer. This involved application of insulating material (plastic tape or rubber tubing) to the surface of the sensor. For each different application of insulator, self-heating tests and plunge tests were performed. Typical results are shown in Figure 10.1. The sensitivity of the self-heating index to changes in time constant were evaluated around the sensor's normal, unmodified condition. Tests on two different sensor designs showed that a one percent change in the self-heating index indicates about a 0.2 percent change in time constant.[6]

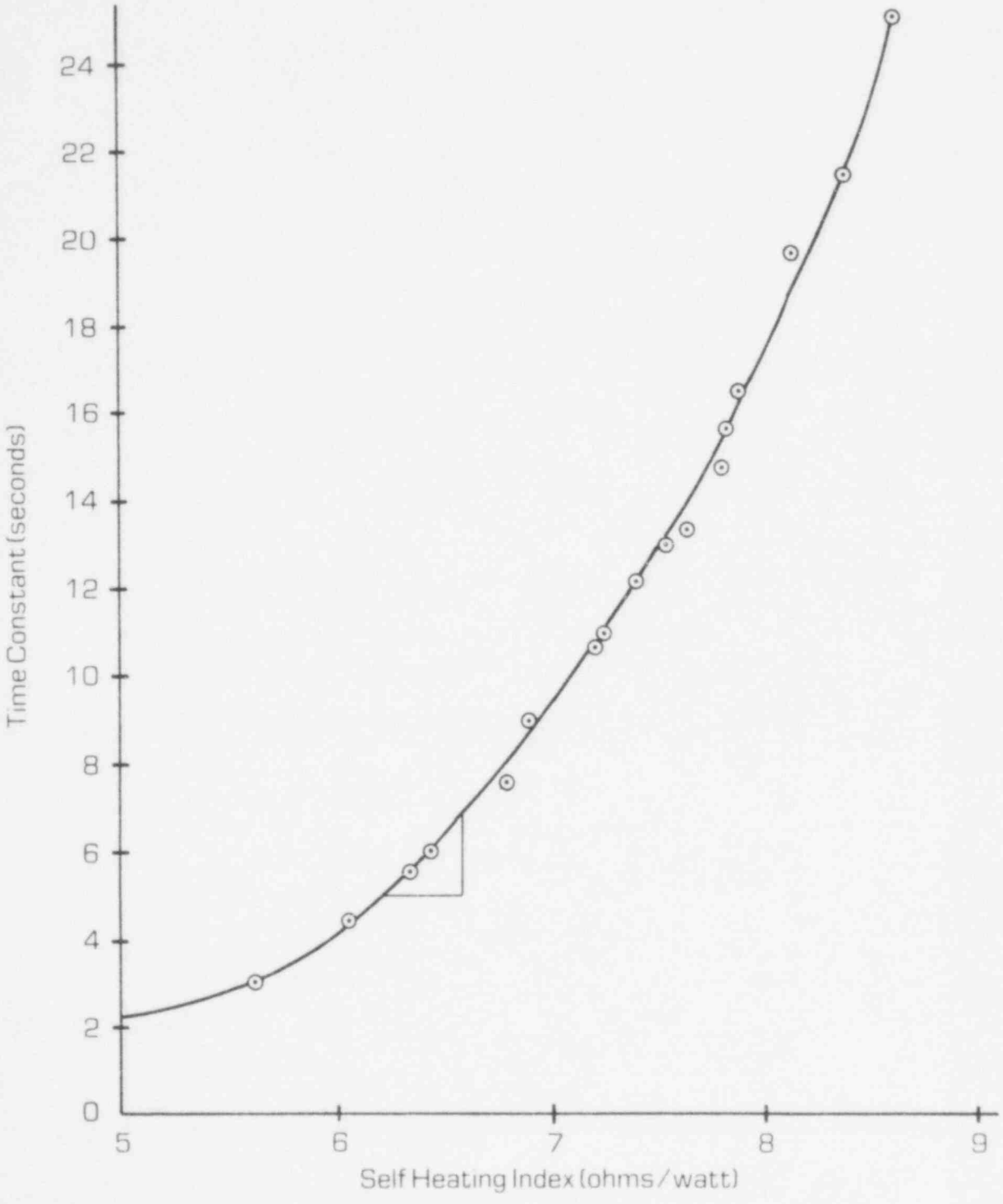

FIGURE 10.1. LABORATORY RESULTS FOR RELATION BETWEEN THE TIME CONSTANT AND THE SELF-HEATING INDEX.

11. In-Plant Testing

11.1 University of Tennessee Program

Tests were performed on three pressurized water reactors as part of the University of Tennessee research program.[5,6] Tests were performed on control system RTDs rather than safety system RTDs. The main purposes of the tests were to establish suitable test procedures and to determine whether plant conditions (such as background noise, process temperature fluctuations, etc.) interferred excessively with the testing. Measurements were made at Turkey Point (a Westinghouse plant), at St. Lucie (a Combustion Engineering plant) and at Oconee (a Babcock and Wilcox plant).

The program included self-heating tests and loop current step response tests. Typical self heating test results appear in Figures 11.1 through 11.3. The expected linear relation between resistance change and power is evident and the scatter is quite small. Consequently, it is concluded that self-heating tests are feasible in operating plants.

LCSR tests were also performed and typical raw data traces appear in Figures 11.4 through 11.6. The results from St. Lucie and Oconee tests are very similar to results obtained in the laboratory. The curves were smooth and repeatable and analysis was accomplished without difficulty.

The Turkey Point results were quite different than typical laboratory data. The data had fluctuations due to fluctuations in the process temperature that interferred with effective analysis of the date. The problem occurred because only a small heating current was used (20 ma) and the sensor is very responsive to process temperature fluctuations because of its fast response. Subsequent tests on the same type of sensor in another Westinghouse plant showed that the problem could be overcome readily with a larger heating current and averaging - (See Section 11.3).

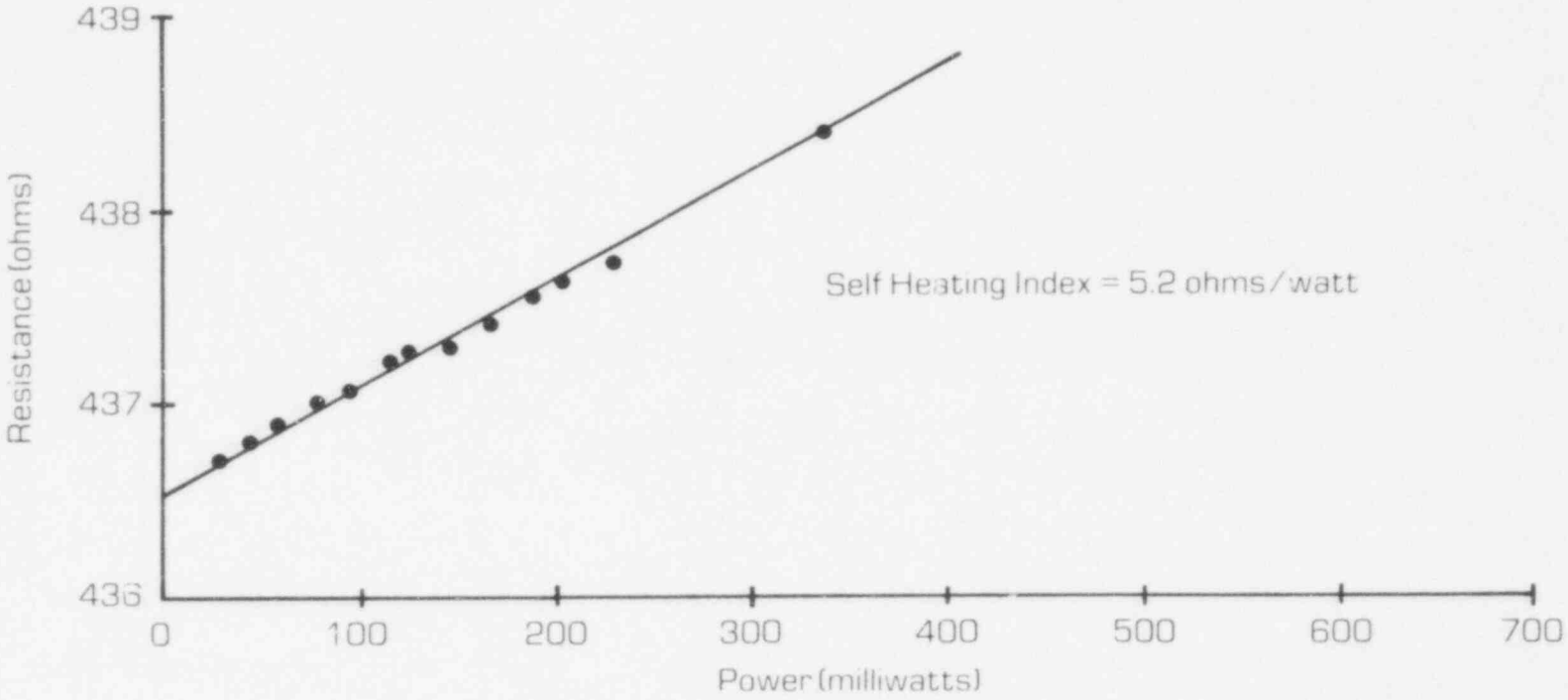

FIGURE 11.1. TYPICAL SELF HEATING RESULTS FROM TURKEY POINT TESTS
(Rosemount 176KF)

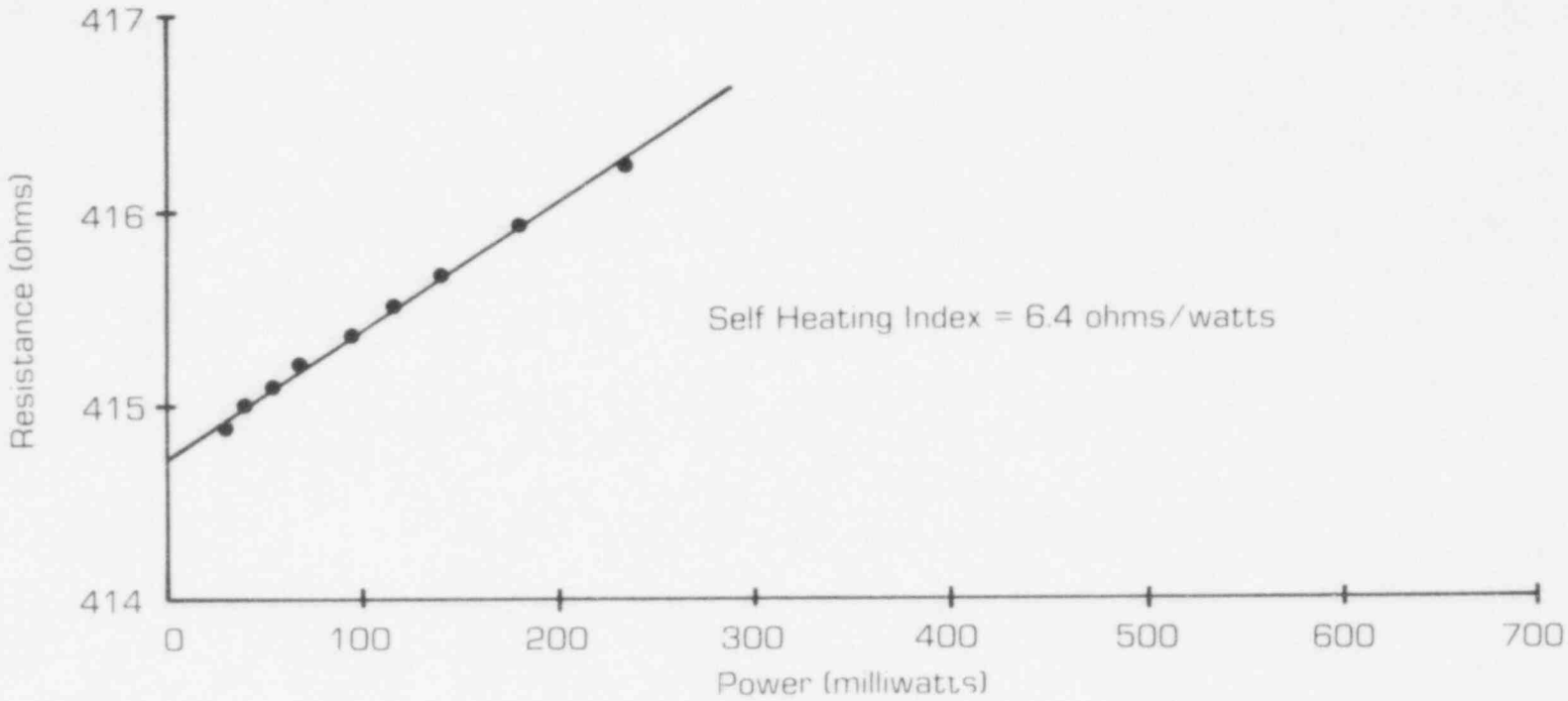

FIGURE 11.2. TYPICAL SELF HEATING RESULTS FROM ST. LUCIE TESTS
(TE 1125 at 540°F)

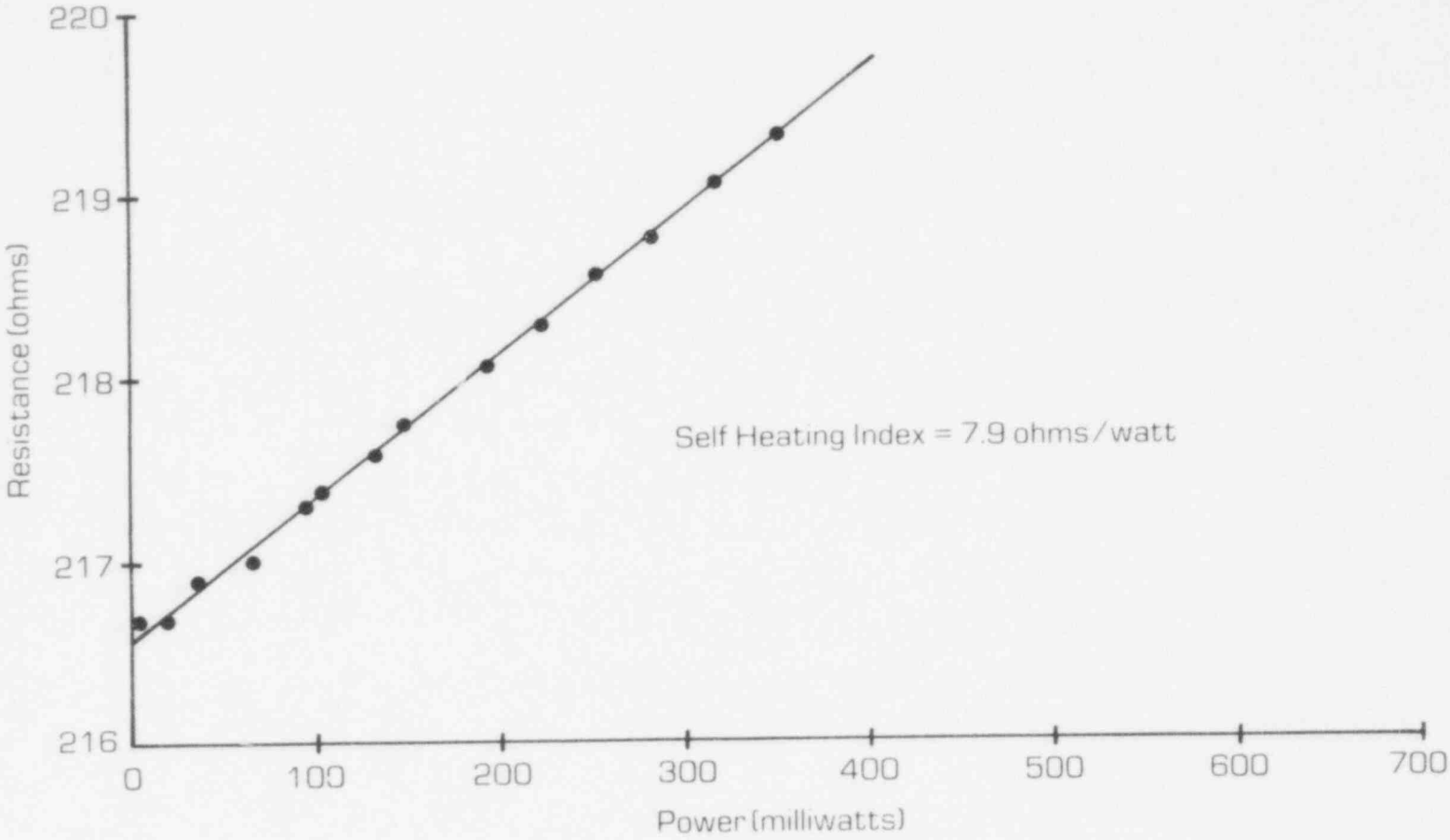

FIGURE 11.3. TYPICAL SELF HEATING RESULTS FROM OCONEE TESTS

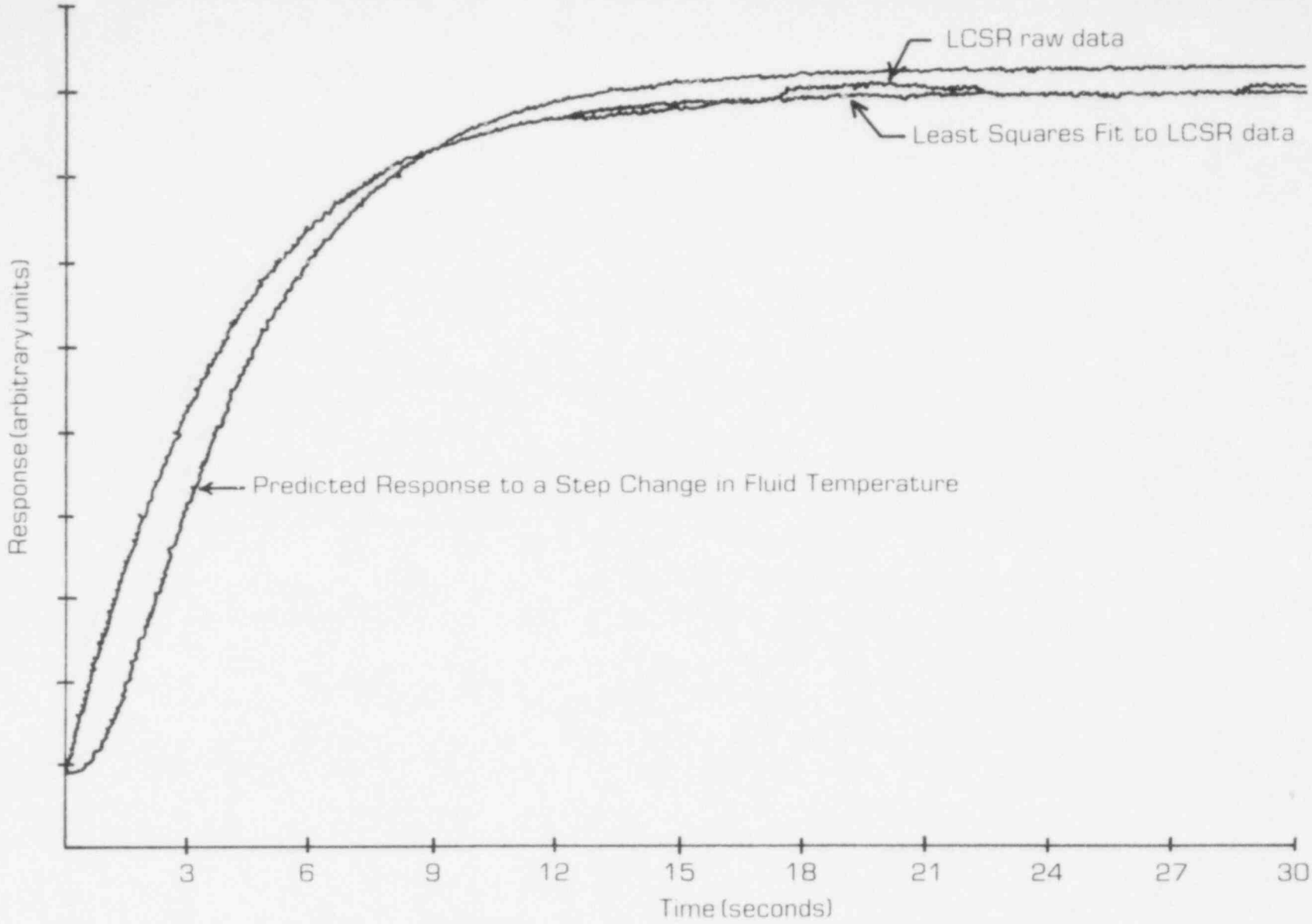

FIGURE 11.4. TYPICAL RESULTS FROM A LOOP CURRENT STEP RESPONSE TEST AT ST. LUCIE NUCLEAR STATION

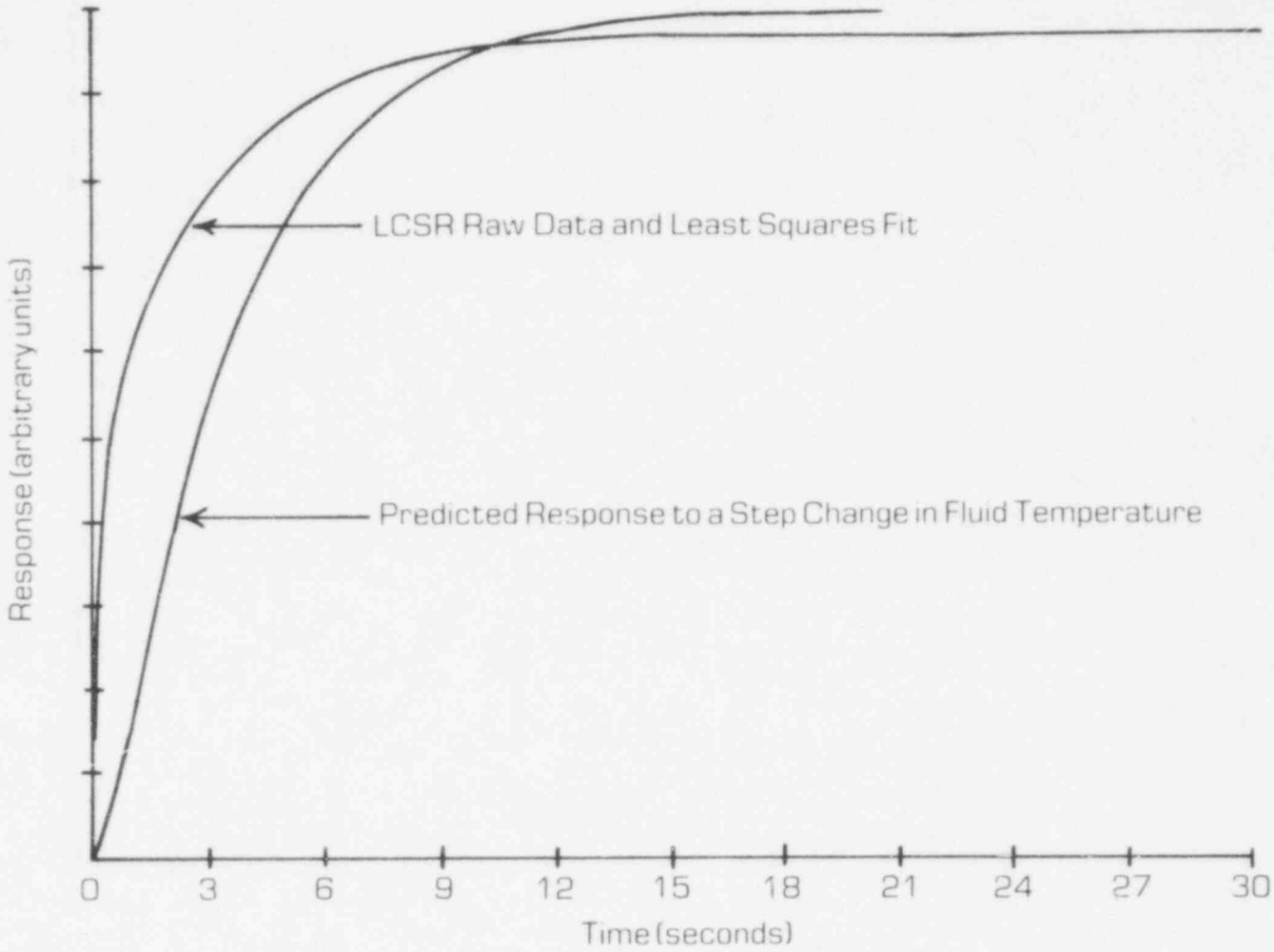

FIGURE 11.5. TYPICAL RESULTS FROM A LOOP CURRENT RESPONSE TEST AT OCONEE NUCLEAR STATION

FIGURE 11.6. TYPICAL LCSR DATA AT TURKEY POINT

11.2 Test Procedure

A standard test procedure was developed based on laboratory experience and in plant testing experience. It is shown in Appendix D.

11.3 AMS Test Program

AMS Corporation has performed five testing programs in three pressurized water reactors for utility customers. The plants were Millstone 2, Arkansas Nuclear One-Unit 2, and Farley 1. The test procedures of Appendix D were followed.

Typical self heating test results appear in Figures 11.7 through 11.9. As in the earlier in-plant tests, the data were adequate to define a reliable self-heating curve.

Typical LCSR raw data appear in Figures 11.10 through 11.12. The data from the Combustion Engineering plants (Millstone 2 and Arkansas Nuclear One - Unit 2) are similar in quality to the earlier tests at St. Lucie. The curves show some influence of process temperature variations, but they are generally smooth and quite suitable for analysis. The data from Farley are much better than the earlier data from Turkey Point (both are Westinghouse plants) because a higher heating current was used. The Farley data are not as smooth as the data from the Combustion Engineering plants because the Farley sensor (Rosemount 176KF) is much faster than the sensors used in Combustion Engineering plants (Rosemount 104) and more responsive to process temperature fluctuations. Nevertheless, the Farley data are suitable for analysis. The benefits of averaging several transients to reduce noise effects are illustrated in Figures 11.13 and 11.14. These may be compared with corresponding individual transients shown in Figures 11.10 and 11.12. The averaged data sets are preferred for analysis.

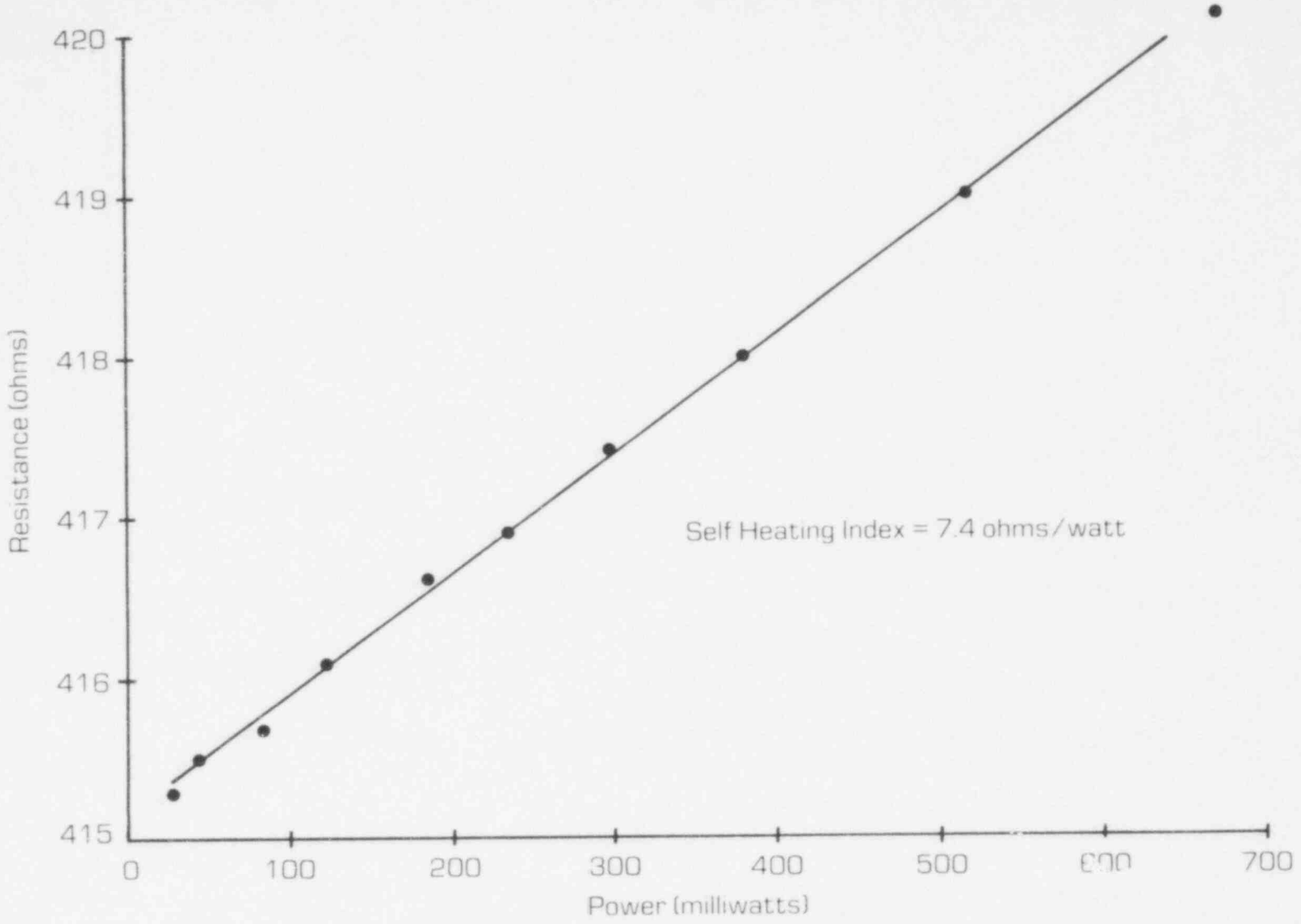

FIGURE 11.7. SELF HEATING CURVE FOR MILLSTONE 2 RTD

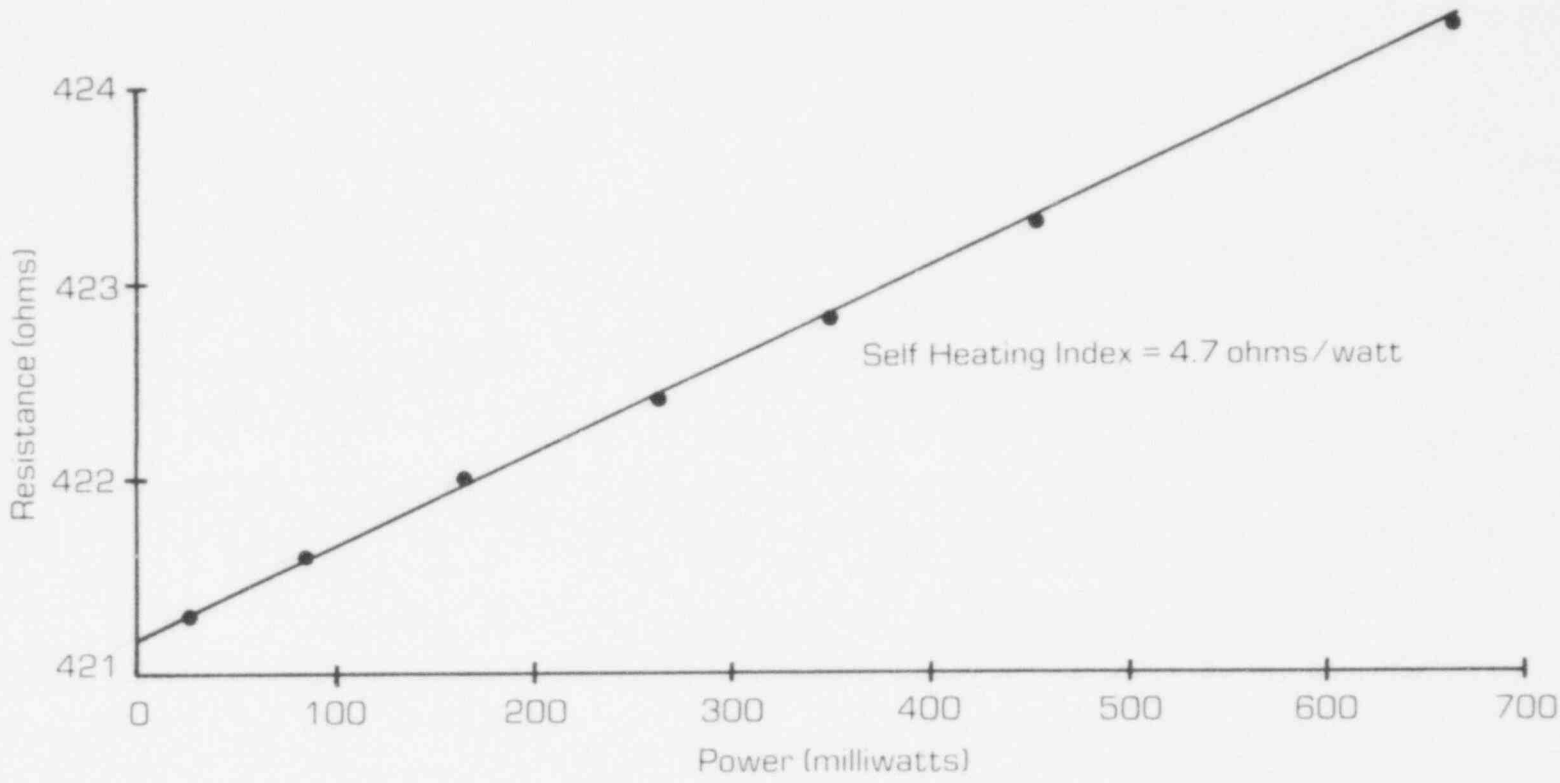

FIGURE 11.8. SELF HEATING CURVE FOR ARKANSAS NUCLEAR ONE UNIT 2 RTD

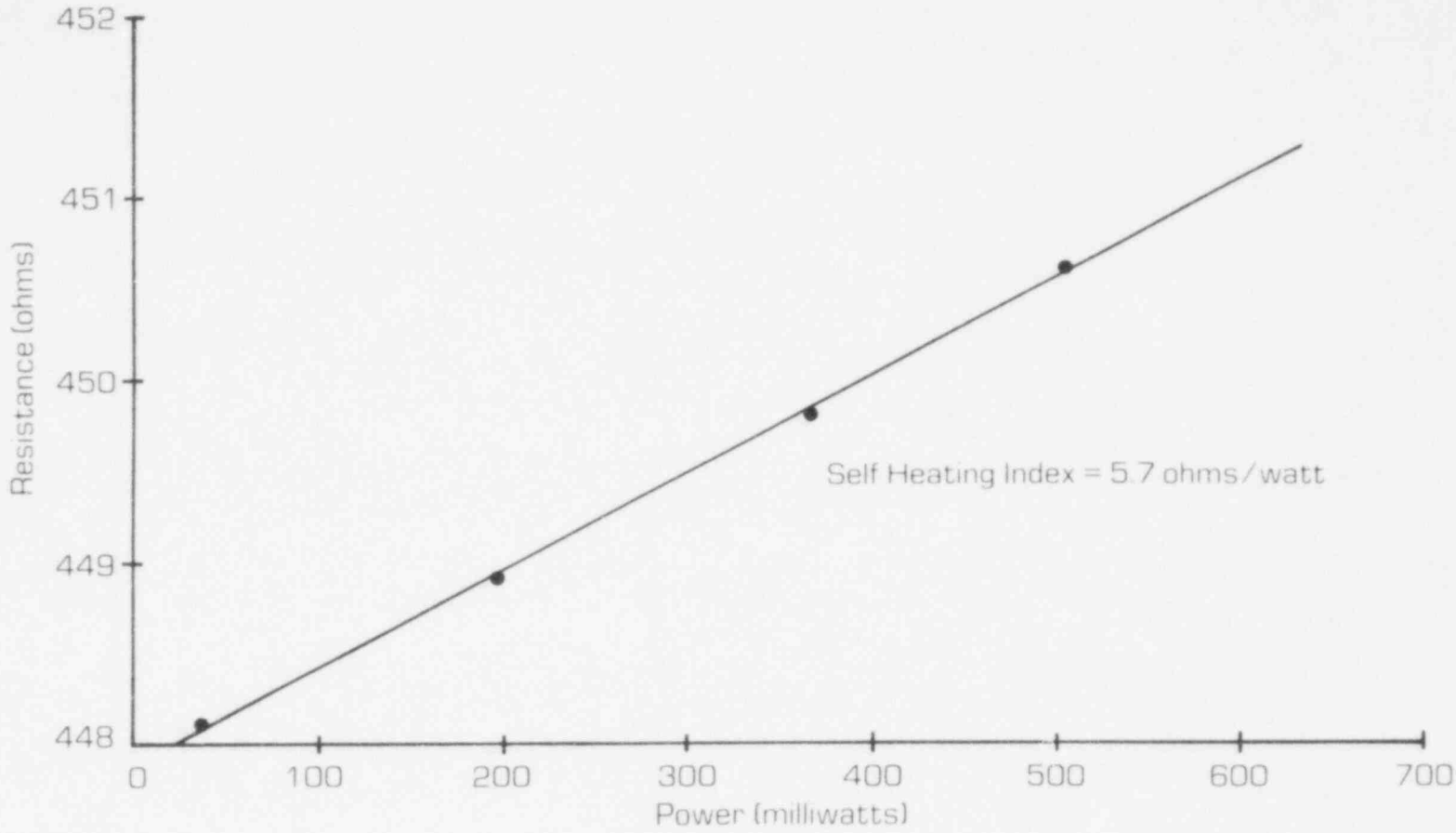

FIGURE 11.9. SELF HEATING CURVE FOR FARLEY 1 RTD

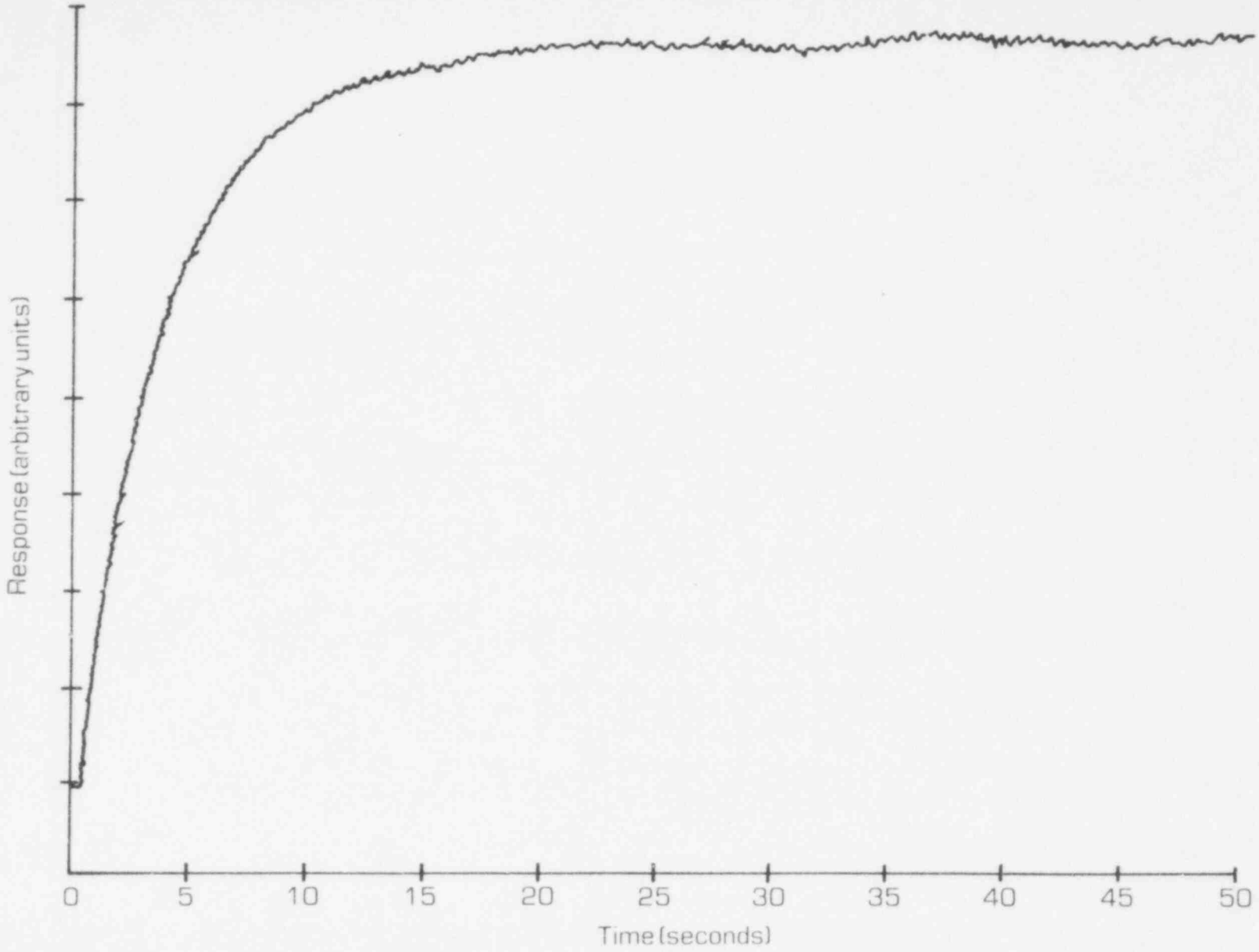

FIGURE 11.10. TYPICAL LCSR DATA AT MILLSTONE 2

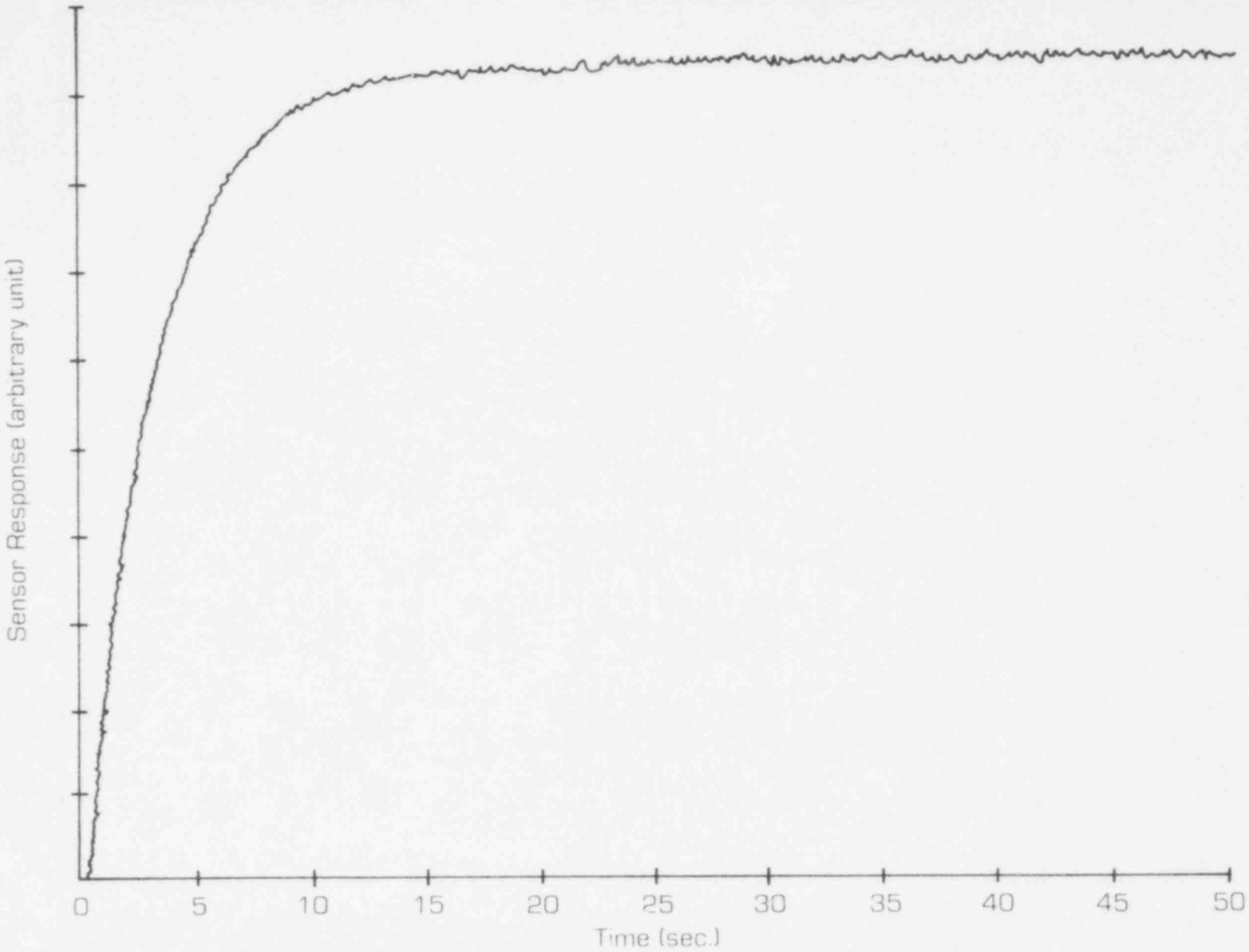

FIGURE 11.11. LCSR TRANSIENT FOR ARKANSAS NUCLEAR ONE UNIT 2 RTD

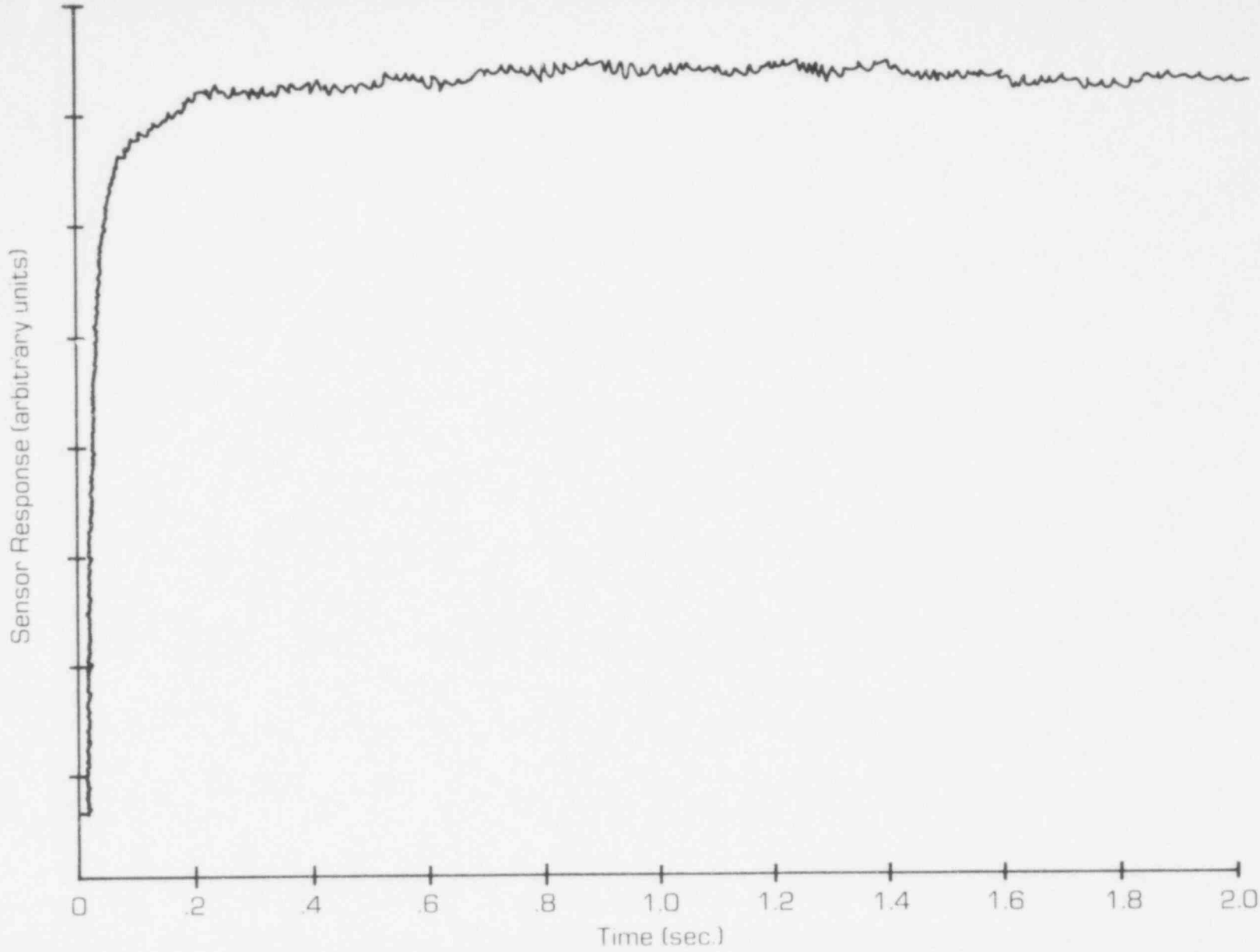

FIGURE 11.12. A TYPICAL LCSR TRANSIENT FROM FARLEY TESTS

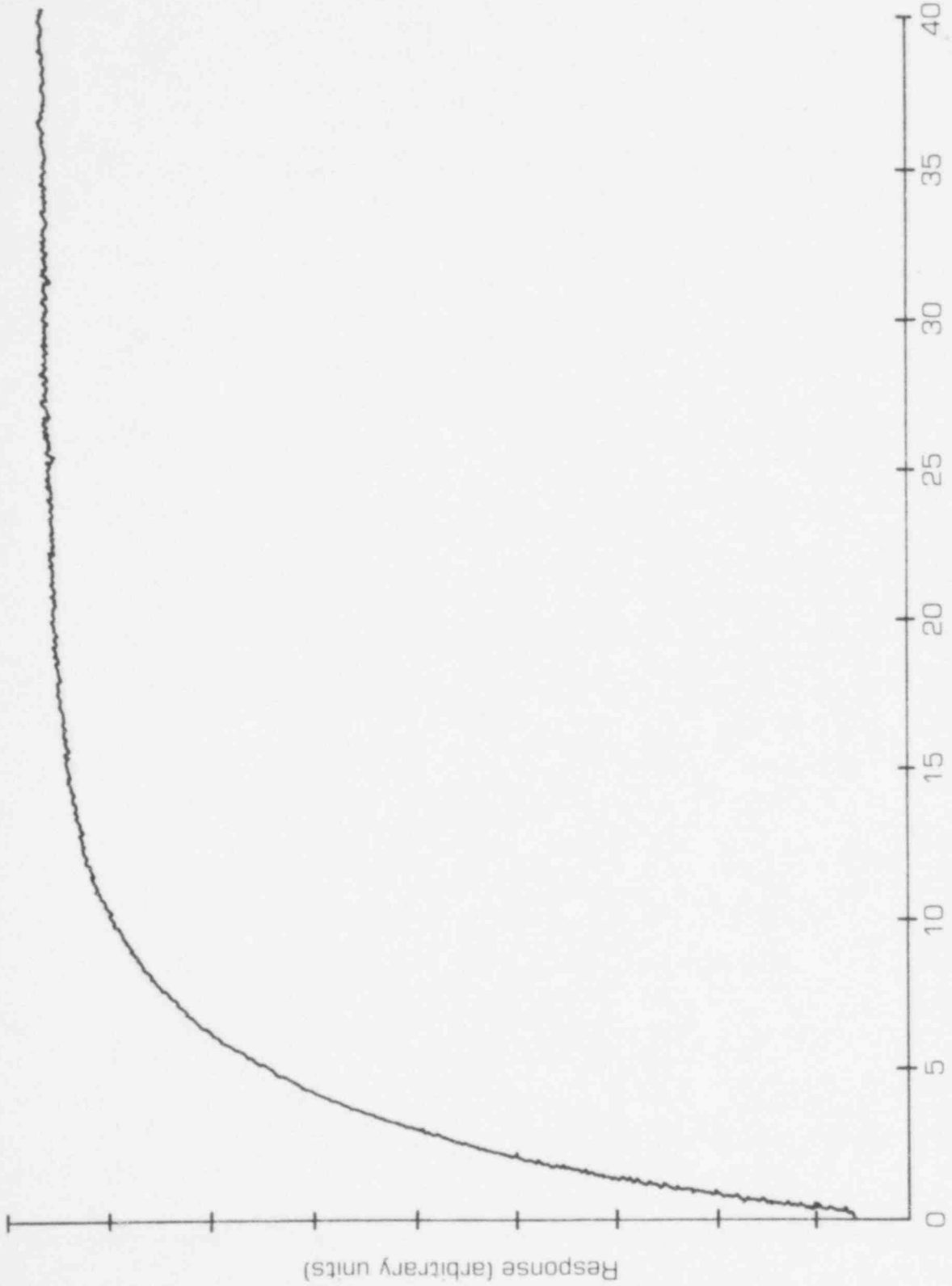

FIGURE 11.13. TYPICAL DATA SET OBTAINED BY AVERAGING MULTIPLE TEST RECORDS AT MILLSTONE 2

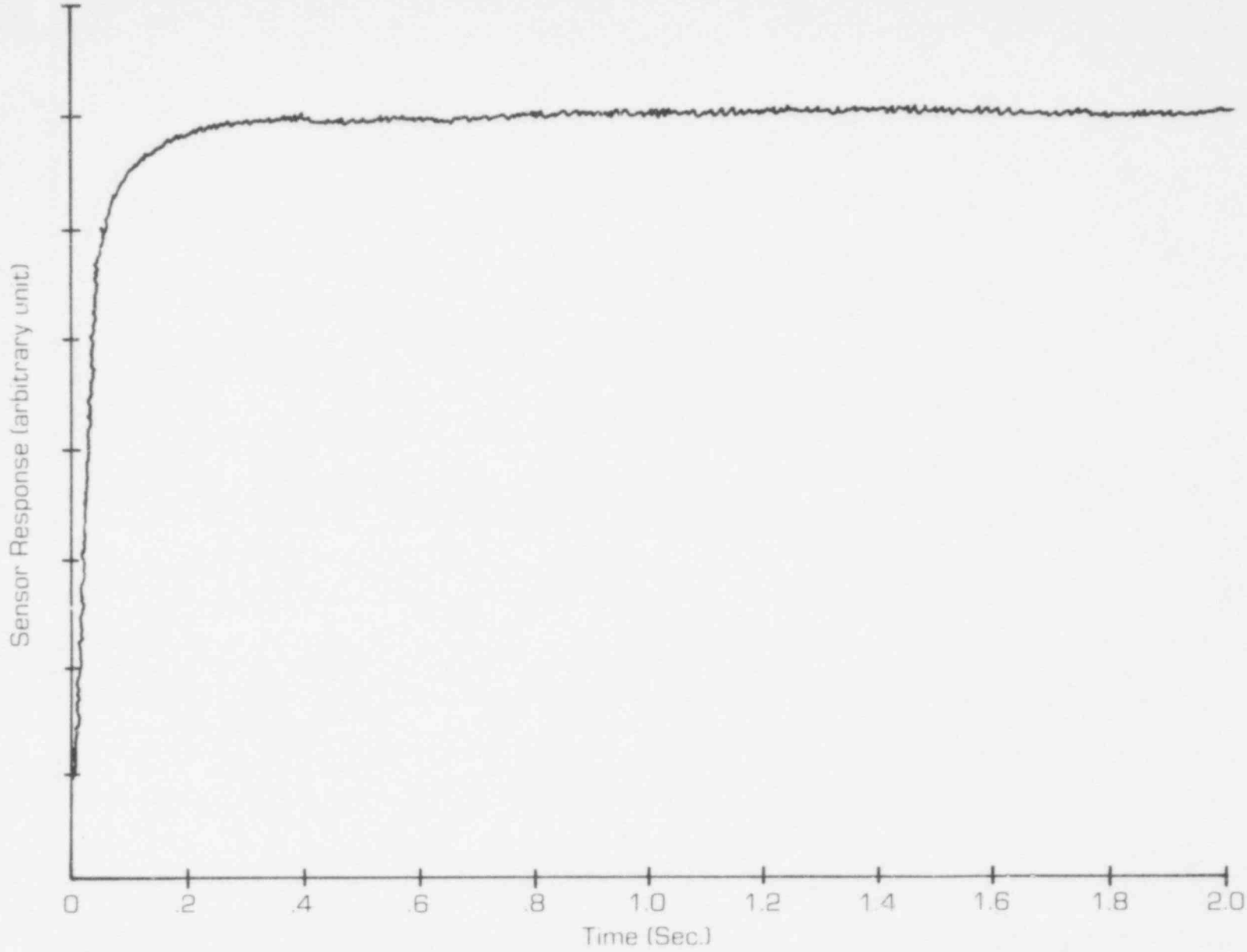

FIGURE 11.14. A TYPICAL AVERAGED LCSR TRANSIENT FROM FARLEY TESTS

11.4 Millstone 2 Tests

The reference plant for this report is Millstone 2. Consequently, the detailed results will be presented for tests on that plant.

11.4.1 First Test Program

The first test program was performed by AMS Corporation in December, 1977. Northeast Utilities contracted for these tests in order to evaluate the test procedure as a method for subsequent tests to be performed for compliance with Regulatory Guide 1.118. The procedure of Appendix D was used to test sixteen safety system sensors.

Results of a typical self heating test performed in 1977 appear in Figure 11.15. Self heating index results for all sensors tested appear in Table 11.1. For comparison, laboratory values for the self heating index for other similar RTDs (with thermowell) varied from 6.1 to 8.8 ohms per watt.

Typical LCSR raw data from 1977 appear in Figure 11.16. Analysis results appear in Table 11.1. These analyses were performed before the correction factors (Section 5.2) had been developed to account for undetectable modes in the transient. Consequently, the results in Table 11.1 have a bias that causes the estimates to be low by as much as twenty percent.

11.4.2 Second Test Program

The Millstone 2 sensors were tested a second time in December 1978. The test procedures were the same as for the first Millstone 2 test. The analysis was modified because of the development of the correction factors to correct for higher mode contributions. Consequently, two sets of LCSR results are of interest: the uncorrected values for comparison with the first tests and the corrected values for giving the best estimates of sensor behavior.

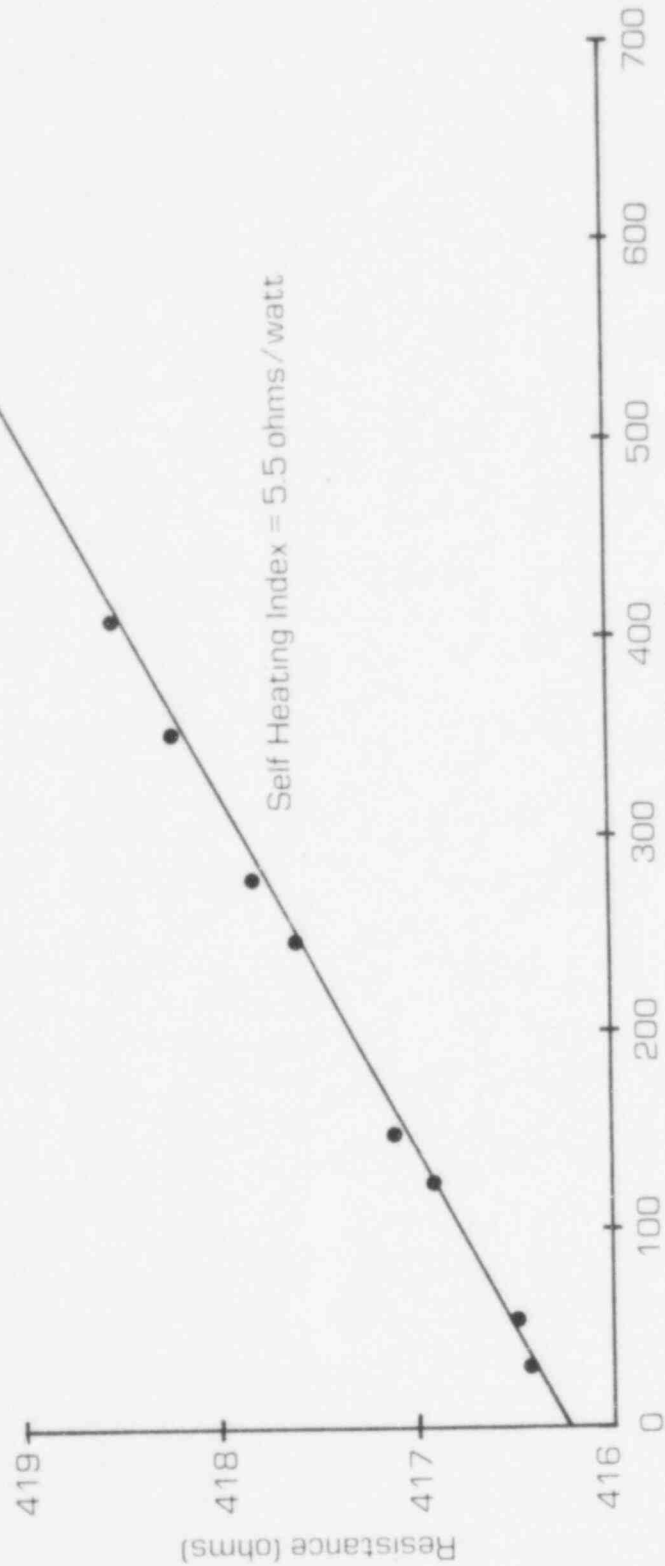

FIGURE 11.15. SELF HEATING CURVE FOR MILLSTONE 2 RTD

Table 11.1

Comparison of Response Time Test Results at Millstone 2*

	Tests of August 1977		Tests of December 1978	
Sensor S/N	Time Constant (sec)	Self Heating Index (ohms/watt)	Time Constant (sec)	Self Heating Index (ohms/watt)
A7770	3.2	5.6	5.2	7.4
A7765	2.8	4.5	3.2	4.8
75313	4.7	6.2	5.6	6.5
A7774	3.8	5.8	4.3	6.2
2456	--**	--**	5.3	7.5
2455	--**	--**	4.5	6.4
2454	--**	--**	4.7	7.5
2453	--**	--**	4.5	5.2
75294	3.7	6.0	4.4	6.4
75299	5.5	8.6	9.3	9.1
75310	4.6	6.2	4.9	6.5
75300	4.6	6.5	4.7	6.5
75297	3.6	4.7	3.6	4.9
80364	4.0	5.6	4.4	6.1
75309	4.0	5.5	4.7	5.8
A7769	3.1	4.8	3.6	5.0

*Since the correction factor had not been developed at the time of the August 1977 measurements, all time constants shown here are uncorrected values.

**These sensors were not included in August 1977 measurements.

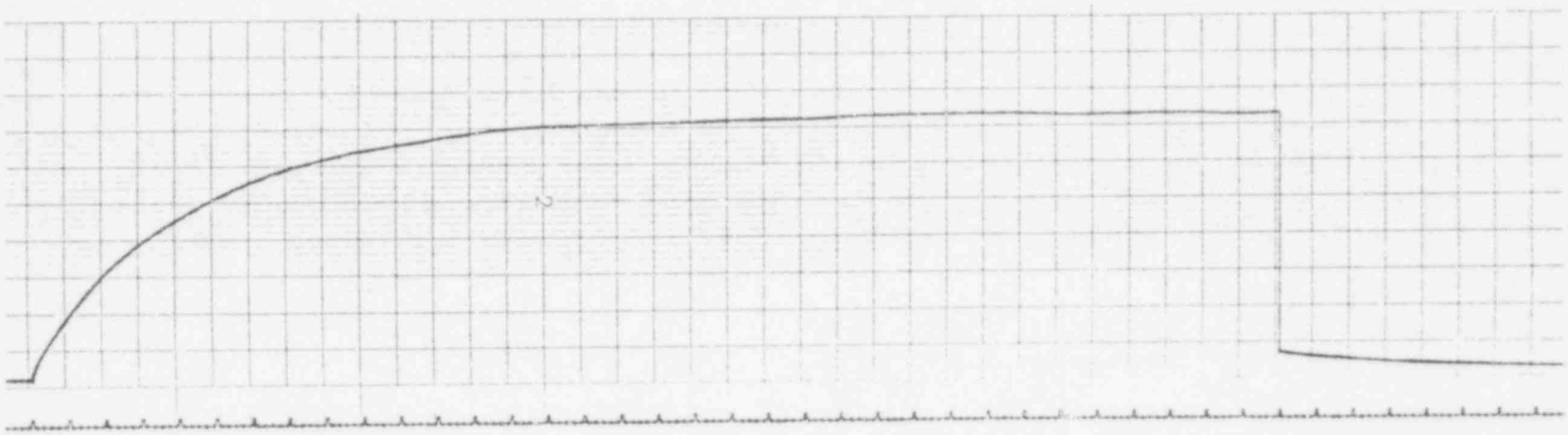

FIGURE 11.16. LCSR TEST TRANSIENT OF MILLSTONE 2 RTD.
BRIDGE BALANCED AT LOW CURRENT.

A typical self heating curve from the 1978 test appears in Figure 11.7. Table 11.1 shows self-heating index results along with comparable results from the first test.

Figure 11.17 shows a typical LCSR transient along with the fit and the predicted response to a step change in fluid temperature. Table 11.2 shows time constant results obtained by analysis of the LCSR data. The table shows uncorrected values and the final corrected values. The results reveal the following:

- The sensor time constants (uncorrected) increased by up to sixty-nine percent between December 1977 and December 1978. The average increase was twenty-one percent.
- The self heating index results revealed the same trends as the time constant measurements. (Sensors had increases in self heating indices that were roughly proportional to the increases in time constants.)

11.5 Conclusions from In-Plant Testing

The conclusions that following from the in-plant testing experience are:

a. By selecting an appropriate combination of heating current and number of cases to be averaged, in-plant LCSR data of comparable quality to laboratory data can be collected.

b. Reliable self-heating data can be collected easily.

c. Self heating data cannot be converted into time constant data using correlations obtained from a given sensor design because of dependence on construction details. However, the self heating index was found to be a sensitive indicator of changes in response characteristics.

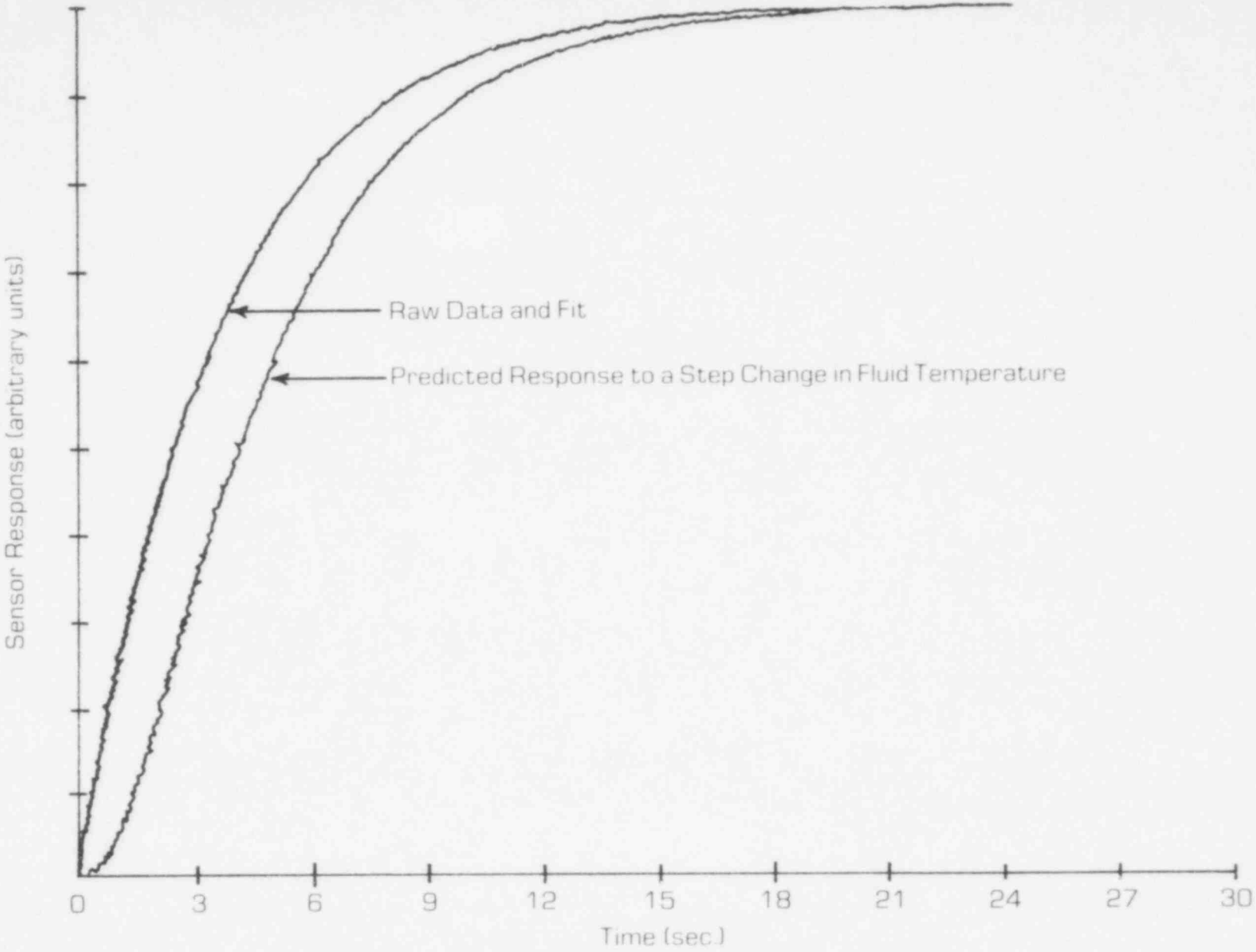

FIGURE 11.17. TYPICAL LCSR TRANSIENT AND ANALYSIS RESULTS FROM MILLSTONE 2

Table 11.2

Response Time Test Results for Millstone 2 RTDs
(Test of December 1978)

Sensor S/N	Uncorrected* Time Constant (Sec)	Corrected** Time Constant (sec)	Self Heating Index (ohms/watt)
A7770	5.2	6.2	7.4
A7765	3.2	3.6	4.8
75313	5.6	6.7	6.5
A7774	4.3	5.2	6.2
2456	5.3	6.4	7.5
2455	4.5	5.4	6.4
2454	4.7	5.2	7.5
2453	4.5	5.4	5.2
75294	4.4	5.3	6.4
75299	9.3	11.2	9.1
75310	4.9	5.5	6.5
75300	4.7	5.6	6.5
75297	3.6	4.1	4.9
80364	4.4	5.0	6.1
75309	4.7	5.6	5.8
A7769	3.6	4.3	5.0

*The uncorrected time constants are based on identification of two exponentials in the experimental data. The higher mode correction factor of Section 5.2 was not used for these results.

**Correction factors ranged from 1.11 to 1.20 for these tests.

12. Conclusions

Loop current step response testing has been developed thoroughly and is completely adequate for testing resistance thermometers in nuclear power reactors. The proof given in this report guarantees its suitability as a substitute test as required in Section C, Item 6 of U.S. Nuclear Regulatory Guide 1.118 (See Section 1.1 of this report for information on the Regulatory Guide).

The proof of adequacy of loop current step response testing has three bases:

- extensive theoretical analysis (Chapters 3, 4 and 5 of this report).
- extensive laboratory testing. In these laboratory tests, it was possible to measure the response of the RTD directly (by plunge testing or injection testing) for comparison with LCSR results. Good agreement was obtained.
- in-plant testing. In-plant tests show that the methods developed in the laboratory are also suitable for plant testing. The test connections are simple and safe, and require little interference to normal operation. In fact, the desired plant condition for testing is full power operation.

Appendix A

Effect of Joule Heating on RTDs

ROSEMOUNT INC., 12001 WEST 78th STREET / EDEN PRAIRIE, MINNESOTA 55344
Mailing Address: P.O. BOX 35129 / MINNEAPOLIS, MINNESOTA 55435
TEL: (612) 941-5560 TWX: 910-576-3103 TELEX: 29-0183

May 21, 1979

Professor Tom Kerlin
Nuclear Engineering Department
University of Tennessee
Knoxville, Tennessee 37916

Dear Sir,

In response to your questions of using the Loop Current Step Response Test method on primary loop temperature sensors furnished to Combustion Engineering, Rosemount finds no problem with applying currents up to 80 milliamps to these sensors.

Currents in excess of this magnitude have been used during testing at Rosemount without damage to the sensor. Recent testing conducted at Rosemount indicates that currents in excess of 300 milliamps with the sensor being at a temperature of 500°F did not cause open elements.

While Rosemount does not have test data available to certify the sensors that have been shipped, it's my opinion that this testing will not damage the sensors.

Please contact me if I can answer further questions.

Sincerely,

L. E. Anderson
Temperature Sensor Design Supervisor

LEA:ddz

RdF CORPORATION
23 Elm Avenue
Hudson, New Hampshire 03051
Tel: (603) 882-5195 TWX: 710-228-1882

May 21, 1979

University of Tennessee
Dept of Nuclear Engineering
Knoxville, Tennessee 37916

Attention: Dr. T.W.Kerlin

Dear Dr. Kerlin:

In response to our telephone conversation on May 17, 1979, concerning RTD's for Nuclear Application: RTD's are usually designed to meet specific time response requirements. This is accomplished, by thermally coupling the sensor as closely as possible with the process medium. This allows energy to be transmitted between the sensor and medium as rapidly as possible. Under these conditions, an intermittant current of 50 - 60 milliamperes generally will not cause self heating in the sensor to be substantially above the medium temperature, thus not cause any permanent damage to the sensing element. Sensing elements with mechanical damage to the sensing wire are susceptible to early failure.

RdF has tested "off the shelf" standard commercial units at 100 milliamperes with the element sheath immersed in 70°F water, flowing at three (3) feet per second. Resistance shifts after exposure to 100 milliamperes are usually less than .08°F.

Dr. T.W.Kerlin May 21, 1979

University of Tennessee

You may use this letter as part of your report to the Nuclear Regulatory Commission on loop current response time testing, and if I can be of further help, please do not hesitate to call.

Yours truly,
RdF Corporation

Randal A Gauthier
Chief Transducer Engineer

RAG:vb

The
LEWIS ENGINEERING
Company
P. O. Box 268
Norwich, New York 13815

Tel. 607-334-3939

May 24, 1979

The University of Tennessee
Nuclear Engineering Department
Knoxville, Tennessee 37916

Attention: Dr. T. Kerlin

Subject: Effect of Loop Current Step Response Test on Lewis Temperature Sensors for Nuclear Applications

Dear Tom:

Lewis Engineering has furnished temperature sensors with standard plunge test response time data for use in coolant loops of nuclear reactors. These platinum resistance temperature detectors, Models 56BPA2 and 56BPA4, are single element, 200 ohm, four wire, thermowell type sensors.

The Loop Current Step Response (LCSR) method of measuring sensor time constant as described in report NP-834, Volume I for EPRI would not be detrimental to these Lewis sensors. In-situ response time testing using the LCSR method, with electric current transients up to 70 milli-amperes, should cause no degradation of the sensors' parameters.

Should you desire to copy or use this statement in your report, per our conversation, please feel free to do so.

Very truly yours,

THE LEWIS ENGINEERING COMPANY

James E. Dann
Engineering Manager
Transducer Division

JED/mlk

927 153

OAK RIDGE NATIONAL LABORATORY
OPERATED BY
UNION CARBIDE CORPORATION
NUCLEAR DIVISION

POST OFFICE BOX X
OAK RIDGE, TENNESSEE 37830

July 17, 1979

Professor T. W. Kerlin
Department of Nuclear Engineering
University of Tennessee
Knoxville, Tennessee 37916

Loop Current Step Response of Thermocouples and Resistance Thermometers

Extensive use of Loop Current Step Response (LCSR) techniques has been made at ORNL over the past 8 years to measure response times of sheathed thermocouples in reactor experiment capsules in the HFIR, plant thermocouples in ORR, and sheathed thermocouples in sodium test loops. Comparisons were made of the results of LCSR tests and more conventional plunge response tests for a wide variety of sheathed thermocouples. Using heating currents typically of 1-1.5 amps for LCSR tests on thermocouples, agreement between LCSR and plunge tests of better than 10% is typical. A few disparities as high as 20% were found, but could be attributed to differences in test conditions, such as surface heat transfer conditions. I estimate several hundred thermocouples have been tested ranging from some as small as 0.020 in. OD to others as large as 0.125 in. OD. No damage from LCSR testing was ever observed.

Tests of the LCSR method were also made for determining response times of platinum resistance thermometers (PRTs) using heating currents typically of 60 ma. No effects on calibration, as determined by changes in the ice point resistance (R_0), were found, although it is customary to restrict the normal measuring currents to 1-3 ma to avoid self heating effects. In a recent study to use the self-heating effect in a PRT as a means for determining whether there was water surrounding the PRT sheath (in the Three Mile Island pressurizer), we ran currents of 200-250 ma through a Rosemount Engineering Model 104MB PRT for periods of 5-6 hours repeatedly over a period of a week with the thermometer at temperatures as high as 550°F. After these tests, the ice point resistance of the PRT was rechecked and found to be 100.003 ohms, well within the normal calibration tolerance. It

is our judgement that currents of as high as 200 ma can be used in LCSR and self-heating tests for PRTs which are properly manufactured to meet RDT and ASTM specifications, so long as the internal platinum element temperature does not exceed the rated temperature for these PRTs.

Very truly yours,

R. L. Shepard
Thermometery Development

RLS:wt

cc: R. M. Carroll

APPENDIX B

TIME RESPONSE CHARACTERIZATION OF SENSORS

B.1 The Concept of Time Constant

The time constant is commonly used to represent the response characteristics of a dynamic system. It has unambiguous meaning only for first order systems (described by a first order differential equation or equivalently, a first order transfer function);

$$\frac{dx}{dt} + ax = au \tag{B.1}$$

or

$$G(s) = \frac{x(s)}{u(s)} = \frac{1}{\frac{1}{a}s+1} . \tag{B.2}$$

If Equation B.2 is solved for a unit step change in the input, u; one obtains

$$x(t) = 1 - e^{-at}. \tag{B.3}$$

If the response is evaluated for $t = \frac{1}{a}$, then

$$x(t = \frac{1}{a}) = 0.632. \tag{B.4}$$

The quantity, $\frac{1}{a}$, is defined as the time constant, τ. It is easily identified from test data by measuring the time required for the response to achieve 63.2 percent of its final value following a step change in the input.

B.2 Higher Order Dynamic Systems

The first order approximation is usually inadequate to represent the dynamics of typical temperature sensors. This means that higher order differential equations or transfer functions are required to represent the dynamics. As is shown in Appendix C, a transfer function without zeroes (no numerator dynamics) is usually adequate:

$$G(s) = \frac{a_o}{s^n + a_1 s^{n-1} + \ldots + a_1 s + a_o} \tag{B.5}$$

or

$$C(s) = \frac{a_o}{(s-s_1)(s-s_2) \ldots (s-s_n)} \tag{B.6}$$

For a step change in the input, the response is

$$x(t) = \frac{a_o}{(-s_1)(-s_2) \ldots (-s_n)} + \frac{a_o e^{s_1 t}}{s_1(s_1-s_2) \ldots (s_1-s_n)}$$

$$+ \frac{a_o e^{s_2 t}}{s_2(s_2-s_1) \ldots (s_2-s_n)} + \ldots \tag{B.7}$$

or

$$x(t) = \frac{a_o}{(-s_1)(-s_2) \ldots (-s_n)} \left[1 + \frac{(-s_1)(-s_2) \ldots (-s_n)}{s_1(s_1-s_2) \ldots (s_1-s_n)} e^{s_1 t} \right.$$

$$\left. + \frac{(-s_1)(-s_2) \ldots (-s_n)}{s_2(s_2-s_1) \ldots (s_2-s_n)} e^{s_2 t} + \ldots \right] \tag{B.8}$$

The s_i are the poles of the system transfer function. They are all negative real numbers for transfer functions for temperature sensors. It is common to introduce the concept of a time constant for each mode of the solution:

$$e^{s_i t} = e^{-t/\tau_i} . \tag{B.9}$$

Thus, we may write

$$\frac{x(t)}{x(\infty)} = 1 + \frac{\dfrac{1}{\tau_1 \tau_2 \cdot \cdot \cdot \tau_n}}{\dfrac{1}{-\tau_1}\left(\dfrac{1}{-\tau_1} + \dfrac{1}{\tau_2}\right) \cdot \cdot \cdot \left(\dfrac{1}{-\tau_1} + \dfrac{1}{\tau_n}\right)} e^{-t/\tau_1}$$

$$+ \frac{\dfrac{1}{\tau_1 \tau_2 \cdot \cdot \cdot \tau_n}}{\dfrac{1}{-\tau_2}\left(\dfrac{1}{-\tau_2} + \dfrac{1}{\tau_1}\right) \cdot \cdot \cdot \left(\dfrac{1}{-\tau_2} + \dfrac{1}{\tau_n}\right)} e^{-t/\tau_2} + \cdot \cdot \cdot \tag{B.10}$$

It is clear that there is no simple relation between the multiple time constants in the response equation. However, it is still accepted practice to define an overall time constant, τ, as the time required to achieve 63.2 percent of the final response following a step change in the input.

It is possible to develop an expression that relates the overall time constant, τ, to the individual time constants, τ_i, using an assumption that is well satisfied in typical temperature sensors. The faster time constants have a decreasing effect on the response compared to the slowest one as time progresses since they decay faster. For example, if we let τ_1 be the slowest time constant and evaluate the second exponential at $t/\tau_1 = 1$, we obtain the following:

τ_1/τ_2	e^{-t/τ_2} (at $t = \tau_1$)
2	.135
3	.050
4	.018
5	.007

Since τ_1/τ_2 is 5 or greater for a sensor, the τ_2 term contribution is small by the time $t = \tau_1$. Since the τ_1 term has the most important effect on τ,

we can also assert that τ_2 and higher terms have a small influence when $t = \tau$. Thus, we may write

$$\frac{x(t)}{x(\infty)} \approx 1 + \frac{\frac{1}{\tau_1 \tau_2 \cdot \cdot \cdot \tau_n}}{\frac{1}{-\tau_1}\left(\frac{1}{-\tau_1} + \frac{1}{\tau_2}\right) \cdot \cdot \cdot \left(\frac{1}{-\tau_1} + \frac{1}{\tau_n}\right)} e^{-t/\tau_1} \qquad (B.11)$$

Now, we can set $x(\tau)/x(\infty) = 0.632$ and solve for τ to obtain:

$$e^{-\tau/\tau_1} = .368 \left(1 - \frac{\tau_2}{\tau_1}\right)\left(1 - \frac{\tau_3}{\tau_1}\right) \cdot \cdot \cdot \left(1 - \frac{\tau_n}{\tau_1}\right) \qquad (B.12)$$

or

$$\tau = \tau_1 \left(1 - \ell n\left(1 - \frac{\tau_2}{\tau_1}\right) - \ell n\left(1 - \frac{\tau_3}{\tau_1}\right) - \cdot \cdot \cdot \ell n\left(1 - \frac{\tau_n}{\tau_1}\right)\right) \qquad (B.13)$$

To illustrate the effect of the faster time constants on the overall time constant, the ratio, τ/τ_1, was evaluated for various values of τ_2/τ_1 with $\tau_i = 0$ for i greater than 2. The results are shown in Figure B.1.

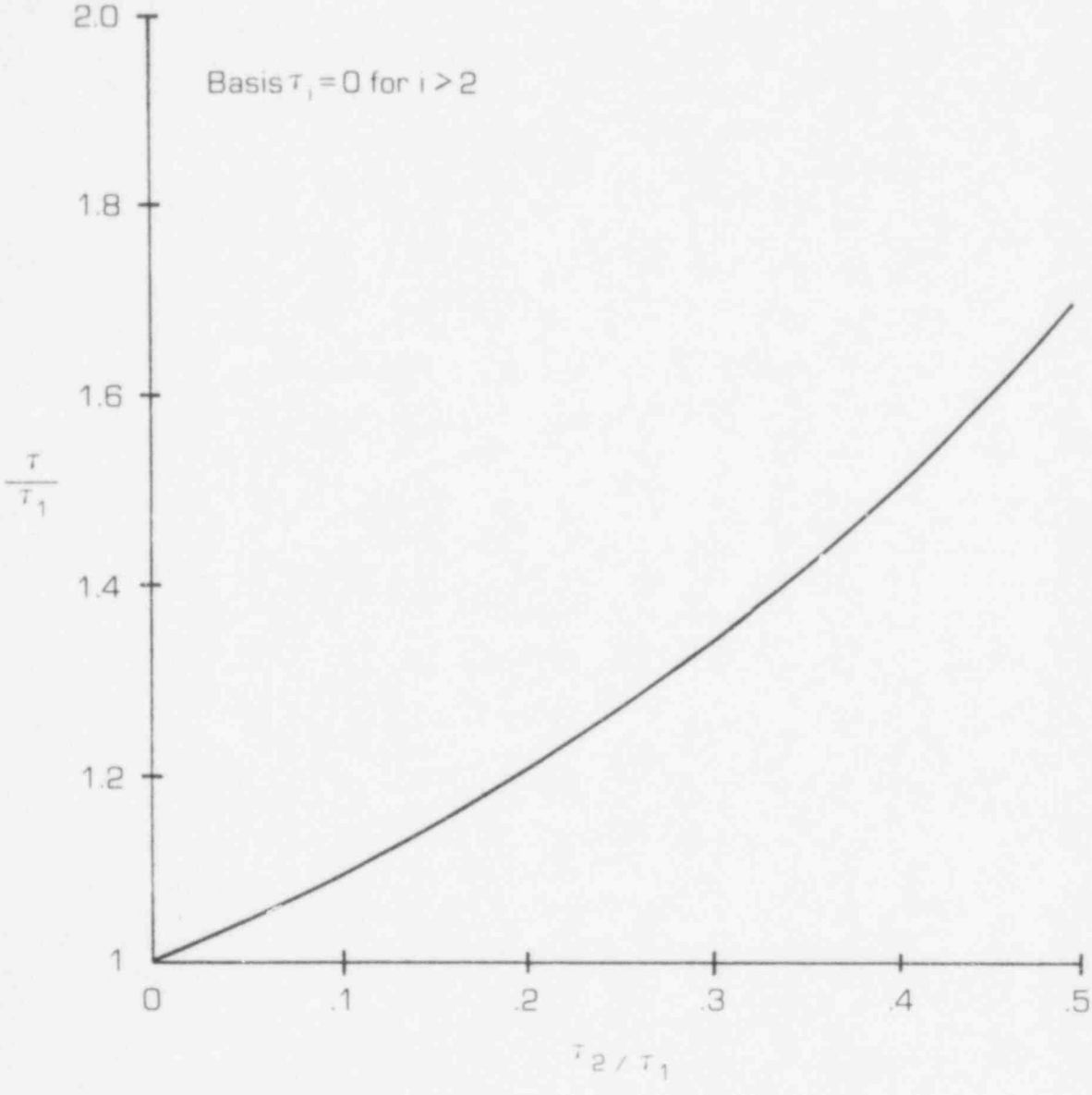

FIGURE B.1. EFFECT OF FASTER TIME CONSTANT ON OVERALL TIME CONSTANT.

B.3 Ramp Response

The ramp response of sensors is of interest because safety studies generally involve ramp changes. The ramp response is obtained readily from the transfer function of a system. First, let us consider a first order system:

$$G(s) = \frac{1}{\tau_s + 1} \tag{B.14}$$

The ramp response is evaluated using the Laplace transform of a ramp with ramp rate K as follows:

$$L\{Kt\} = \frac{K}{s^2} \tag{B.15}$$

Then:

$$x(s) = \frac{K}{s^2(\tau s + 1)} \tag{B.16}$$

The response may be obtained by inverse Laplace transformation:

$$x(t) = K\,[t - \tau + \tau\, e^{-t/\tau}] \tag{B.17}$$

For $t \gg \tau$, the exponential term is insignificant. The response is as shown in Figure B.2. The output, x(t), is delayed relative to the true process value, Kt, by a time that is less than or equal to τ. The asymptotic delay is called the system ramp time delay and is equal to the time constant for a first order system. Note that the ramp time delay is independent of the ramp rate. The asymptotic measurement error is $K\tau$.

Now, we will evaluate the ramp time delay and measurement for sensors described by higher order dynamic models. Consider the transfer function:

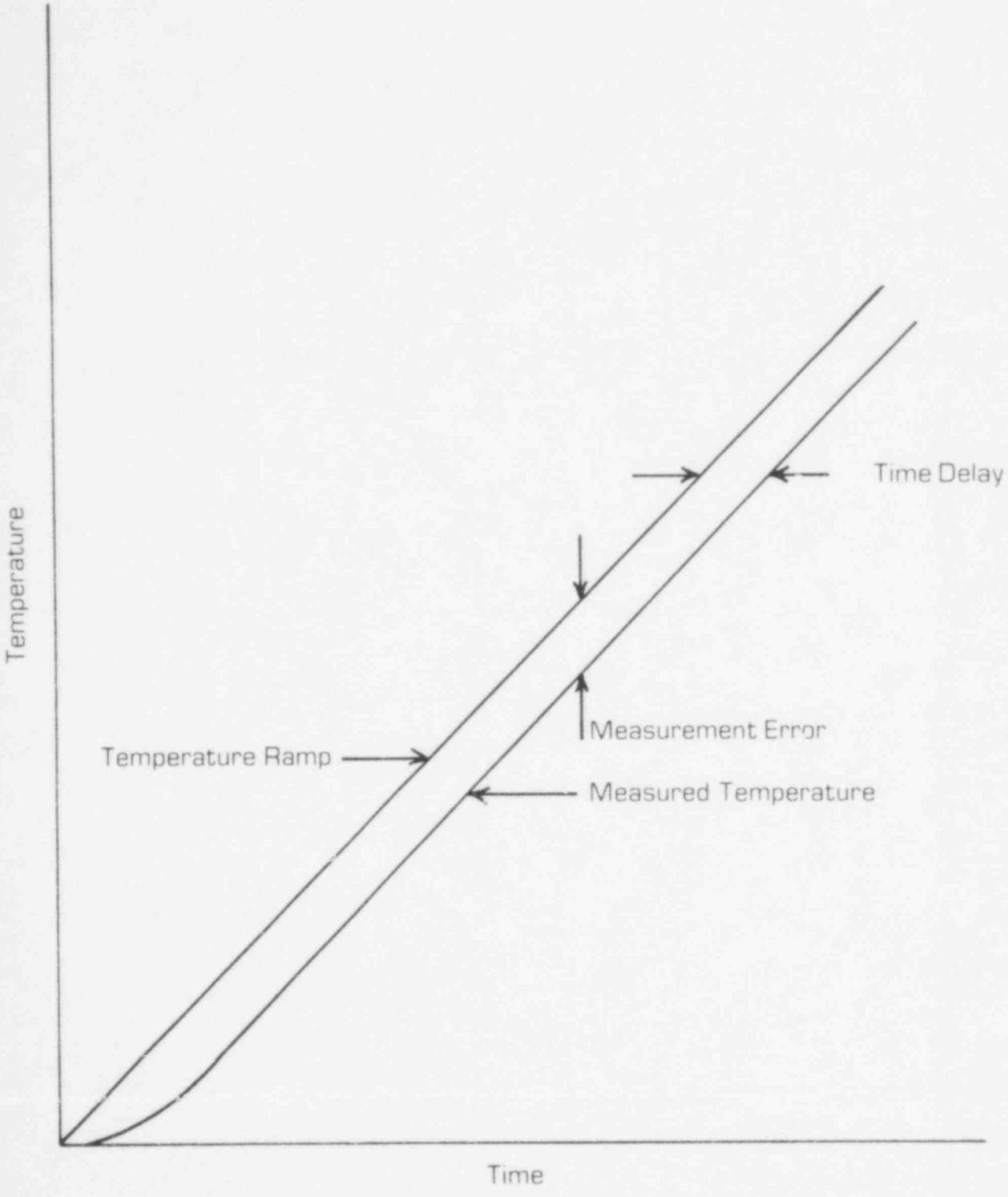

FIGURE B.2. TYPICAL RAMP RESPONSE AND ILLUSTRATION OF RAMP TIME DELAY AND MEASUREMENT ERROR.

$$G(s) = \frac{a_o}{(s-s_1)(s-s_2) \ldots (s-s_n)} \tag{B.18}$$

$$a_o = (-s_1)(-s_2) \ldots (-s_n)$$

and the input, Kt, with Laplace transform, $\frac{K}{s^2}$. The Laplace transform of the output is

$$x(s) = \frac{Ka_o}{s^2(s-s_1)(s-s_2) \ldots (s-s_n)} \tag{B.19}$$

The sensor response may be evaluated by inverse Laplace transformation. The partial fraction method gives

$$x(s) = \frac{A_1}{s^2} + \frac{A_2}{s} + \frac{A_3}{s-s_1} + \frac{A_4}{s-s_2} + \ldots \tag{B.20}$$

The arbitrary constants must be evaluated if the complete response is required. However, we are interested only in determining the ramp delay time and the asymptotic measurement error. Consequently, the exponential terms are of no interest, and we can concentrate on A_1 and A_2. These may be evaluated to give the following result.

$$A_1 = K \tag{B.21}$$

$$A_2 = -K\,[\tau_1 + \tau_2 + \ldots \tau_n] \tag{B.22}$$

Therefore

$$x(t) \sim K[t-(\tau_1 + \tau_2 + \ldots + \tau_n)] \tag{B.23}$$

In this case, we obtain:

$$\text{ramp time delay} = \tau_1 + \tau_2 + \ldots \tau_n \tag{B.24}$$

and

$$\text{asymptotic measurement error} = K[\tau_1 + \tau_2 + \ldots \tau_n] \tag{B.25}$$

B.4 Relation Between Time Constant and Ramp Time Delay

The time constant and the ramp time delay are given by:

$$\text{time constant} = \tau_1 \left[1 - \ell\eta\left(1 - \frac{\tau_2}{\tau_1}\right) - \ell\eta\left(1 - \frac{\tau_3}{\tau_1}\right) - \ldots\right] \tag{B.26}$$

and

$$\text{ramp time delay} = \tau_1\left[1 + \frac{\tau_2}{\tau_1} + \frac{\tau_3}{\tau_1} + \ldots\right]. \tag{B.27}$$

Insertion of numerical values into these expressions shows that the ramp delay time is always less than the time constant, but the difference is small for values of the τ_i that are typical of temperature sensors. To illustrate this, the percent differences between the time constant and the ramp time delay was evaluated for a two-term representation (τ_1 and τ_2). The error is shown in Figure B.3. We note that for a typical ratio of 0.20, the difference is less than two percent.

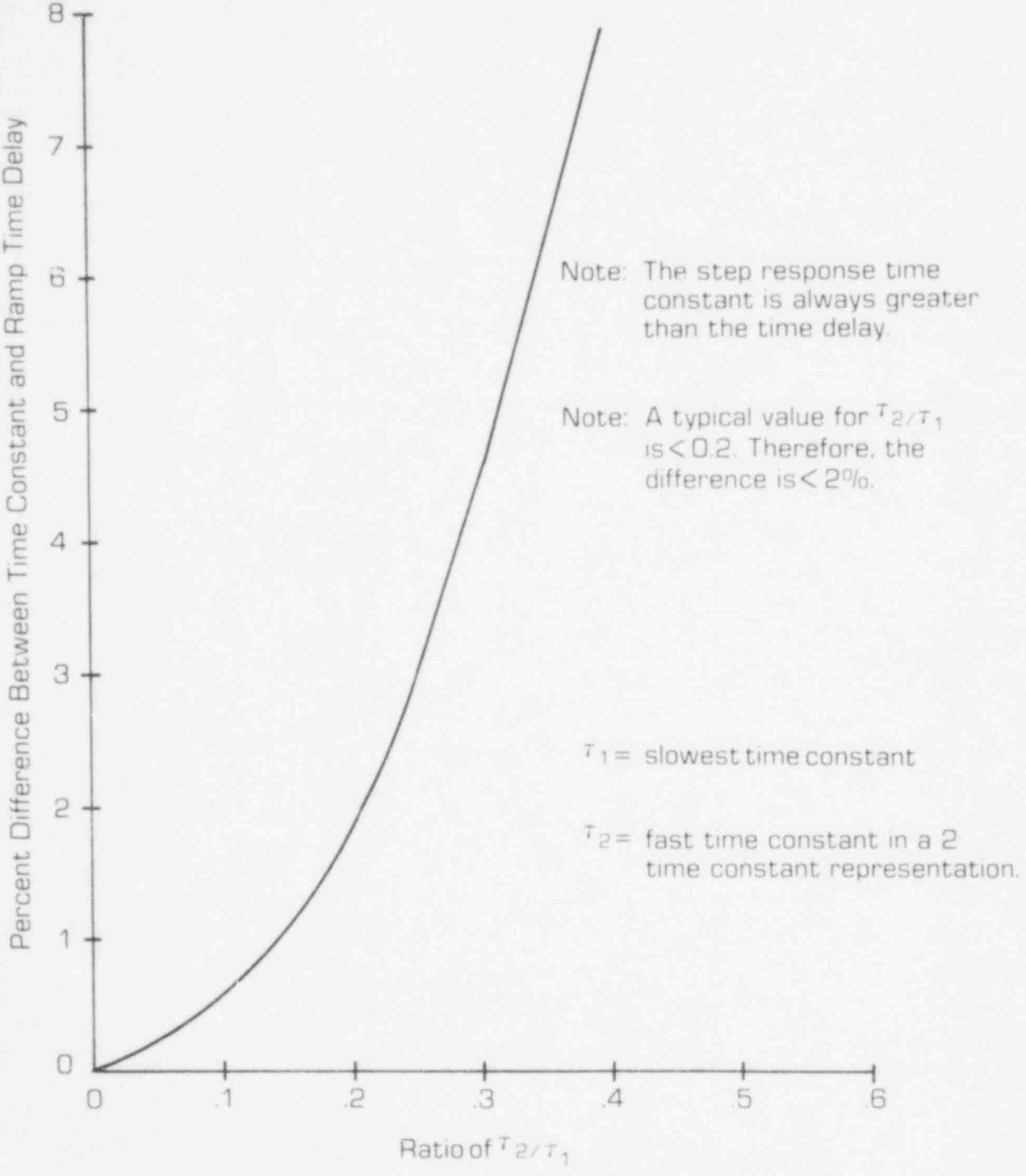

FIGURE B.3. RELATION BETWEEN PLUNGE TIME CONSTANT AND RAMP TIME DELAY.

927 165

APPENDIX C

THE LOOP CURRENT STEP RESPONSE TRANSFORMATION

C.1 Introduction

The result of interest is the time constant associated with a step change in fluid temperature external to the sensor. The time constant is defined to be the time required for the sensor output to reach 63.2 percent of its final steady-state value after a step change in fluid temperature. This time constant is usually obtained from a plunge test in a laboratory environment. Since the plunge test cannot be used to obtain the time constant of an installed RTD, the LCSR test is proposed as one method to obtain an estimate of the desired plunge test time constant.

A transformation is needed to convert LCSR data into a prediction of the response that would occur following a fluid temperature step change. The transformation may be developed using a general nodal model for sensor heat transfer. The development is independent of the number of nodes included in the model, so use of this approach does not imply any restrictive assumptions. The following sections give some details on RTD heat transfer that permit formulation of a transformation and that define the conditions for validity of the transformation.

C.2 Mathematical Development of the LCSR Transformation

An analytical transformation for converting loop current step response (LCSR) test results into plunge test results may be developed using a general nodal model for sensor heat transfer. Consider first a system with predominantly one-dimensional heat transfer. In this case, the nodal model may be represented schematically as shown in Figure C.1. The accuracy of such a model may be made as great as desired by using enough nodes.

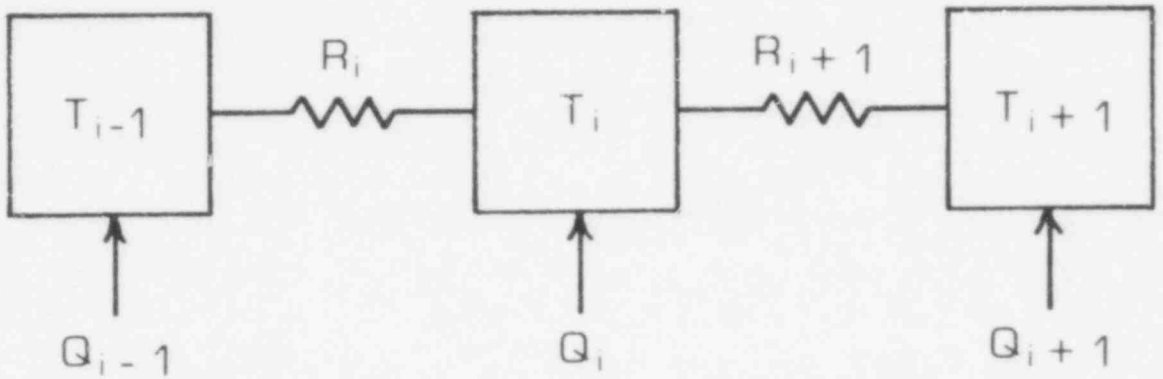

FIGURE C.1. SCHEMATIC OF A ONE-DIMENSIONAL NODE-TO-NODE HEAT TRANSFER MODEL.

The dynamic heat transfer equation for node i is:

$$(MC)_i \frac{dT_i}{dt} = \frac{1}{R_{i-1}} (T_{i-1} - T_i) - \frac{1}{R_i} (T_i - T_{i+1}) + Q_i \qquad (B.1)$$

where

Q_i = heat generation rate in node i

M_i = mass of material in node i

C_i = specific heat capacity of material in node i

R_i = heat transfer resistance for node i-1 to node i

T_i = temperature of node i.

Dividing through by $(MC)_i$ and defining constants gives

$$\frac{dT_i}{dt} = a_{i,i-1} T_{i-1} - a_{i,i} T_i + a_{i,i+1} T_{i+1} + b_i Q_i \qquad (B.2)$$

where

$$a_{i,i-1} = \frac{1}{(MC)_i R_{i-1}}$$

$$a_{i,i} = \frac{1}{(MC)_i} \left(\frac{1}{R_{i-1}} + \frac{1}{R_i}\right)$$

$$a_{i,i+1} = \frac{1}{(MC)_i R_i}$$

$$b_i = \frac{1}{(MC)_i}$$

The nodal equations may be applied to a series of nodes, starting at the node closest to the center (i=1) and ending with the node closest to the surface (i=N). The equations have the form:

$$\frac{dT_1}{dt} = -a_{11}\ T_1 + a_{12}\ T_2 + b_1\ Q_1$$

$$\frac{dT_2}{dt} = a_{21}\ T_1 - a_{22}\ T_2 + a_{23}\ T_3 + b_2\ Q_2$$

$$\frac{dT_3}{dt} = a_{32}\ T_2 - a_{33}\ T_3 + a_{34}\ T_4 + b_3\ Q_3$$

.

.

.

$$\frac{dT_N}{dt} = a_{N,N-1}\ T_{N-1} - a_{N,N}\ T_N + C_{N,F}\ T_F + b_N\ Q_N$$

where

T_F = fluid temperature.

These equations may be written in matrix form:

$$\frac{d\bar{x}}{dt} = A\ \bar{x} + B\ \bar{q} + \bar{c}\ T_F \qquad (C.3)$$

where

$$\bar{x} = \begin{bmatrix} T_1 \\ T_2 \\ T_3 \\ . \\ . \\ . \\ T_N \end{bmatrix} \qquad A = \begin{bmatrix} -a_{11} & a_{12} & 0 & 0 & \cdots \\ a_{21} & -a_{22} & a_{23} & 0 & \cdots \\ 0 & a_{32} & a_{33} & a_{34} & \cdots \\ . & & & & \\ . & & & & \\ . & & & & \\ & & & a_{N,N-1} & -a_{N,N} \end{bmatrix}$$

$$B = \begin{bmatrix} b_1 & 0 & 0 & & \\ 0 & b_2 & 0 & & \\ 0 & 0 & b_3 & \cdots & \\ & & & & b_N \end{bmatrix} \qquad \bar{q} = \begin{bmatrix} Q_1 \\ Q_2 \\ Q_3 \\ \cdot \\ \cdot \\ \cdot \\ Q_N \end{bmatrix}$$

Laplace transformation gives:

$$[sI-A]\ \bar{x}(s) = \bar{c}\ T_F(s) + B\ \bar{q}(s). \tag{C.4}$$

The Laplace transform solution for the response of any node, x_i, may be found using Cramer's rule. Let us consider several cases:

Case 1--no heat capacity in region between the filament and the center of the sensor, no heat generation in any nodes, fluid temperature perturbation, one dimensional heat transfer

$$T_1(s) = \frac{F(s)}{|\ sI-A\ |} \tag{C.5}$$

where

$$F(s) = \begin{vmatrix} 0 & -a_{12} & 0 & 0 & \cdots & & \\ 0 & (s+a_{22}) & -a_{23} & 0 & \cdots & & \\ 0 & -a_{32} & (s+a_{33}) & -a_{34} & \cdots & & \\ 0 & 0 & -a_{34} & (s+a_{44}) & \cdots & & \\ \cdot & \cdot & \cdot & \cdot & \cdots & & \\ \cdot & \cdot & \cdot & \cdot & \cdots & & \\ \cdot & \cdot & \cdot & \cdot & \cdots & & \\ C_{N,F}T_F(s) & \cdot & \cdot & \cdot & \cdots & -a_{N,N-1} & (s+a_{N,N}) \end{vmatrix} \tag{C.6}$$

This may be written

$$F(s) = C_{N,F}\, T_F(s)\, (-1)^{(N+f)} \begin{vmatrix} -a_{12} & 0 & 0 & \cdots & \\ (s+a_{22}) & -a_{23} & 0 & \cdots & \\ -a_{32} & (s+a_{33}) & -a_{34} & \cdots & \\ \cdot & \cdot & \cdot & \cdots & \\ \cdot & \cdot & \cdot & \cdots & \\ \cdot & \cdot & \cdot & \cdots & -a_{N-1,N-1} \end{vmatrix} \tag{C.7}$$

This determinant is for a matrix in lower triangular form (all elements above the diagonal are zero). The determinant is given by the product of the diagonals, all of which are constants. Therefore, for a fluid temperature perturbation in a one-dimensional heat transfer system, the response of the innermost node is characterized by a transfer function with no zeroes. If the sensing element in an RTD is centrally located, or if there is insignificant heat capacity between the filament and the center of the sensor, then this type of transfer function describes the response characteristics of the sensor.

The transfer function may be written

$$\frac{T_1(s)}{T_F(s)} = \left| \frac{K}{sI-A} \right|$$

$$= \frac{K}{(s-p_1)\ (s-p_2)\ \cdots} \tag{C.8}$$

where

p_i = poles (identical to eigenvalues of A).

For a unit step change in T_F, $T_F(s) = \frac{1}{s}$, and we may write:

$$T_1(s) = \frac{K}{s(s-p_1)\ (s-p_2)\ \ldots} \tag{C.9}$$

Inversion of this Laplace transform using the residue theorem gives:

$$T_1(t) = K\left[\frac{1}{(-p_1)\ (-p_2)\ \ldots\ (-p_N)} + \frac{e^{p_1 t}}{(p_1)\ (p_1-p_2)\ \ldots}\right.$$

$$\left. + \frac{e^{p_2 t}}{(p_2)\ (p_2-p_1)\ \ldots} + \ldots\right]. \tag{C.10}$$

Thus, we make the following important observation:

> For an RTD with predominantly one-dimensional heat transfer and with insignificant heat capacity between the sensing element and the center of the sensor, the poles alone (no zeroes) are adequate to characterize the response due to a fluid temperature change.

The implication is that if one can identify the poles by some other test (such as the LCSR), then he can construct the response to a fluid temperature step.

Case 2--significant heat capacity between the filament and the center of the sensor, no heat generation in any nodes, fluid temperature perturbation, one-dimensional heat transfer

This case may be analyzed for the response of any non-central node, but for notational simplicity, let us consider the response of the second node. In this case

$$T_2(s) = \frac{R(s)}{|\,sI-A\,|} \tag{C.11}$$

where

$$F(s) = \begin{vmatrix} (s+a_{11}) & 0 & 0 & 0 & \cdots \\ -a_{21} & 0 & -a_{23} & 0 & \cdots \\ 0 & 0 & (s+a_{33}) & -a_{34} & \cdots \\ . & . & . & . & \cdots \\ . & . & . & . & \cdots \\ . & . & . & . & \cdots \\ . & C_{N,F}T_F(s) & . & . & \cdots \end{vmatrix} \qquad (C.12)$$

This may be written

$$F(s) = C_{N,F}\, T_F(s)\, (-1)^{2+N} \begin{vmatrix} (s+a_{11}) & 0 & 0 & 0 & \cdots \\ -a_{21} & -a_{23} & 0 & 0 & \cdots \\ 0 & (s+a_{33}) & -a_{34} & 0 & \cdots \\ . & . & . & . & \cdots \\ . & . & . & . & \cdots \\ . & . & . & . & \cdots \end{vmatrix} \qquad (C.13)$$

Again, we observe that the matrix is triangular, but the diagonals are not all constant. In this case, the transfer function will have one zero. For the response of nodes further from the center, there will be more zeroes. Thus, the poles alone are not adequate to construct the response for an RTD if the sensing element is not located at a position with insignificant heat capacity between the filament and the center of the sensor.

Case 3--insignificant heat capacity between the filament and the center of the sensor, heat generation in central node, constant fluid temperature, one-dimensional heat transfer

$$T_1(s) = \left| \frac{F(s)}{sI-A} \right| \tag{C.14}$$

where

$$F(s) = \begin{vmatrix} b_1 Q_1 & -a_{12} & 0 & 0 & \cdots \\ 0 & (s+a_{22}) & -a_{23} & 0 & \cdots \\ 0 & & (s+a_{33}) & -a_{34} & \cdots \\ \cdot & \cdot & \cdot & \cdot & \cdots \\ \cdot & \cdot & \cdot & \cdot & \cdots \\ \cdot & \cdot & \cdot & \cdot & \cdots \end{vmatrix} \tag{C.15}$$

This may be written

$$F(s) = b_1 Q_1 \begin{vmatrix} (s+a_{22}) & -a_{23} & 0 & 0 & \cdots \\ -a_{32} & (s+a_{33}) & -a_{34} & 0 & \cdots \\ 0 & -a_{43} & (s+a_{44}) & -a_{45} & \cdots \\ \cdot & \cdot & \cdot & \cdot & \cdots \\ \cdot & \cdot & \cdot & \cdot & \cdots \\ \cdot & \cdot & \cdot & \cdot & \cdots \end{vmatrix} \tag{C.16}$$

In this case, the matrix is not triangular, and the transfer function will have zeroes.

The transfer function may be written:

$$\frac{T_1(s)}{Q_1(s)} = K^1 \frac{(s-z_1)\ (s-z_2)\ \cdots\ (s-z_M)}{(s-p_1)\ (s-p_2)\ \cdots\ (s-p_N)} . \tag{C.17}$$

For a unit step change in Q_1 ($Q_1(s) = \frac{1}{s}$), we obtain

$$T_1(s) = \frac{K^1(s-z_1)\ (s-z_2)\ \ldots\ (s-z_M)}{s(s-p_1)\ (s-p_2)\ \ldots\ (s-p_N)} \ . \qquad \text{(C.18)}$$

Inversion by the residue theorem gives:

$$T_1(t) = K^1\left[\frac{(-z_1)\ (-z_2)\ \ldots\ (-z_M)}{(-p_1)\ (-p_2)\ \ldots\ (-p_N)} + \frac{(p_1-z_1)\ (p_1-z_2)\ \ldots\ (p_1-z_M)}{(p_1)\ (p_1-p_2)\ \ldots\ (p_1-p_N)}\ e^{p_1 t}\right.$$

$$\left. + \frac{(p_2-z_1)\ (p_2-z_2)\ \ldots\ (p_2-z_M)}{(p_2)\ (p_2-p_1)\ \ldots\ (p_2-p_N)}\ e^{p_2 t} + \ldots\right]. \qquad \text{(C.19)}$$

Note that the response is determined by the zeroes as well as the poles. However, the poles are the same as for the fluid temperature change case. Thus, if we can identify the poles from a LCSR test, we can construct the equivalent fluid perturbation response using Equation (C.10).

Case 4--insignificant heat capacity between the filament and the center of the sensor, no heat generation in any nodes, fluid temperature perturbation, multi-dimensional heat transfer

In this case, there is branching in the heat transfer (see Figure C.2). This means that the temperature of a node may be influenced by more than just two neighboring nodes as in the one-dimensional case. In the one-dimensional case, all of the elements of the A matrix are on the diagonal or in the position adjacent to the diagonal. In the multi-dimensional case, coupling terms appear in other positions (always symmetrically positioned around the diagonal). Thus F(s) may be written

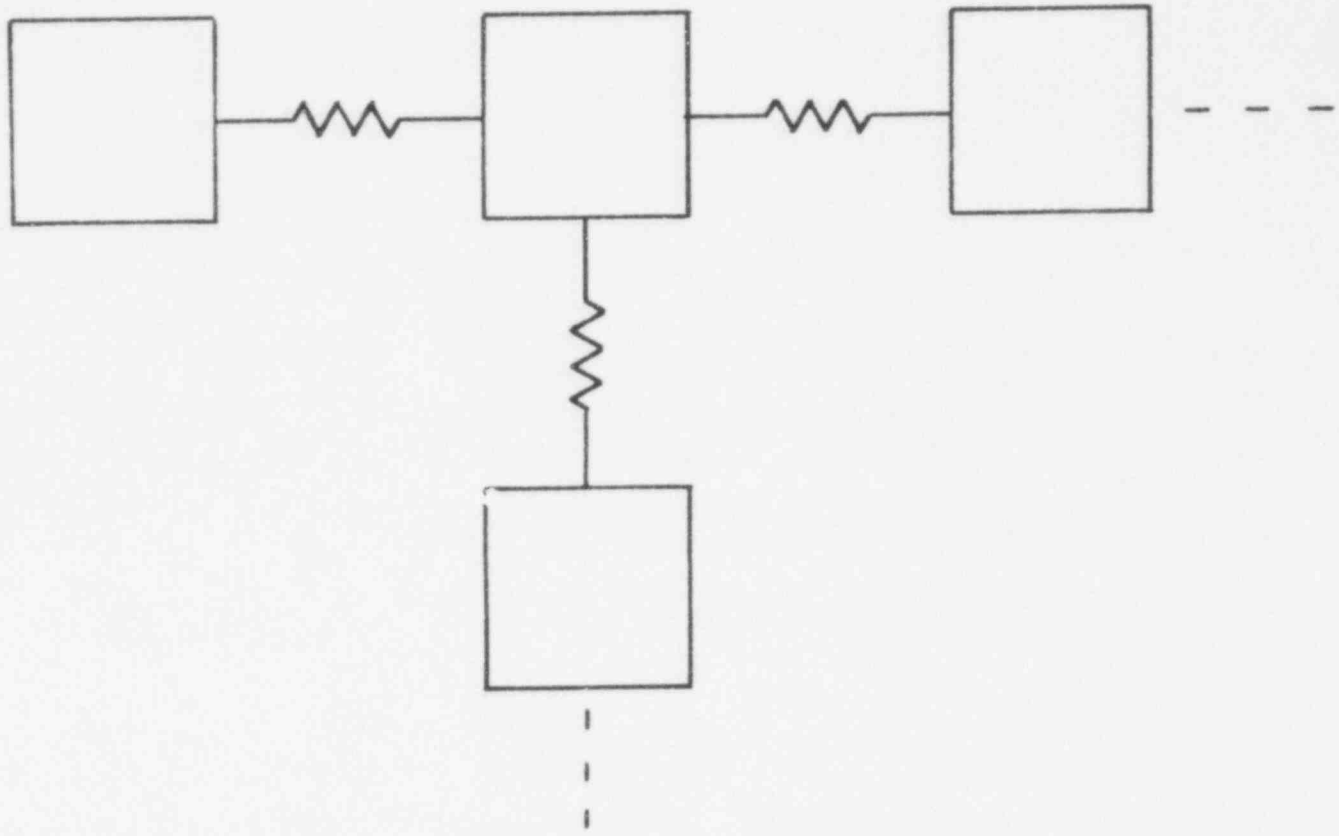

FIGURE C.2. SCHEMATIC OF A MULTI-DIMENSIONAL NODE-TO-NODE HEAT TRANSFER

$$F(s) = \begin{vmatrix} 0 & -a_{12} & * & * & \cdots \\ 0 & (s+a_{22}) & -a_{23} & * & \cdots \\ \cdot & -a_{32} & (s+a_{33}) & -a_{34} & \cdots \\ \cdot & * & * & * & \cdots \\ \cdot & \cdot & \cdot & \cdot & \cdots \\ \cdot & \cdot & \cdot & \cdot & \cdots \\ \cdot & \cdot & \cdot & \cdot & \cdots \\ C_{N,F}{}^{T}{}_{F}(s) & \cdot & \cdot & \cdot & \cdots \end{vmatrix} \qquad (C.20)$$

where

* = possible new coupling terms.

In this case, the matrix is not triangular and zeroes can occur. This means that the availability of the poles through some sort of measurement is not sufficient for construction of the response to a fluid temperature step.

C.3 Steps in Implementing the LCSR Transformation

The steps for obtaining the plunge test time constant are:

1. perform a LCSR test
2. identify the poles associated with the LCSR data
3. construct the step response for a fluid temperature perturbation using Equation (C.10).

APPENDIX D

TEST PROCEDURE

A test procedure for performing a combined self heating, loop current step response test program is presented below.

1. Set up the equipment as near as possible to the cabinet where the RTD leads are connected to the plant transmitters. The equipment includes:
   - The test instrument (bridge, switchable power supply, adjustable decade resistors, adjustable-gain amplifier to amplify the voltage drop across the bridge, and a digital voltmeter that can monitor the amplifier output or can be switched to measure the voltage drop across a fixed bridge resistor to provide the current).
   - A strip chart recorder connected to the bridge amplifier output.
   - A data recording system (analog or digital) connected to the bridge amplifier output and to the current switch status (open or closed) indicator output.
2. Connect a spare RTD to the test instrument. The RTD should be immersed in water to within two inches of the top connector on the RTD.
3. Turn on the power supply with the current selector switch set to LOW and the power supply voltage at its lowest setting.
4. Adjust the power supply to give 1-5 ma.
5. Balance the bridge (adjust the decade resistor until the bridge amplifier output goes to zero).
6. Check to be sure that the resistance is correct for the water temperature.
7. Switch the current selector switch to HIGH.

8. Adjust the power supply to give 40 ma (typical) through the sensor.
9. Adjust the amplifier gain to give an output voltage that is suitable for the recording equipment.
10. Switch the current selector switch to LOW.
11. Wait until the bridge amplifier output settles out.
12. Turn on the strip chart recorder.
13. Switch the current selector switch to HIGH.
14. Wait until the bridge amplifier output settles out.
15. Measure the time required for the output to reach 63.2 percent of its total variation.
16. Compare this time with a reference value (obtained on previous tests on the same sensor in still water).
17. If the difference in times is more than fifteen percent, check equipment and procedure.
18. If the difference in times is less than fifteen percent, set the current selector switch to LOW and continue. Otherwise, check equipment.
19. Turn off the power supply
20. Disconnect the spare RTD.
21. Remove the selected plant RTD leads from its in-plant transmitter.
22. Connect the in-plant RTD leads to the test instrument. If the RTD has more than two leads, select only one from each side of the filament.
23. Turn on the power supply and adjust to give 1-5 ma through the RTD.
24. Balance the bridge.

25. Check the noise level at the bridge amplifier output.
26. Set the power supply to its lowest value.
27. Switch the current selector switch to HIGH.
28. Start the self heating test. Increase the power supply voltage to give a current through the RTD of about 10 ma.
29. Wait until the bridge amplifier output settles out.
30. Rebalance the bridge.
31. Calculate the power dissipated in the RTD filament.
32. Record the resistance and power.
33. Repeat steps 23 through 32 for current values up to 40 ma (typical).
34. Plot resistance versus power on linear graph paper. If the data indicate a well-defined straight line, go to step 35. If the data indicate scatter, repeat steps 23 through 32 for more data points.
35. Start the Loop Current Step Response (LCSR) tests. Balance the bridge at low current then set the current selector switch to HIGH.
36. Set the power supply voltage to give a current of 40 ma (typical) through the RTD.
37. Adjust the amplifier gain to give an input voltage that is suitable for the recording equipment.
38. Set the current selector switch to LOW.
39. Wait for the bridge amplifier output to settle out.
40. Start the strip chart recorder and the data recording equipment.
41. Switch the current selector switch to HIGH.
42. Wait until the bridge amplifier output settles out.
43. Switch the current selector switch to LOW.

44. Repeat steps 38 through 43 at least five times (more for noisy or unstationary data).

45. Set the current selector switch to LOW.

46. Turn off the power supply.

47. Disconnect the sensor.

48. Repeat steps 22 through 47 for the next sensor to be tested.

49. Complete tests on all sensors.

50. Remove test equipment.

References

1. U.S. Nuclear Regulatory Commission, "Regulatory Guide 1.118 - Periodic Testing of Electric Power and Protection Systems" USNRC, Washington, D.C., Revision 1, November 1977

2. The Institute of Electrical and Electronics Engineers, "IEEE Standard: Criteria for Protection Systems for Nuclear Power Generating Stations" Standard 279-1971, IEEE, New York, 1971

3. The Institute of Electrical and Electronics Engineers, "IEEE Standard Criteria for the Periodic Testing of Nuclear Power Generating Station Class IE Power and Protection Systems," Standard 338-1975, IEEE, New York, 1975

4. T. W. Kerlin, "Analytical Methods for Interpreting In-Situ Measurements of Response Times in Thermocouples and Resistance Thermometers," Oak Ridge National Laboratory Report ORNL-TM-4912 (March 1976)

5. T. W. Kerlin, et. al., "In-Situ Response Time Testing of Platinum Resistance Thermometers," EPRI Report NP-459 (January, 1977)

6. T. W. Kerlin, et. al. "In-Situ Response Time Testing of Platinum Resistance Thermometers," EPRI Report NP-834 (July, 1978)

7. T. W. Kerlin, L. F. Miller and H. M. Hashemian, "In-Situ Response Time Testing of Platinum Resistance Thermometers," ISA Transactions, 17, 71-88 (1978)

8. B. R. Upadhyaya and T. W. Kerlin, "In-Situ Response Time Testing of Platinum Resistance Thermometers - Noise Analysis Method" EPRI Report NP-834, Vol. 2, July 1978

9. B. R. Upadhyaya and T. W. Kerlin, "Estimation of Response Time Characteristics of Platinum Resistance Thermometers by the Noise Analysis Technique" ISA Transactions, 17, 21-38 (1978)

10. H. M. Hashemian, T. W. Kerlin, B. R. Upadhyaya, "Apparatus for Measuring the Degradation of a Sensor Time Constant" Patent Application filed with U.S. Patent Office

11. M. Skorska, personal communication, Nuclear Engineering Department, University of Tenenssee, Knoxville, Tennessee

12. W. P. Poore, "Resistance Thermometer Characteristics and Time Response Testing" Thesis, Nuclear Engineering Department, University of Tennessee, Knoxville, Tennessee (to be published)

13. T. W. Kerlin, "Accuracy of Loop Current Step Response Test Results" (to be published)